Winter 1988

A Mathematical Model of the Dynamics of an Optically Pumped Four-Level Solid State Laser System

Lila Freeman Roberts
Old Dominion University

A MATHEMATICAL MODEL OF THE DYNAMICS OF AN OPTICALLY PUMPED FOUR-LEVEL SOLID STATE LASER SYSTEM

by

LILA FREEMAN ROBERTS

B.S. May 1977, North Carolina State University, Raleigh, NC

M.S. August 1986, Old Dominion University, Norfolk, VA

A Dissertation Submitted to the Faculty of Old Dominion University
in Partial Fulfilment of the Requirements for the Degree of

DOCTOR OF PHILOSOPHY
in
COMPUTATIONAL AND APPLIED MATHEMATICS

December, 1988

Approved by:

J. Swetits (Director)

ABSTRACT

A Mathematical Model of the Dynamics of an Optically Pumped Four-Level Solid State Laser System

Lila Freeman Roberts

Old Dominion University, 1988
Director: Dr. John J. Swetits

This is a study of a mathematical model of the dynamics of an optically pumped four-level solid state laser system. A general mathematical model that describes the spatial and temporal evolution of the electron populations in the laser rod as well as the development of the left and right traveling photon fluxes in the cavity is developed. The model consists of a coupled set of first order semilinear partial differential equations. While the model was developed for Titanium-doped sapphire lasers, it is applicable to three and four level lasers in general.

The analysis of the model is conducted in two parts. First, by formally taking an average over the spatial variable, the system of partial differential equations is reduced to a system of ordinary differential equations describing the temporal behavior of the spatially-averaged dynamic quantities. Several qualitative properties of the solutions of this system are proved and stability of the solutions under various operating conditions is investigated. The rate equations are solved numerically and the effects on the solutions of changes in the physical parameters are discussed.

The second part of this study is concerned with the qualitative and numerical

analysis of the spatial and temporal model of a Ti: Sapphire ring laser. Several qualitative properties of the solution are established. The system of partial differential equations is solved numerically by integration along the characteristic lines using an implicit integration scheme developed for this problem. The computed solutions are compared to those obtained by using a stable finite difference approximation. The results of the comparison demonstrate that the implicit integration scheme is viable as well as efficient for numerically solving the system of partial differential equations and can be considered a useful analytical tool for studying the dynamics of this type of laser system.

All computer codes are written in FORTRAN and currently run on a DEC VAX 11/750.

Acknowledgements

It would be impractical for me to attempt to name every person who has contributed in a positive way to the work that I have accomplished. However, I will attempt to acknowledge many of those people. I first would like to express my appreciation to the Mathematics faculty at Old Dominion University for their support and encouragement. Special thanks are in order for Dr. Philip Wohl, Graduate Program Director, whose advice and kind words were deeply appreciated during my stay at Old Dominion University.

The research that led to this dissertation was supported by NASA Training Grant NGT-47-003-804. I would like to thank the people in the Flight Electronics Division at NASA Langley Research Center, in particular those people in the Laser Technology and Applications Branch for their patience and help in every aspect of my work. I am particularly indebeted to Dr. Charles E. Byvik for his efforts in securing support for me and for his friendship which I value highly.

I would like to thank my dissertation committee, Dr. John J. Swetits, Dr. John Heinbockel, Dr. Stan Weinstein, and Dr. A.M. Buoncristiani for their helpful suggestions and constructive criticism of my work. I especially thank Dr. Swetits, Chair of the committee, for his confidence in me and for his seemingly infinite patience. I am very appreciative of the encouragement I have received from Dr. Heinbockel throughout my years as a graduate student. I thank Dr. Buoncristiani for helpful conversations and for being my good friend.

During the time I was at Old Dominion university I was fortunate to meet

a number of fellow graduate students who became my friends and confidantes and to them I give special thanks. I also thank Barbara Jeffrey, Mathematics Department Secretary, who typed this dissertation and without whom I would never have been able to wade through mountains of administrative paperwork while I was a graduate student.

Last, but not least, I express loving appreciation to my husband, Lonnie, without whose encouragement, understanding, and patience this work would never have been completed.

TABLE OF CONTENTS

LIST OF FIGURES

Chapter 1

Introduction

During the last several years, solid state lasers have been developed that have the potential for meeting the rigorous performance requirements for space-based remote sensing of the atmosphere. One of the materials that has shown promise in achieving the performance objectives is $Ti^{3+} : Al_2O_3$, or Titanium doped Sapphire, first demonstrated in 1982 [18].

In a solid state laser, a dopant ion substitutes for an ion in the host material. Specifically, in Ti:Sapphire, the Ti^{3+} ion substitutes for the Al^{3+} ion in Al_2O_3. Strong coupling between the optically active Titanium ion and the host lattice broaden the absorption and emission lines [5]. Narrow line width operation is achieved by using a line-narrowing technique such as injection seeding [10]. In order to design a stable and efficient laser and to understand the effect on laser output of line-narrowing techniques, it is necessary to gain an understanding of the development of the dynamical processes of the laser. This is a study

of a mathematical model of an end-pumped Ti:Sapphire laser. The model was developed for this laser system but is sufficiently general to be applied, with minor modifications, to both three and four-level laser systems.

The model consists of a coupled set of rate equations that describe the spatial and temporal development of the dynamical variables. The model presented here allows for the introduction of an injected signal and thus the effect on laser output of injection seeding can be studied.

A general time dependent rate equation model for three and four level lasers is given in [12]. Moulton [16] has employed a rate equation approach to investigate the temporal process in a $Co : MgF_2$ laser system. The rate equations were solved numerically and experimental results were compared with the numerical solutions. Moulton also applied this approach to a study of an injection locked Ti:Sapphire ring laser [18]. Ganiel, et.al. [10], numerically solved the coupled space and time dependent rate equations for an injection locked pulsed dye laser system. The purpose of the present study is to establish general analytical properties of the solutions to both the temporal and the spatial-temporal models for a Ti:Sapphire laser. In addition, the numerical treatment of the models will be discussed in detail.

In Chapter 2, a general mathematical model that describes the spatial and temporal evolution of the electron population in the active region of the laser system as well as the development of left and right traveling photon fluxes in the laser rod and cavity is presented. The model, based on a four-level model of the

transitions between electronic levels of the Titanium ion, consists of a system of first order semilinear partial differential equations. The cavity configuration is assumed to be a simple ring with injection seeding allowed through a mirror in the cavity. Boundary conditions appropriate for this arrangement are given.

Chapter 3 deals with a simplified version of the model described in Chapter 2 obtainied by taking an average over the spatial variable. By formally integrating over the spatial variable, the system of partial equations is reduced to a system of nonlinear ordinary differential equations. General qualitative results are given and a linearized analysis gives stability properties of the equilibrium solutions. The numerical treatment of the system of equations is discussed and numerical results are given for both constant and time dependent pumping rates. The effects on the computed solutions of physical parameters that cannot be directly measured are studied.

The spatial and temporal model is studied in detail in Chapter 4. Some qualitative results are established and the solutions to this model are found to exhibit some of the same qualitative properties as the corresponding elements in the spatially averaged model. The approach used to solve the system of partial differential equations numerically is motivated by reducing it to a system of ordinary differential equations along the characteristics [8]. Numerical integration in the active region is performed using a Modified Euler technique (as in [7]) and the results are compared to those obtained by using Euler's Method and a stable finite difference approximation [11].

Most of the physical parameters used can be obtained by direct measurement. Characteristics of Ti:Sapphire used in the model are summarized in Figures 2.1- 2.3 ([4], [17]) which show the absorption and emission spectra and the temperature dependence of the fluorescence lifetime.

All computer codes are written in FORTRAN and currently run on a DEC VAX11/750. Two computer programs are included in the appendices. In Appendix I, the computer program is given that calculates the equilibrium solutions for the spatially averaged model with a constant pumping rate and determines the stability properties of the solution. The program also determines the nature of the linearized eigenvalues which is used to predict the occurrence of oscillations in the computed solutions of the rate equations. Appendix II contains the computer program that solves the spatial and temporal model using the Modified Euler Method to integrate along the characteristics of the system.

Chapter 2

A Descripton of the Model of the Laser Dynamics

2.1 The Population Rate Equation

The emission and absorption spectra of Ti:Sapphire [4], [17], superimposed on an energy level diagram for the Ti^{3+} ion are shown in Figure 2.4. These spectra are the basis for an idealized four level model, Figure 2.5, of the lasing action of Titanium in Sapphire. The electron population density in the i^{th} energy level at position x in the crystal and time t is denoted by $n_i(x,t)$; $i = 0,1,2,3$.

A narrow band pump excites the ground state electrons to a level in the absorption band which is determined by the wavelength of the pump. The electrons then undergo a rapid non-radiative transition to the upper laser level. The population density in the lasing levels, n_2 and n_1, can be changed by stimulated emission and absorption. In addition, the populations in each of the levels above the ground state can change due to non-radiative transitions to the lower levels.

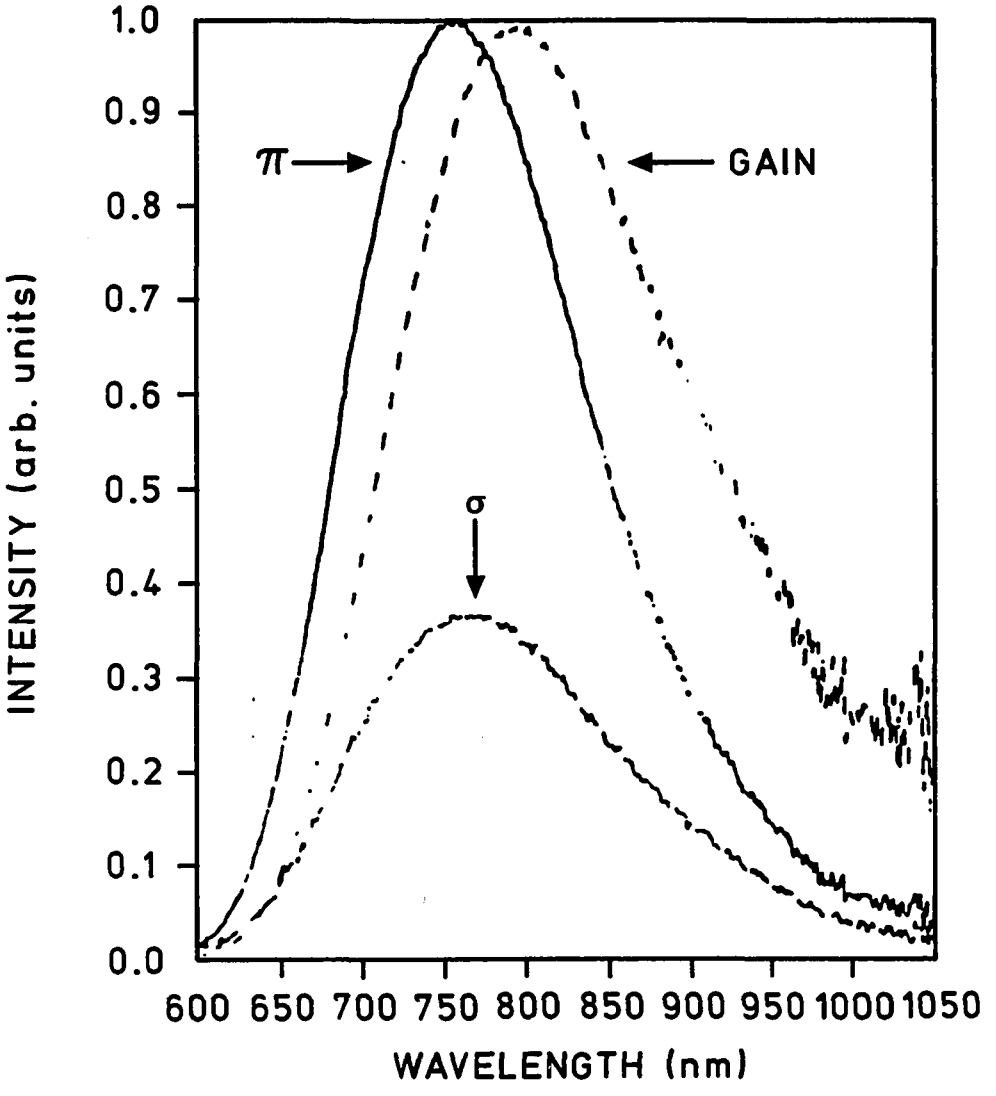

Figure 2.1 Polarized fluorescence spectra and calculated gain line shape for Ti:Al_2O-3.

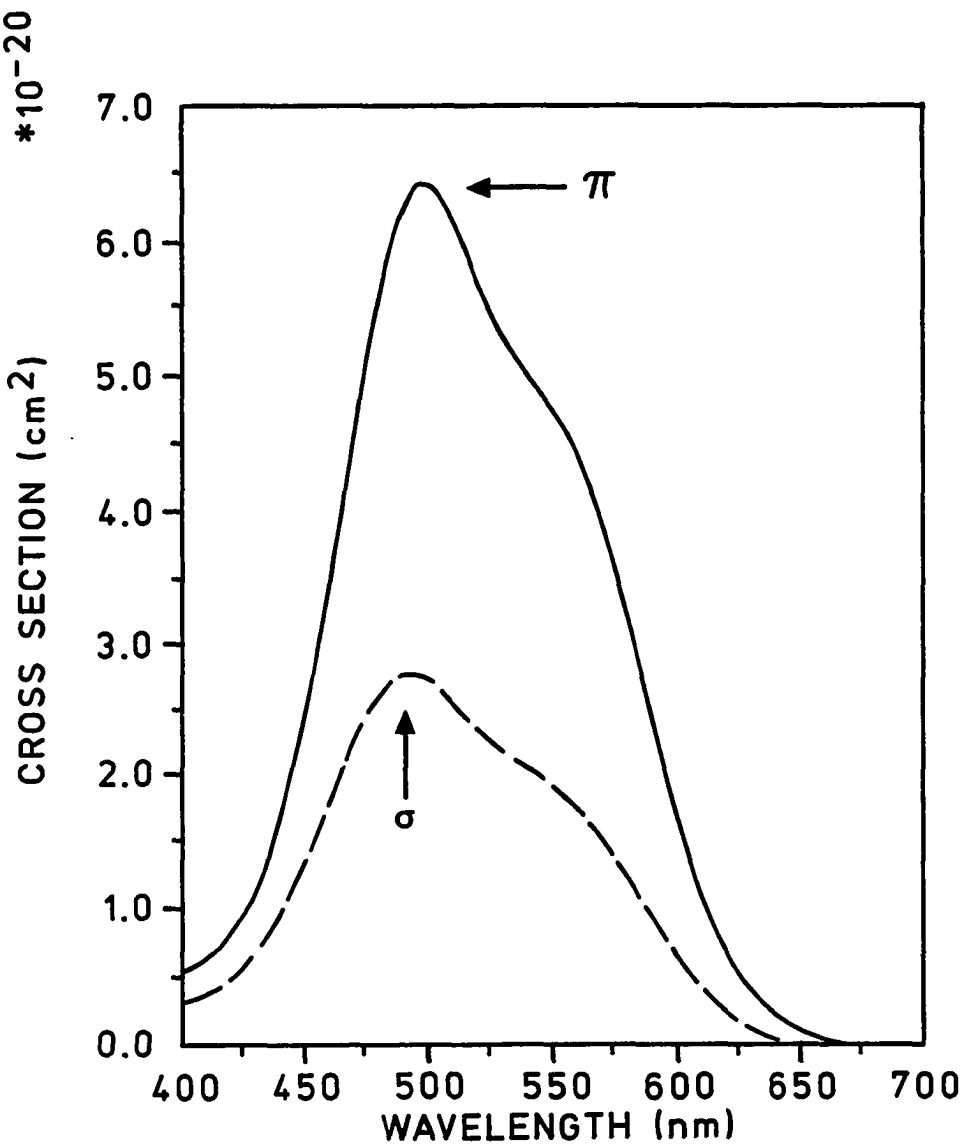

Figure 2.2 Polarized absorption cross sections for the $^2T_2 \rightarrow E$ transition in Ti:Al-20_3.

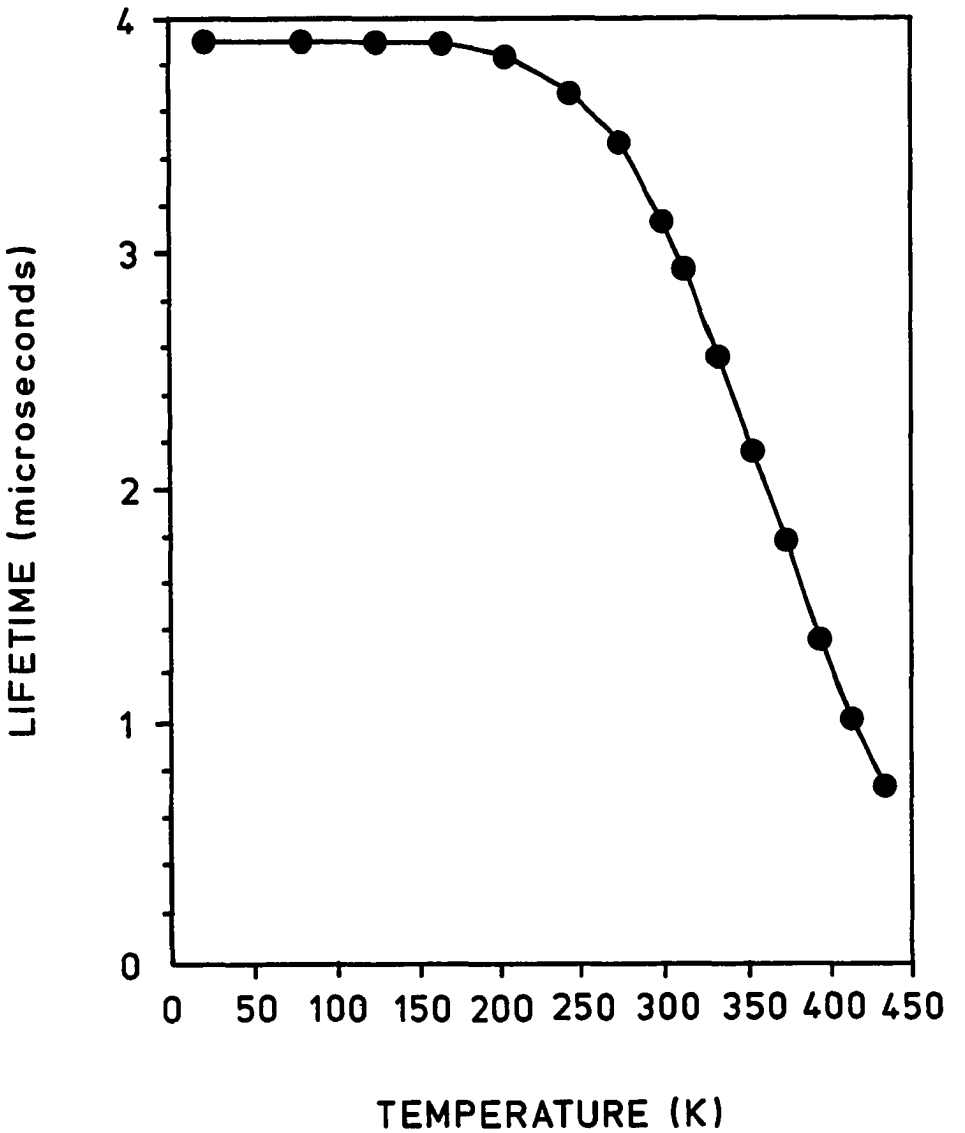

Figure 2.3 Fluorescence lifetime versus temperature for the transition in Ti:Al_2O_3.

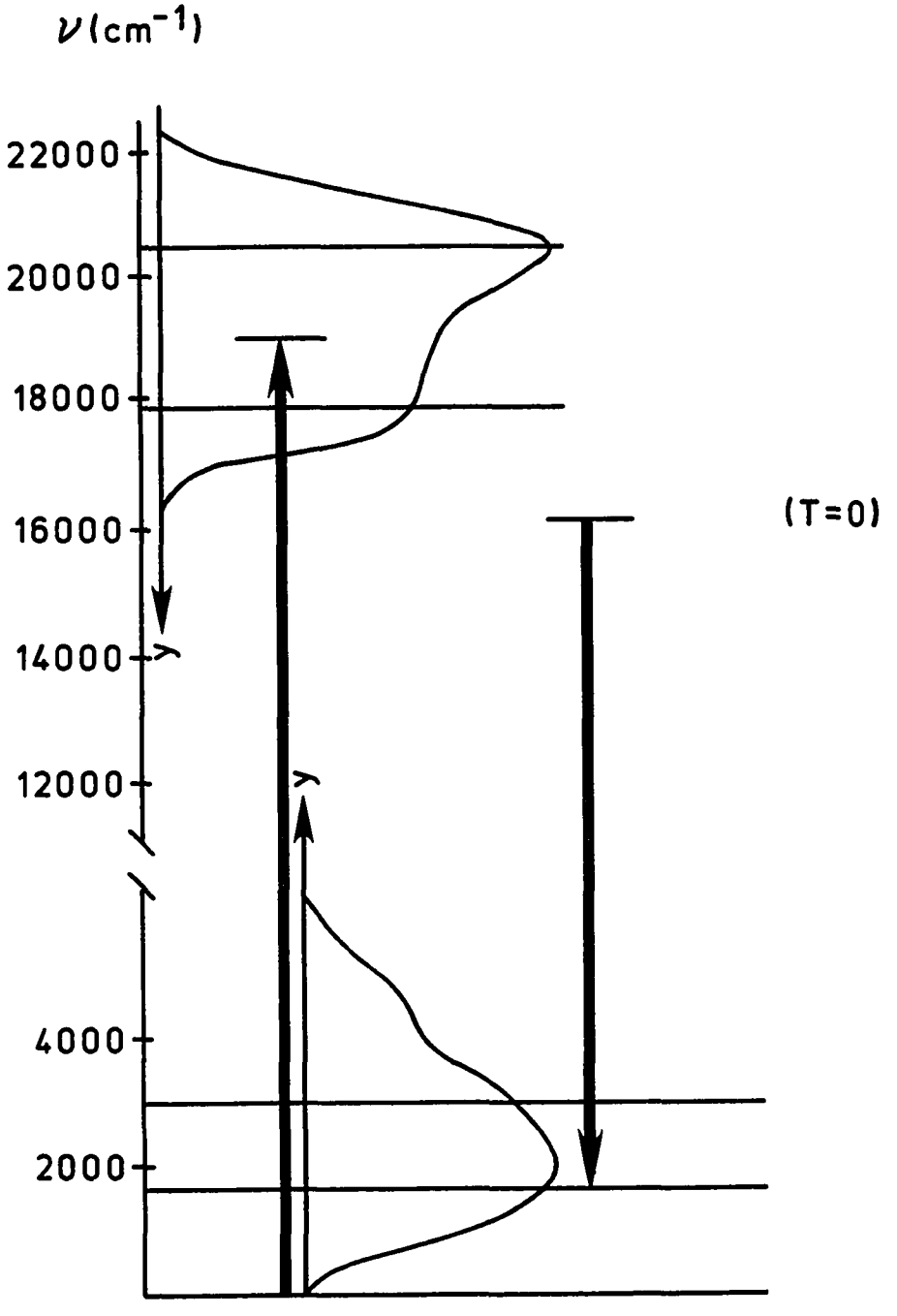

Figure 2.4 Emission and absorption spectra superimposed on an enery level diagram for the t^{3+} ion.

Ground state electrons are pumped to level 3 at a rate

$$W_{o3}(x,t)n_0(x,t)$$

where $W_{03}(x,t)$ is the pumping rate giving the number of photons per second available to pump electrons from the ground state to level 3. The pumped electrons then undergo transitions to the lower levels at a rate

$$\frac{n_3(x,t)}{\tau_{30}} + \frac{n_3(x,t)}{\tau_{31}} + \frac{n_3(x,t)}{\tau_{32}} = \frac{n_3(x,t)}{\tau_3}$$

where $\tau_{30}^{-1}, \tau_{31}^{-1}, \tau_{32}^{1}$ represent the transition rates from level 3 to levels 0, 1, and 2, respectively. Electrons arrive at level 2 at a rate

$$\frac{n_3(x,t)}{\tau_{32}}$$

and are transferred to the lower levels at a rate

$$\frac{n_2(x,t)}{\tau_{21}} + \frac{n_2(x,t)}{\tau_{20}} = \frac{n_2(x,t)}{\tau_2}.$$

The 2 $\rightarrow$ 1 transition is the lasing transition so the population at level 2 is depleted due to induced emission by the quantity

$$\left[n_2(x,t) - \frac{g_2}{g_1}n_1(x,t)\right]\int_0^\infty \sigma(\lambda)F(x,t;\lambda)d\lambda.$$

In this expression g_1 and g_2 are the degeneracies of electronic levels 1 and 2, and $F(x,t;\lambda)$ is the total photon flux in both directions

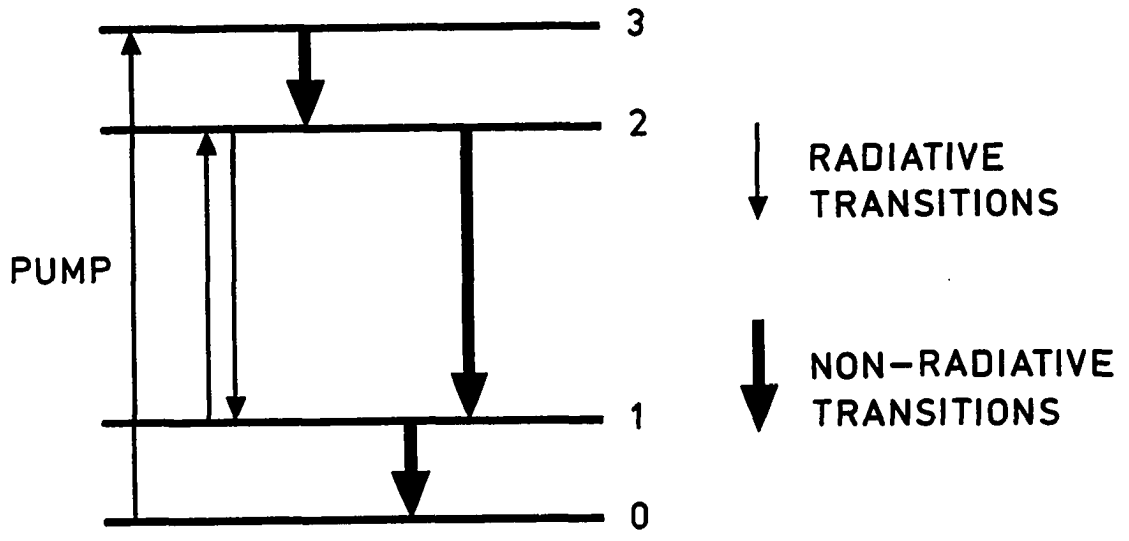

Figure 2.5 Idealized four level model for the lasing action of Titanium in Sapphire. Only those non-radiative transitions to or from the lasing levels are shown.

$$F(x,t;\lambda) = F_+(x,t;\lambda) + F_-(x,t;\lambda).$$

The quantity

$$\int_0^\infty \sigma(\lambda)F(x,t;\lambda)d\lambda$$

represents the probability that stimulated emission will occur. Here, $\sigma(\lambda)$ is the emission cross section. Electrons are transferred to level 1 at the rate

$$\frac{n_3(x,t)}{\tau_{31}} + \frac{n_2(x,t)}{\tau_{21}} + \left[n_2(x,t) - \frac{g_2}{g_2}n_1(x,t)\right]\int_0^\infty \sigma(\lambda)F(x,t;\lambda)d\lambda$$

by transitions from the upper levels and by stimulated emission. The electrons then undergo a decay to level 0 at a rate

$$\frac{n_1(x,t)}{\tau_1} = \frac{n_1(x,t)}{\tau_{10}}.$$

Finally, the ground state is populated via transitions from levels 3,2, and 1 and electrons are lost due to pumping. Hence, the rate equations decribing the rates of change of the population densities in the active medium for each of the electronic levels are given below.

$$\begin{aligned}
\frac{\partial n_3(x,t)}{\partial t} &= W_{03}(x,t)n_0(x,t) - \frac{n_3(x,t)}{\tau_3} \\
\frac{\partial n_2(x,t)}{\partial t} &= \frac{n_3(x,t)}{\tau_{32}} - \frac{n_2(x,t)}{\tau_2}
\end{aligned}$$

$$
\begin{aligned}
& -[n_2(x,t) - \frac{g_2}{g_1} n_1(x,t)] \int_0^\infty \sigma(\lambda) F(x,t;\lambda) d\lambda \qquad (2.1.1) \\
\frac{\partial n_1(x,t)}{\partial t} &= \frac{n_3(x,t)}{\tau_{31}} + \frac{n_2(x,t)}{\tau_{21}} - \frac{n_1(x,t)}{\tau_1} \\
& +[n_2(x,t) - \frac{g_2}{g_1} n_1(x,t)] \int_0^\infty \sigma(\lambda) F(x,t;\lambda) d\lambda \\
\frac{\partial n_0(x,t)}{\partial t} &= \frac{n_3(x,t)}{\tau_{30}} + \frac{n_2(x,t)}{\tau_{21}} + \frac{n_1(x,t)}{\tau_1} - W_{03}(x,t) n_0(x,t)
\end{aligned}
$$

The quantities τ_i and τ_{ij}^{-1} represent the lifetime for the i^{th} level and the transition rate from level i to level j, respectively. They are related by

$$\tau_i^{-1} = \sum_{j=0}^{i-1} \tau_{ij}^{-1} \qquad i = 1,2,3.$$

The population densities are constrained by the relation

$$n_T = n_0(x,t) + n_1(x,t) + n_2(x,t) + n_3(x,t) \qquad (2.1.2)$$

where n_T is the concentration of optically active ions, assumed to be homogeneous throughout the crystal and independent of time. Indeed, equations (2.1.1) give

$$\frac{\partial n_0}{\partial t} + \frac{\partial n_1}{\partial t} + \frac{\partial n_2}{\partial t} + \frac{\partial n_3}{\partial t} = 0.$$

The right hand sides of the equations (2.1.1) account for the changes in the population densities in each of the electronic levels due to both radiative and non-radiative transitions.

The population rate equations can be simplified by making certain assumptions that describe the physical processes in a four-level laser system. The radiationless transition from the pumped level n_3 to the upper lasing level n_2 is fast so the electrons stay at the pumped level for a very short time. Consequently the electrons do not accumulate at the pumped level. Therefore the assumptions

$$\tau_3 \ll \tau_1, \tau_2 \quad , \quad \frac{\partial n_3}{\partial t} = 0, \quad n_3 \ll n_i \text{ for } i = 0,1,2, \text{ and } n_3 \ll n_T.$$

can be made. Under these assumptions, $n_3(x,t)$ can be replaced by $W_{03}(x,t)n_0(x,t)\tau_3$. In addition, the constraint condition (2.1.2) can be approximated by

$$n_T \approx n_0(x,t) + n_1(x,t) + n_2(x,t).$$

It is further assumed that the dominant decay path from the pumped level is the $3 \rightarrow 2$ path so that $\tau_{32} \ll \tau_{31}$ and τ_{30}. Then

$$\frac{1}{\tau_3} = \frac{1}{\tau_{30}} + \frac{1}{\tau_{31}} + \frac{1}{\tau_{32}} \approx \frac{1}{\tau_{32}}$$

so that $\tau_3 \approx \tau_{32}$.

The pumped electrons are transferred to the second level at a rate

$$\frac{n_3(x,t)}{\tau_{32}} \approx W_{03}(x,t)n_0(x,t)\frac{\tau_3}{\tau_{32}} = W(x,t)n_0(x,t)$$

where

$$W(x,t) = W_{03}(x,t)\frac{\tau_3}{\tau_{32}}.$$

The quantity $\eta = \frac{\tau_3}{\tau_{32}}$, called the branching ratio, is expected to be close to unity.

The total decay from level 2 has both radiative and non-radiative contributions which are related by

$$\frac{1}{\tau_2} = \frac{1}{\tau_{f\ell}} + \frac{1}{\tau_{NR}}$$

where $\tau_{f\ell}$ is the fluorescence lifetime for the material and τ_{NR}^{-1} is the rate for the non-radiative transition from level 2. With the assumption that $\tau_{21} \approx \tau_{f\ell}$ and those described above, the equations for the population densities are reduced to

$$\begin{aligned}
\frac{\partial n_2(x,t)}{\partial t} &= W(x,t)n_0(x,t) - \frac{n_2(x,t)}{\tau_2} \\
&\quad -[n_2(x,t) - \frac{g_2}{g_1}n_1(x,t)]\int_0^\infty \sigma(\lambda)F(x,t;\lambda)d\lambda \\
\frac{\partial n_1(x,t)}{\partial t} &= \frac{n_2(x,t)}{\tau_{f\ell}} - \frac{n_1(x,t)}{\tau_1} \\
&\quad +[n_2(x,t) - \frac{g_2}{g_1}n_1(x,t)]\int_0^\infty \sigma(\lambda)F(x,t;\lambda)d\lambda
\end{aligned} \tag{2.1.3}$$

subject to the constraint

$$n_T = n_0(x,t) + n_1(x,t) + n_2(x,t).$$

Equations (2.1.3) can be rewritten in terms of the population inversion $n(x,t)$ which is defined by

$$n(x,t) = n_2(x,t) - \frac{g_2}{g_1} n_1(x,t).$$

Then,

$$\frac{\partial n_1(x,t)}{\partial t} = \frac{n(x,t)}{\tau_{f\ell}} + [\frac{g_2}{g_1} \cdot \frac{1}{\tau_{f\ell}} - \frac{1}{\tau_1}]n_1(x,t) + n(x,t) \int_0^\infty \sigma(\lambda) F(x,t;\lambda) d\lambda$$

and

$$\begin{aligned}
\frac{\partial n(x,t)}{\partial t} &= \frac{\partial n_2(x,t)}{\partial t} - \frac{g_2}{g_1} \frac{\partial n_1(x,t)}{\partial t} \\
&= W(x,t)n_0(x,t) - n(x,t) \int_0^\infty \sigma(\lambda) F(x,t;\lambda) d\lambda - [n(x,t) + \frac{g_2}{g_1} n_1(x,t)] \frac{1}{\tau_2} \\
&- \frac{g_2}{g_1} [\frac{n(x,t)}{\tau_{f\ell}} + [\frac{g_2}{g_1} \cdot \frac{1}{\tau_{f\ell}} - \frac{1}{\tau_1}]n_1(x,t) + n(x,t) \int_0^\infty \sigma(\lambda) F(x,t;\lambda) d\lambda] \\
&= W(x,t)n_0(x,t) + [-\frac{1}{\tau_2} - \frac{g_2}{g_1} \cdot \frac{1}{\tau_{f\ell}}]n(x,t) \\
&+ [-\frac{g_2}{g_1} \cdot \frac{1}{\tau_2} - \frac{g_2}{g_1} (\frac{g_2}{g_1} \cdot \frac{1}{\tau_{f\ell}} - \frac{1}{\tau_1})]n_1(x,t) \\
&- [1 + \frac{g_2}{g_1}]n(x,t) \int_0^\infty \sigma(\lambda) F(x,t;\lambda) d\lambda.
\end{aligned}$$

Now let $\gamma = 1 + \frac{g_2}{g_1}$ and define

$$c_{11} = -\frac{1}{\tau_2} - \frac{(\gamma-1)}{\tau_{fl}}; c_{12} = (1-\gamma)[\frac{1}{\tau_2} + \frac{(\gamma-1)}{\tau_{fl}} - \frac{1}{\tau_1}];$$
$$c_{21} = \frac{1}{\tau_{fl}} \; ; \; c_{22} = \frac{\gamma-1}{\tau_{fl}} - \frac{1}{\tau_1}. \qquad (2.1.4)$$

Then, in terms of the population inversion, equations (2.1.3) can be written as

$$\frac{\partial n(x,t)}{\partial t} = c_{11}n(x,t) + c_{12}n_1(x,t) - \gamma n(x,t)\int_0^\infty \sigma(\lambda)F(x,t;\lambda)d\lambda$$
$$+W(x,t)n_0(x,t) \qquad (2.1.5)$$
$$\frac{\partial n_1(x,t)}{\partial t} = c_{21}n(x,t) + c_{22}n_1(x,t) + n(x,t)\int_0^\infty \sigma(\lambda)F(x,t;\lambda)d\lambda$$

where

$$n_0(x,t) = n_T - \gamma n_1(x,t) - n(x,t).$$

This is the form of the population rate equations that will be used in the subsequent discussion.

2.2 The Photon Equations

In this section the equations that describe the changes in the photon flux as it passes through an active medium are discussed. Consider a one-dimensional flux distribution of photons where the x-axis is taken to be defined by the propagation of the laser beam. At any position in the crystal there will be a flux

in both directions at all wavelengths denoted by $F_+(x,t;\lambda)$ and $F_-(x,t;\lambda)$ for right and left traveling photons, respectively. The active medium is assumed to be homogeneous with refractive index n.

As photons pass through an active medium, their number is changed by interaction with the optically active ions. The equations that account for the increases in photon flux due to spontaneous and stimulated emission and decreases resulting from absorption and scattering losses are obtained as in [23] and are given below.

$$\begin{aligned} \frac{1}{v}\frac{\partial F_+(x,t;\lambda)}{\partial t} &+ \frac{\partial F_+(x,t;\lambda)}{\partial x} = [\sigma(\lambda)n(x,t) - \alpha(\lambda)]F_+(x,t;\lambda) \\ &+ S_+(x,t;\lambda) \\ \frac{1}{v}\frac{\partial F_-(x,t;\lambda)}{\partial t} &- \frac{\partial F_-(x,t;\lambda)}{\partial x} = [\sigma(\lambda)n(x,t) - \alpha(\lambda)]F_-(x,t;\lambda) \\ &+ S_-(x,t;\lambda) \end{aligned} \tag{2.2.1}$$

The left hand sides of equations (2.2.1) represent the net spatial and temporal change in the corresponding photon flux as it propagates through the active medium with velocity $v = \frac{c}{n}$, where c is the speed of light in a vacuum. On the right hand sides, the changes in the photon fluxes brought about by interaction with the material are described. These changes have three components, namely, the contribution to photon fluxes due to spontaneous emission given by $S_\pm(x,t;\lambda)$, increases resulting from stimulated emission described by $\sigma(\lambda)n(x,t)F_\pm(x,t;\lambda)$ and decreases to photon fluxes from absorption and scattering losses given by $\alpha(\lambda)F_\pm(x,t;\lambda)$. $\alpha(\lambda)$ is the absorption coefficient for the material and is a function of wavelength.

The spontaneous emission functions $S_{\pm}(x,t;\lambda)$ can be expressed as a product of three factors

$$S_{\pm}(x,t;\lambda) = \frac{n_2(x,t)}{\tau_{f\ell}} \cdot (8\pi^2 c \frac{\sigma(\lambda)}{\lambda^4} \tau_{f\ell}) \cdot \Omega_{\pm}(x). \qquad (2.2.2)$$

The first factor represents the rate of fluorescent decay from the upper laser level and can be rewritten in terms of the population inversion

$$\frac{n_2(x,t)}{\tau_{f\ell}} = [n(x,t) + \frac{g_2}{g_1} n_1(x,t)] \frac{1}{\tau_{f\ell}}.$$

The second factor in (2.2.2) gives the probability for emission at wavelength λ. The third factor is a geometric factor which gives the fraction of emitted photons which can be considered to contribute to the right or left photon flux. The geometrical term depends on the length ℓ of the crystal and some limiting radius r which defines the field of view of the emitting ion. The latter quantity is taken to be the radius of a cylindrical crystal. The geometrical factors are given by

$$\Omega_{+}(x) = \frac{1}{2}\left[1 - \frac{(\ell - x)}{\sqrt{(\ell - 1)^2 + r^2}}\right]$$

and

$$\Omega_{-}(x) = \frac{1}{2}\left[1 - \frac{x}{\sqrt{x^2 + r^2}}\right].$$

for an Aperature Limited System and by

$$\Omega_+(x;\lambda) = \frac{\Delta\lambda}{4\pi}\left[\frac{n^3}{\pi W_{\text{pump}}}\lambda^2\right]$$

for a Diffraction Limited System [6].

In the remainder of the cavity, the propagation of the right and left traveling fluxes is described by

$$\begin{aligned}\frac{1}{c}\frac{\partial \hat{F}_+(x,t;\lambda)}{\partial t} &+ \frac{\partial \hat{F}_+(x,t;\lambda)}{\partial x} = 0\\ \frac{1}{c}\frac{\partial \hat{F}_+(x,t;\lambda)}{\partial t} &- \frac{\partial \hat{F}_+(x,t;\lambda)}{\partial x} = 0.\end{aligned} \qquad (2.2.3)$$

2.3 The Pump Pulse

The laser system is assumed to be end-pumped so the pumping rate has both space and time dependence. As the pump pulse moves through the crystal, the pumping photons are absorbed by the materials. The equation that describes the propagation of the pump pulse through the material is given below.

$$\frac{1}{v}\frac{\partial W(x,t)}{\partial t} + \frac{\partial W(x,t)}{\partial t} = -\sigma_{ab} n_o(x,t) W(x,t) \qquad (2.3.1)$$

Here, σ_{ab} is the absorption cross section at the pumping wavelength. The expression on the right hand side of (2.3.1) accounts for the absorption of the

pump pulse by the ground state electrons. In terms of the population inversion and the lower laser level population density, (2.3.1) becomes

$$\frac{1}{v}\frac{\partial W(x,t)}{\partial t}+\frac{\partial W(x,t)}{\partial x}=-\sigma_{ab}[n_T-n(x,t)-\gamma n_1(x,t)]W(x,t) \qquad (2.3.2)$$

where n_T and γ are as described previously in Section 2.1

2.4 Normalization

The coupled system of partial differential equations defined by equations (2.1.5) and (2.2.1) constitute the spatial and temporal model of the dynamics of the active medium of the laser. Equations (2.2.3) model the behavior of right and left traveling photon fluxes in the remainder of the cavity.

The dependent variables are normalized by a quantity n_{norm}. Let

$$\begin{aligned} N(x,t) &= \frac{n(x,t)}{n_{\text{norm}}} \\ N_1(x,t) &= \frac{n_1(x,t)}{n_{\text{norm}}} \\ N_0(x,t) &= \frac{n_0(x,t)}{n_{\text{norm}}}=\frac{n_T}{n_{\text{norm}}}-N(x,t)-\gamma N_1(x,t) \end{aligned}$$

be the normalized population concentrations in the crystal.

The photon fluxes are related to the photon concentrations $\phi_{\pm}(x,t;\lambda)$, by

$$v\phi_{\pm}(x,t;\lambda)=F_{\pm}(x,t;\lambda)$$

in the active medium and by

$$c\hat{\phi}_{\pm}(x,t;\lambda) = \hat{F}_{\pm}(x,t;\lambda)$$

in the remainder of the cavity. These quantities are also normalized by n_{norm}, so let

$$\Phi_{\pm}(x,t;\lambda) = \frac{\phi_{\pm}(x,t;\lambda)}{n_{\text{norm}}}$$

be the normalized photon concentration in the active region and $\hat{\Phi}_{\pm}(x,t;\lambda) = \frac{\hat{\phi}_{\pm}(x,t;\lambda)}{n_{\text{norm}}}$ be the normalized photon concentrations in the rest of the cavity. Finally, the time variable is scaled to a standard time interval, τ_{norm}. With these changes, the equations describing the dynamics in the active region become

$$\begin{aligned}
\frac{\partial N(x,t)}{\partial t} &= c_{11}N(x,t) + c_{12}N_1(x,t) - \gamma\beta N(x,t)\int_0^{\infty}\sigma(\lambda)\Phi(x,t;\lambda)d\lambda \\
&\quad + W(x,t)\left[\frac{n_T}{n_{\text{norm}}} - N(x,t) - \gamma N_1(x,t)\right] \\
\frac{\partial N_1(x,t)}{\partial t} &= c_{21}N(x,t) + c_{22}N_1(x,t) + \beta N(x,t)\int_0^{\infty}\sigma(\lambda)\Phi(x,t;\lambda)d\lambda \\
\frac{1}{v\cdot\tau_{\text{norm}}}\frac{\partial\Phi_{\pm}(x,t;\lambda)}{\partial t} &\pm \frac{\partial\Phi_{\pm}(x,t;\lambda)}{\partial x} = [n_{\text{norm}}\sigma(\lambda)N(x,t) \\
&\quad - \alpha(\lambda)]\Phi_{\pm}(x,t;\lambda) \\
&\quad + \frac{1}{v\cdot\tau_{\text{norm}}}S_{\pm}(x,t;\lambda) \qquad (2.4.1)
\end{aligned}$$

where

$$\beta = n_{\text{norm}} \tau_{\text{norm}} v$$

$$\Phi(x,t;\lambda) = \{\Phi_+(x,t;\lambda) + \Phi_-(x,t;\lambda)\}$$

and all other quantities are as described previously. The equation describing the propagation of the pump pulse becomes

$$\frac{1}{v \cdot \tau_{\text{norm}}} \frac{\partial W(x,t)}{\partial t} + \frac{\partial W(x,t)}{\partial x} = -\sigma_{ab} n_{\text{norm}} [\frac{n_T}{n_{\text{norm}}} - N(x,t) - \gamma N_1(x,t)] W(x,t) \tag{2.4.2}$$

Equations (2.4.1) and (2.4.2) are subject to the constraint

$$\frac{n_T}{n_{\text{norm}}} = N_0(x,t) + N(x,t) + \gamma N_1(x,t).$$

In the remainder of the cavity the equations describing the propagation of the normalized photon concentrations are

$$\frac{1}{c \cdot \tau_{\text{norm}}} \frac{\partial \hat{\Phi}_\pm(x,t;\lambda)}{\partial t} \pm \frac{\partial \hat{\Phi}_\pm(x,t;\lambda)}{\partial x} = 0 \tag{2.4.3}$$

2.5 Initial and Boundary Conditions

The initial conditions for the normalized population concentrations in the active region are given below

$$N(x,0) = a_1(x)$$

$$N_1(x,0) = a_2(x)$$

and in the entire cavity, the normalized photon concentrations have the initial profile

$$\Phi_{\pm}(x,0;\lambda) = f_{\pm}(x;\lambda).$$

The pump pulse is initially given by

$$W(x,0) = W(x).$$

If the laser starts from a quiescent state, the upper level population in the crystal and the photons in the entire cavity are negligible, so the quantities $a_1(x), a_2(x), f_{\pm}(x;\lambda)$ would in that case be taken to be zero.

Since the photon concentrations and pump pulse have spatial as well as time derivatives, boundary conditions must also be specified. The boundary conditions describe the optical environment of the laser. The cavity configuration considered here is a simple ring cavity in which the only optical elements are mirrors and the crystal. A schematic diagram is presented in Figure 2.6.

The pump pulse is introduced at the position $x = 0$ and the positive direction is taken to be the clockwise direction in the cavity. The length of the crystal is ℓ and the cavity has length L. Mirrors are located at positions L_1, L_2, and L_3 and have corresponding reflection and transmission coefficients R_i and T_i for $i = 1,2,3$. The crystal has surface reflection and transmission parameters, T_s and R_s, called the Fresnel coefficients for the material. R_s is given by

$$R_s = \frac{(n-1)^2}{(n+1)^2}$$

and so

$$\begin{aligned} T_s &= 1 - R_s \\ &= \frac{4n}{(n+1)^2} \end{aligned}$$

where n is the index of refraction.

The mirror at $x = L_1$ is taken to be an output coupler and at this position an injection signal, $I_{\pm}(t;\lambda)$, may be introduced in the system in either direction.

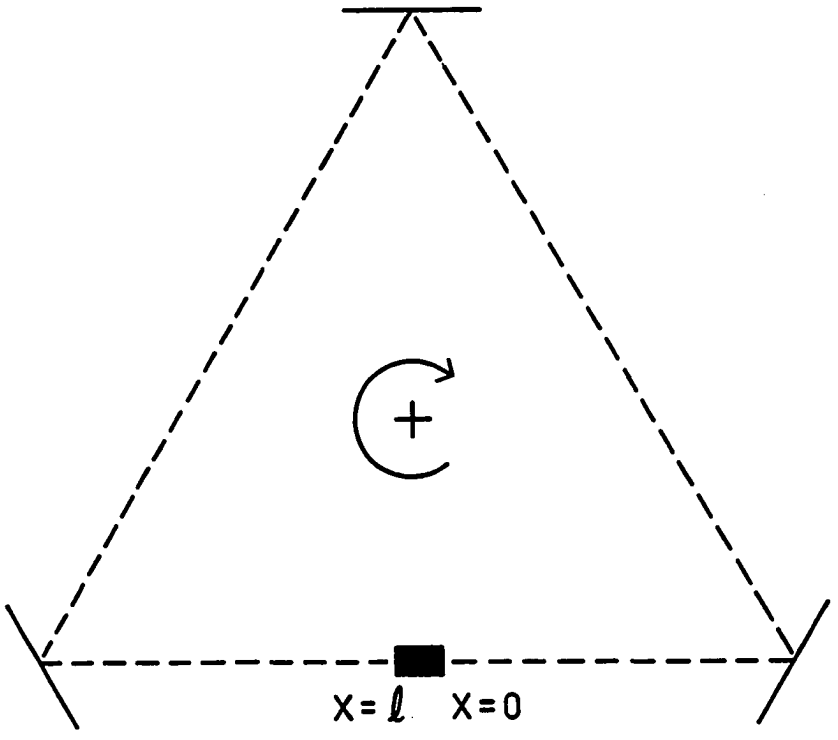

Figure 2.6 A schematic diagram of a simple ring laser cavity. The laser rod has length ℓ and is end pumped (at x=0). Mirrors are located at $x=L_1$, $x = L-2$, and $x = L_3$. The clockwise direction is taken to be positive.

Boundary conditions that describe the optical configuration described above are as follows

$$\Phi_+(0+,t;\lambda) = T_s\hat{\Phi}_+(L-,t;\lambda) + R_s\Phi_-(0+,t;\lambda)$$

$$\hat{\Phi}_-(L-,t;\lambda) = T_s\Phi_-(0+,t;\lambda) + R_s\hat{\Phi}_+(L-,t;\lambda)$$

$$\Phi_-(\ell-,t;\lambda) = T_s\hat{\Phi}_-(\ell+,t;\lambda) + R_s\Phi_+(\ell-,t;\lambda)$$

$$\hat{\Phi}_+(\ell+,t;\lambda) = T_s\Phi_+(\ell-,t;\lambda) + R_S\hat{\Phi}_-(\ell+,t;\lambda)$$

$$\hat{\Phi}_+(L_1+,t;\lambda) = R_1\hat{\Phi}_+(L_1^-,t;\lambda) + I_+(t;\lambda)$$

$$\hat{\Phi}_-(L_1-,t;\lambda) = R_1\hat{\Phi}_-(L_1^+,t;\lambda) + I_-(t;\lambda)$$

$$\hat{\Phi}_+(L_2+,t;\lambda) = R_2\hat{\Phi}_+(L_2^-,t;\lambda)$$

$$\hat{\Phi}_-(L_2-,t;\lambda) = R_2\hat{\Phi}_-(L_2^+,t;\lambda)$$

$$\hat{\Phi}_+(L_3+,t;\lambda) = R_3\hat{\Phi}_+(L_3^-,t;\lambda)$$

$$\hat{\Phi}_-(L_3-,t;\lambda) = R_3\hat{\phi}_-(L_3^+,t;\lambda).$$

The initial and boundary value problem defined by the above conditions and equations (2.4.1), (2.4.2),(2.4.3) are the subject of the present study.

Chapter 3

Analysis of the Spatially Averaged Model

3.1 The Spatially Averaged Model

In this section, the rate equations (2.4.1) are simplified by a heuristic derivation of a model in which the population and photon concentrations are averaged over the spatial variable. For simplicity, only those photons at a particular wavelength, $\bar{\lambda}$, wil be considered. Without loss of generality, the pump pulse is assumed to have a specified temporal dependence, $W_p(t)$. It is further assumed that $n_{\text{norm}} = n_T$ and that the material is homogeneous so that emission and absorption properties of the materials do not depend on the spatial variable. As in [23] the average is taken over the length of the active medium.

Incorporating these assumptions into the population equations, they are formally integrated over the length of the active medium to obtain

$$
\begin{aligned}
\frac{d}{dt}\left\{\frac{1}{\ell}\int_0^{\ell} N(x,t)dx\right\} &= c_{11}\left\{\frac{1}{\ell}\int_0^{\ell} N(x,t)dx\right\} \\
&+ c_{12}\left\{\frac{1}{\ell}\int_0^{\ell} N_1(x,t)dx\right\} \\
&\quad -\gamma\beta\sigma\left\{\frac{1}{\ell}\int_0^{\ell} N(x,t)\Phi(x,t)dx\right\} \\
&+ W_p(t)\left\{\frac{1}{\ell}\int_0^{\ell}[1-N(x,t)-\alpha N_1(x,t)]dx\right\} \\
\frac{d}{dt}\left\{\frac{1}{\ell}\int_0^{\ell} N_1(x,t)dx\right\} &= c_{21}\left\{\frac{1}{\ell}\int_0^{\ell} N(x,t)dx\right\} \\
&+ c_{22}\left\{\frac{1}{\ell}\int_0^{\ell} N_1(x,t)dx\right\} \\
&\quad +\beta\sigma\left\{\frac{1}{\ell}\int_0^{\ell} N(x,t)\Phi(x,t)dx\right\} \qquad (3.1.1)
\end{aligned}
$$

where σ is the emission cross section at $\bar{\lambda}$ and all other parameters are as discussed previously.

The photon concentration equations are added, giving

$$
\begin{aligned}
\frac{1}{v\cdot\tau_{\text{norm}}}\frac{\partial\Phi(x,t)}{\partial t} &+ \frac{\partial}{\partial x}[\Phi_+(x,t)-\Phi_-(x,t)] \\
&= [n_{\text{norm}}\sigma N(x,t)-\alpha]\,\Phi(x,t) \\
&+ \frac{1}{v\cdot\tau_{\text{norm}}}[S_+(x,t)+S_-(x,t)]\,. \qquad (3.1.2)
\end{aligned}
$$

Here, α is the absorption coefficient at $\bar{\lambda}$. Integrating (3.1.2) over the length of the active medium yields

$$\frac{\ell}{v \cdot \tau_{\text{norm}}} \frac{d}{dt}\left\{\frac{1}{\ell}\int_0^{\ell}\Phi(x,t)dx\right\} + [\Phi_+(\ell,t) - \Phi_-(\ell,t)] - [\Phi_+(0,t) - \Phi_-(0,t)]$$
$$= \ell\beta\sigma\left\{\frac{1}{\ell}\int_0^{\ell}N(x,t)\Phi(x,t)dx\right\} \qquad (3.1.3)$$
$$- \alpha\ell\left\{\frac{1}{\ell}\int_0^{\ell}\Phi(x,t)dx\right\}$$
$$+ \frac{\ell}{v \cdot \tau_{\text{norm}}}\left\{\frac{1}{\ell}\int_0^{\ell}[S_+(x,t) + S_-(x,t)]\,dx\right\}$$

The term $[S_+(x,t) + S_-(x,t)]$ is the contribution to the photon concentration in the laser beam coming from spontaneous emission of the excited electron. The spatial average $\frac{1}{\ell}\int_0^{\ell}[S_+(x,t) + S_-(x,t)]\,dx$ is expressed as a fraction Sp_0 of the total fluorescence decay rate, $\tau_{f\ell}$, so that

$$\frac{1}{\ell}\int_0^{\ell}[S_+(x,t) + S_-(x,t)]\,dx = \frac{Sp_0}{\tau_{f\ell}}\left\{\frac{1}{\ell}\int_0^{\ell}N(x,t)dx + \frac{(\gamma-1)}{\ell}\int_0^{\ell}N_1(x,t)dx\right\}$$
$$= c_{31}\left\{\frac{1}{\ell}\int_0^{\ell}N(x,t)dx\right\} + c_{32}\left\{\frac{1}{\ell}\int_0^{\ell}N_1(x,t)dx\right\}$$

where $c_{31} = \frac{Sp_0}{\tau_{f\ell}}$, $c_{32} = \frac{(\gamma-1)Sp_0}{\tau_{f\ell}}$, and Sp_0 depends on the geometry of the laser cavity and on the fluorescence spectrum of the lasing ion [5]

The following approximation is also made [23]

$$\frac{1}{\ell}\int_0^{\ell} N(x,t)\Phi(x,t)dx \approx \left\{\frac{1}{\ell}\int_0^{\ell} N(x,t)dx\right\}\cdot\left\{\frac{1}{\ell}\int_0^{\ell}\Phi(x,t)dx\right\}.$$

Boundary conditions that account for the presence of the mirrors in the ring laser cavity are also incorporated:

$$\begin{aligned}\Phi_-(\ell^-,t) &= R_1R_2R_3T_s\hat{\Phi}_-(\ell^+,t)\\ \Phi_+(0^+,t) &= R_1R_2R_3T_s\hat{\Phi}_+(L^-,t).\end{aligned}$$

Equation (3.1.3) can now be written as

$$\begin{aligned}\frac{d}{dt}\{\frac{1}{\ell}\int_0^{\ell}\Phi(x,t)dx\} &= \frac{-v\cdot\tau_{\text{norm}}}{\ell}\left\{[\Phi_+(\ell^-,t)-R_1R_2R_3T_s\hat{\Phi}_-(\ell^+,t)]\right.\\ &\quad\left.+[\Phi_-(0^+,t)-R_1R_2R_3T_s\hat{\Phi}_+(L^-,t)]\right\}\\ &- \alpha v\cdot\tau_{\text{norm}}\left\{\frac{1}{\ell}\int_0^{\ell}\Phi(x,t)dx\right\}+\beta\sigma\left\{\frac{1}{\ell}\int_0^{\ell}N(x,t)dx\right\}\\ &\quad\left\{\frac{1}{\ell}\int_0^{\ell}\Phi(x,t)dx\right\}\\ &+ c_{31}\left\{\frac{1}{\ell}\int_0^{\ell}N(x,t)dx\right\}+c_{32}\left\{\frac{1}{\ell}\int_0^{\ell}N(x,t)dx\right\}.\end{aligned}$$

The first expression on the right hand side can be considered in the following way. In terms of a standard time scale, τ_{norm}, the photon concentration in each direction is related to the corresponding photon flux by

$$v \cdot \tau_{\text{norm}} \Phi_{\pm}(x,t) = F_{\pm}(x,t)$$

so that

$$\begin{aligned} v \cdot \tau_{\text{norm}} \{ & [\Phi_{+}(\ell^{-},t) - R_1 R_2 R_3 T_s \Phi_{-}(\ell^{+},t)] \\ & + [\Phi_{-}(0^{+},t) - R_1 R_2 R_3 T_s \Phi_{+}(L^{-},t)] \} \\ & = [F_{+}(\ell,t) - R_1 R_2 R_3 T_s F_{-}(\ell,t)] \\ & + [F_{-}(0,t) - R_1 R_2 R_3 T_s F_{+}(0,t)] \\ & = F_{\text{out}}(t) \end{aligned}$$

where $F_{\text{out}}(t)$ is the total flux coming from the crystal. Now, $F_{\text{out}}(t)$ may be written [23]

$$F_{\text{out}}(t) = \ell \left\{ \frac{1}{\ell} \int_0^{\ell} F(x,t) dx \right\} \alpha_{rad}$$

where α_{rad} is the coefficient giving the fraction of photons lost due to radiation from the crystal.

Thus equation (3.1.3) can rewritten

$$\begin{aligned}\frac{d}{dt}\left\{\frac{1}{\ell}\int_0^{\ell}\Phi(x,t)dx\right\} &= c_{31}\left\{\frac{1}{\ell}\int_0^{\ell}N(x,t)dx\right\}\\ &+ c_{32}\left\{\frac{1}{\ell}\int_0^{\ell}N(x,t)dx\right\}\\ &+ c_{33}\left\{\frac{1}{\ell}\int_0^{\ell}\Phi(x,t)dx\right\}\\ &+ \beta\sigma\left\{\frac{1}{\ell}\int_0^{\ell}\Phi(x,t)dx\right\}\left\{\frac{1}{\ell}\int_0^{\ell}N_1(x,t)dx\right\}\end{aligned}$$

where $c_{33} = -v \cdot \tau_{\text{norm}}[\alpha_{rad} + \alpha]$ represents the fraction of photons lost by all mechanisms in the cavity including losses due to absorption, scattering, and reflection. Since a photon will have some average lifetime in the cavity before being lost by the above mechanisms, it is convenient to express the losses in terms of the cavity lifetime, τ_c, where

$$c_{33} = -\frac{1}{\tau_c}$$

and $\tau_c = \frac{2L}{c \cdot \tau_{\text{norm}}}[2\alpha\ell + \ell_m - \ln(R_1R_2R_3T_S^4)]^{-1}$ ([12], [6]) for the ring laser cavity described in Chapter 2. Here, ℓ_m represents miscellaneous losses due to scattering and absorption by the optical elements in the cavity. All other parameters are as previously defined.

If the laser system is injection seeded, then an accounting for the photons which are introduced to the system in this way must be made. In the spatial and temporal model, this accounting was made by introducing photons at an appropriate boundary. For the spatially averaged model, the contribution from

injection seeding is assumed to have a specified temporal distribution, I(t), that gives the number of photons per time unit introduced by an injected signal.

Now let

$$\begin{aligned} n(t) &= \frac{1}{\ell}\int_0^{\ell} N(x,t)dx \\ n_1(t) &= \frac{1}{\ell}\int_0^{\ell} N_1(x,t)dx \\ \phi(t) &= \frac{1}{\ell}\int_0^{\ell} \Phi(x,t)dx. \end{aligned}$$

Then the spatial and temporal model given in (2.4.1) is reduced to the nonlinear system of ordinary differential equations

$$\begin{aligned} \frac{dn(t)}{dt} &= c_{11}n(t) + c_{12}n_1(t) - \gamma\beta\sigma n(t)\phi(t) + W_p(t)[1 - n(t) - \gamma n_1(t)] \\ \frac{dn_1(t)}{dt} &= c_{21}n(t) + c_{22}n_1(t) + \beta\sigma n(t)\phi(t) \\ \frac{d\phi(t)}{dt} &= c_{31}n(t) + c_{32}n_1(t) + c_{33}\phi(t) + \beta\sigma n(t)\phi(t) + I(t) \end{aligned} \qquad (3.1.4)$$

The remainder of this chapter deals with the qualitative and numerical analysis of the initial value problem defined by (3.1.4) subject to the initial conditions

$$\begin{aligned} n(0) &= a_1 \\ n_1(0) &= a_2 \\ \phi(0) &= a_3 \quad \text{where} \quad a_i \geq 0 \qquad (i = 1,2,3). \end{aligned} \qquad (3.1.5)$$

3.2 Qualitative Properties of the Solutions

This section establishes a number of qualitative properties of the solutions to the system (3.1.5). Throughout this section the material parameters are assumed to satisfy

$$0 < \tau_1 << \tau_2 < \tau_{fl}$$

$$0 \leq Sp_0$$

$$0 < \tau_c$$

$$1 < \gamma.$$

Theorem 1 *Let $W_p(t) > 0$ and $I(t) \geq 0$ be continuous functions on $[0, +\infty)$. If $n(0) \geq 0, n_1(0) \geq 0$, and $\phi(0) \geq 0$, then*

(i) if $n(0) + \gamma n_1(0) < 1$, then $n(t) + \gamma n_1(t) < 1$ for all t;

(ii) if $n(0) + \gamma n_1(0) \geq 1$, then there exists T such that $n(t) + \gamma n_1(t) < 1$ for all $t > T$;

(iii) $n(t) \geq 0, n_1(t) \geq 0$, and $\phi(t) \geq 0$ for all t.

Theorem 2 *Let $Wp(t)$ and $I(t)$ satisfy the conditions in Theorem 3.1.*

(i) If $W_p(t)$ and $I(t)$ are integrable on $[0, +\infty)$, then $n(t), n_1(t)$, and $\phi(t)$ are integrable on $[0, +\infty)$.

(ii) If $W_p(t)$ and $I(t)$ are bounded on $[0,+\infty)$, then $n(t), n_1(t)$ and $\phi(t)$ are bounded on $[0,+\infty)$.

Proof of Theorem 1:

(i) Since $n(0)+\gamma n_1(0) < 1$, then by continuity, $n(t)+\gamma n_1(t) < 1$ for t close to zero. Suppose there exists T such that $n(T)+\gamma n_1(T) = 1$ and $n(t)+\gamma n_1(t) < 1$ for $t < T$.

Then, at $t = T$,

$$\frac{d}{dt}(n+\gamma n_1) = (c_{11}+\gamma c_{21})n + (c_{12}+\gamma c_{22})n_1 > 0. \qquad (3.2.1)$$

Suppose $n(T) \geq 0$ and $n_1(T) \geq 0$. Now $n(T)+\gamma n_1(T) = 1$ so not both $n(T)$ and $n_1(T)$ are zero. Also, $c_{11}+\gamma c_{21} < 0$ and $c_{12}+\gamma c_{22} < 0$.

So, at $t = T$,

$$\frac{d}{dt}(n+\gamma n_1) < 0$$

which is a contradiction to (3.2.1).

Now suppose that $n_1(T) < 0$. Since $n_1(0) \geq 0$, there exists $T_1 < T$ such that $n_1(T_1) = 0$ and $n_1(t) \geq 0$ for $0 \leq t \leq T_1$.

Then, at $t = T_1$,

$$\begin{aligned} \frac{dn_1}{dt} &= c_{21}n + \beta\sigma n\phi \\ &= (c_{21}+\beta\sigma\phi)n \\ &\leq 0 \end{aligned}$$

Suppose $n(T_1) < 0$ and $c_{21} + \beta\sigma\phi(T_1) \geq 0$. Then there exists $T_2 < T_1$, such that $n(T_2) = 0$ and $n(t) \geq 0$ for $0 \leq t \leq T_2$. At $t = T_2$,

$$\begin{aligned} \frac{dn}{dt} &= c_{12}n_1(T_2) + W_p(T_2)(1 - \gamma n_1(T_2)) \\ &> 0 \end{aligned}$$

since $c_{12} > 0, n_1(T_2) \geq 0, W_P(T_2) > 0$, and $1 - \gamma n_1(T_2) > 0$. Hence n increases to the right of T_2 and so $n(t)$ cannot be negative for $0 \leq t \leq T_1$. Therefore, $n(T_1) \geq 0$.

Now suppose $c_{21} + \beta\sigma\phi(T_1) \leq 0$. Since $c_{21} > 0$ and $\beta\sigma > 0$, it follows that $\phi(T_1) < 0$. Then there exists $T_3 < T_1$ such that $\phi(T_3) = 0$ and $\phi(t) \geq 0$ for $0 \leq t \leq T_3$. So, at $t = T_3$

$$\begin{aligned} \frac{d\phi}{dt} &= c_{31}n + c_{32}n_1 + I(T_3) \\ &\geq 0 \end{aligned}$$

since $I(T_3) \geq 0$ and all other quantities are nonnegative. If $I(T_3) > 0$, then $\phi(t)$ increases to the right of T_3 so it follows that $\phi(T_1) \geq 0$. If $I(T_3) = 0$ and at least one of $n(T_3)$ or $n_1(T_3)$ is positive, then $\phi(t)$ increases to the right of T_3 and so $\phi(T_1) \geq 0$. If $I(T_3) = 0$ and both $n(T_3)$ and $n_1(T_3)$ are zero, then at $t = T_3$,

$$\frac{d^2\phi}{dt^2} = c_{31}W_p(T_3) > 0$$

since $c_{31} > 0$ and $W_p(T_3) > 0$. Therefore ϕ increases to the right of T_3 and in this case it is also true that $\phi(T_1) \geq 0$.

Suppose $n(T_1) = 0$ so that at $t = T_1$,

$$\frac{dn_1}{dt} = 0.$$

Then, at $t = T_1$,

$$\frac{dn}{dt} = W_p(T_1) > 0.$$

In addition, at $t = T_1$,

$$\begin{aligned} \frac{d^2n}{dt^2} &= c_{21}\frac{dn}{dt} + c_{22} = \frac{dn_1}{dt} + \beta\sigma\left[\phi\frac{dn}{dt} + n\frac{d\phi}{dt}\right] \\ &= c_{21}W_p(T_1) + \beta\sigma\phi(T_1)W_p(T_1) \\ &> 0 \end{aligned}$$

since $c_{21} > 0, W_p(T_1) > 0, \beta\sigma > 0$ and $\phi(T_1) \geq 0$. Therefore n_1 increases to the right of T_1. It follows that $n_1(t) \geq 0$.

Suppose now that $n(T) < 0$. Choose $T_1 < T$ such that $n(T_1) = 0$ and $n(t) \geq 0$ for $0 \leq t \leq T_1$. Then at $t = T_1$,

$$\begin{aligned} \frac{dn}{dt} &= c_{21}n_1 + W_p(T_1)(1 - \gamma n_1) \\ &> 0 \end{aligned}$$

since $c_{21} > 0, n_1(T_1) \geq 0, W_p(T_1) > 0$ and $1 - \gamma n_1(T_1) > 0$. Hence n increases to the right of T_1. Therefore $n(T) \geq 0$.

The above argument shows that at least one of $n(T)$ or $n_1(T)$ is strictly positive, so at $t = T$,

$$\frac{d}{dt}(n + \gamma n_1) < 0$$

which is a contradiction to (3.2.1). Thus, for all t, $n(t) + \gamma n_1(t) < 1$.

(ii) The proof of (i) shows that if $n(0) + \gamma n_1(0) = 1$, then $n(t) + \gamma n_1(t) < 1$ for all t> 0

Suppose $n(0) + \gamma n_1(0) > 1$. Then, for t close to zero,

$$\begin{aligned} \frac{d}{dt}(n + \gamma n_1) &= (c_{11} + \gamma c_{21} n) + (c_{12} + \gamma c_{22}) n_1 \\ &< 0 \end{aligned}$$

since $c_{11} + \gamma c_{21} < 0$ and $c_{12} + \gamma c_{22} < 0$. Thus $n + \gamma n_1$ is decreasing for t close to zero.

Suppose there exists $\xi \geq 1$ such that $(n + \gamma n_1) \geq \xi \geq 1$ for all t. Then

$$\begin{aligned} \frac{d}{dt}(n + \gamma n_1) &= (c_{11} + \gamma c_{21})(n + \gamma n_1) + (c_{12} + \gamma c_{22} - \gamma(c_{11} + \gamma c_{21})) n_1 \\ &\leq (c_{11} + \gamma c_{21}) \xi \end{aligned}$$

since $c_{12} + \gamma c_{22} - \gamma(c_{11} + \gamma c_{21}) < 0$ and $c_{11} + \gamma c_{21} < 0$. But then

$$n(t) + \gamma n_1(t) - [n(0) + \gamma n_1(0)] \leq (c_{11} + \gamma c_{21})\xi t$$

or

$$n(t) + \gamma n_1(t) \leq [n(0) + \gamma n_1(0)] + (c_{11} + \gamma c_{21})\xi t.$$

Thus, it follows that

$$\lim_{t \to +\infty} [n(t) + \gamma n_1(t)] = -\infty$$

which contradicts $n + \gamma n_1 \geq \xi \geq 1$ for all t.

Hence, there exists T such at $n(t) + \gamma n_1(T) = 1$ and $n(t) + \gamma n_1(t) < 1$ for t close to T. The analysis used to prove (i) now applies to show that $n(t)+\gamma n_1(t) <$ 1. for all $t > T$.

(iii) The arguments in (i) show that n and n_1 are nonnegative on an interval where $n + \gamma n_1 < 1$. Hence, if $n(0) + \gamma n_1(0) \leq 1$, then $n(t) \geq 0$ and $n_1(t) \geq 0$ for all t.

Suppose there exists T such that $n(t) \geq 0$ and $n_1(t) \geq 0$ for $0 \leq t \leq T$ and $\phi(T) < 0$. Then choose $T_1 < T$ such that $\phi(T_1) = 0$. At $t = T_1$,

$$\begin{aligned}\frac{d\phi}{dt} &= c_{31} + c_{32}n_1 + I(T_1) \\ &\geq 0\end{aligned}$$

since $c_{31} \geq 0, c_{32} \geq 0, n(T_1) \geq 0, n_1(T_1) \geq 0$ and $I(T_1) \geq 0$. Hence, ϕ is nondecreasing to the right of T_1, which contradicts $\phi(T) < 0$. thus, $\phi(t) \geq 0$ for all t.

Finally, suppose $n(0) + \gamma n_1(0) > 1$. Choose T such that $n(T) + \gamma n_1(T) = 1$ and $n(t) + \gamma n_1(t) < 1$ for $0 \leq t \leq T$. Suppose $n(T_1) < 0$ for some $T_1 < T$. Then there exist $T_2 < T_1$ such that $n(T_2) = 0$ and $n(t) \geq 0$ for $0 \leq t \leq T_2$. Then at $t = T_2$

$$\begin{aligned}\frac{dn}{dt} &= c_{12}n_1 + W_p(1 - \gamma n_1) \\ &> c_{12}n_1\end{aligned}$$

since $W_p(T_2) > 0$ and $1 - \gamma n_1(T_2) > 0$.

If $n_1(T_2) < 0$ then there exist $T_3 < T_2$ such that $n_1(T_3) = 0$ and $n_1(t) \geq 0$ for $0 \leq t \leq T_3$.

Then at $t = T_3$

$$\begin{aligned}\frac{dn_1}{dt} &= (c_{21} + \beta\sigma\phi)n \\ &\geq 0\end{aligned}$$

since $c_{21} > 0, \beta\sigma > 0$, and $\phi(T_3) \geq 0$.

If $n(T_3) = 0$, then at T_3

$$\begin{aligned} \frac{d^2 n_1}{dt^2} &= c_{21} W_p(T_3) + \beta\sigma\phi(T_3) \\ &> 0. \end{aligned}$$

Therefore n_1 increases to the right of T_3.

If $n(T_3) > 0$, then at T_3

$$\frac{dn_1}{dt} > 0.$$

Therefore, in either case n_1 increases to the right of T_3. Hence $n_1(t) \geq 0$ for all t.

Thus at $t = T_2$

$$\begin{aligned} \frac{dn}{dt} &> c_{21} n_1 \\ &\geq 0. \end{aligned}$$

Therefore n is nondecreasing to the right of T_2. Hence, $n(t) \geq 0$ for all t.

Proof of Theorem 2:

(i) Fix T so that $n(t) + \gamma n_1(t) < 1$ for $t > T$. Then for $t > T$,

$$\begin{aligned}\frac{d}{dt}(n+\gamma n_1) &= (c_{11}+\gamma c_{21})(n+\gamma n_1)\\ &+ (c_{12}+\gamma c_{22}-\gamma(c_{11}+\gamma c_{21}))n_1\\ &+ W_p(1-n-\gamma n_1)\\ &\leq (c_{11}+\gamma c_{21})(n+\gamma n_1)\\ &+ W_p(1-n-\gamma n_1)]\end{aligned}$$

since $c_{21}+\gamma c_{22}-\gamma(c_{11}-\gamma c_{21})<0$ and $n_1(t)\geq 0$. Hence

$$\frac{d}{dt}\left(e^{\int_T^t[W_p-c_{11}-\gamma c_{21}]dt'}(n+\gamma n_1)\right)\leq e^{\int_T^t[W_p-c_{11}-\gamma c_{21}]dt'}W_p.$$

Thus,

$$\begin{aligned}e^{\int_T^t[W_p-c_{11}-\gamma c_{21}]dt'}(n+\gamma n_1)-[n(T)-\gamma n_1(T)]\\ \leq \int_T^t e^{\int_t^u[W_p-c_{11}-\gamma c_{21}]dt}W_p(u)du.\end{aligned}$$

It folllows that

$$\begin{aligned}0\leq n+\gamma n_1 &\leq e^{-\int_T^t[W_p-c_{11}-\gamma c_{21}]dt'}\int_T^t e^{\int_T^u[W_p-c_{11}-\gamma c_{21}]dt'}W_p(u)du\\ &+ e^{-\int_T^t[W_p-c_{11}-\gamma c_{21}]dt'}[n(T)+\gamma n_1(T)]\\ &= \int_T^t e^{-\int_u^t[W_p-c_{11}-\gamma c_{21}]dt'}W_p(u)du\\ &+ e^{-\int_T^t[W_p-c_{11}-\gamma c_{21}]dt'}[n(T)+\gamma n_1(T)]\end{aligned}$$

Hence

$$\begin{aligned} 0 &\leq \int_T^S [n(t) + \gamma n_1(t)]dt \\ &\leq \int_T^s \int_T^t e^{-\int_u^t [W_p - c_{11} - \gamma c_{21}]dt'} W_p(u)dudt \\ &+ \int_T^s e^{-\int_T^t [W_p - c_{11} - \gamma c_{21}]dt'} [n(T) + \gamma n_1(T)dt. \end{aligned}$$

Note that $e^{-\int_u^t W_p dt'} \leq 1$ since $W_p(t) > 0$ for all t.

Therefore,

$$\begin{aligned} 0 &\leq \int_T^s [n(t) + \gamma n_1(t)]dt \\ &\leq \int_T^s W_p(u) \int_u^s e^{[c_{11} + \gamma c_{21}](t-u)} dudt \\ &\quad + \int_T^s e^{[c_{11} - \gamma c_{21}](t-T)} [n(T) + \gamma n_1(T)]dt \\ &= \int_T^s W_p(u) \left[\frac{e^{[c_{11} + \gamma c_{21}](s-u)} - 1}{c_{11} + \gamma c_{21}} \right] du \\ &\quad + [n(T) + \gamma n_1(T)] \left[\frac{e^{[c_{11} + \gamma c_{12}](s-T)} - 1}{c_{11} + \gamma c_{21}} \right]. \end{aligned}$$

Since $c_{11} + \gamma c_{21} < 0$ and $W_p(t)$ is integrable on $[0, +\infty)$ it follows that $(n + \gamma n_1)(t)$ is integrable on $[0, +\infty)$. Both $n(t)$ and $n_1(t)$ are nonnegative so it follows that $n(t)$ and $n_1(t)$ are integrable on $[0, +\infty)$.

Now, $E(t) = e^{\int_T^t [c_{33} + \beta\sigma n]dt'}$.

Then

$$\begin{aligned} \phi(t) &- E(t)\phi(T) \\ &= E(t)\left[\int_T^t e^{-\int_T^u [c_{33} + \beta\sigma n]dt'} \cdot [c_{31}n + c_{32}n_1 + I(u)]du\right] \end{aligned}$$

so that

$$\begin{aligned} \phi(t) &= \int_T^t e^{\int_u^t [c_{33} + \beta\sigma n]dt'} [c_{31} + c_{32}n_1 + I(u)]du \\ &+ E(t)\phi(T). \end{aligned}$$

Hence,

$$\begin{aligned} 0 \leq \int_T^s \phi(t)dt &= \int_T^s \int_T^t e^{\int_u^t [c_{33} + \beta\sigma n]dt'} [c_{31} + c_{32}n_1 + I(u)]dudt \\ &+ \int_T^s e^{\int_T^t [c_{33} + \beta\sigma n]dt'} \phi(T)dt \\ &= \int_T^s [c_{31}n + c_{32}n_1 + I(u)] \int_u^s e^{c_{33}(t-u) + \int_u^t \beta\sigma n dt'} dtdu \\ &+ \int_T^s e^{c_{33}(t-u) + \int_T^t \beta\sigma n dt'} \phi(T)dt. \end{aligned}$$

Now $n(t)$ is integrable on $[0, +\infty)$ so

$$\beta\sigma \int_u^t n dt' \leq \beta\sigma \int_T^t n dt' \leq \beta\sigma \int_0^\infty n dt' < \infty.$$

In addition, $n_1(t)$ and $I(t)$ are integrable on $[0, +\infty)$ and $c_{33} < 0$. Therefore $\phi(t)$ is integrable on $[0, +\infty)$.

(ii) Previous discussion shows that $n(t)$ and $n_1(t)$ are bounded on $[0, +\infty)$. Multiplying the last equation in (3.1.5) by γ and adding to the first equation yields

$$\begin{aligned}\frac{d}{dt}(n+\gamma\phi) &= (c_{11}+\gamma c_{31}-W_p)n+(c_{12}+\gamma c_{32}-\gamma W_p)n_1 \\ &\quad +\gamma c_{33}\phi+W_p(t)+\gamma I(t) \\ &= (c_{11}+\gamma c_{31}-W_p)n+(c_{12}+\gamma c_{32}3-\gamma W_p)n_1 \\ &\quad +c_{33}(n+\gamma\phi)+W_p(t)+\gamma I(t).\end{aligned}$$

Thus

$$\begin{aligned}\frac{d}{dt}(n+\gamma\phi)-c_{33}(n+\gamma\phi) &= (c_{11}+\gamma c_{31}-W_p)n+(c_{12}+\gamma c_{32}-\gamma W_p)n_1 \\ &\quad + W_p(t)+\gamma I(t).\end{aligned}$$

and so

$$\begin{aligned}\frac{d}{dt}\left(e^{-c_{33}t}(n+\gamma\phi)\right) &= [(c_{11}+\gamma c_{31}-W_p-c_{33})n+(c_{12}+\gamma c_{32}-\gamma W_p)n_1 \\ &\quad +W_p(t)+\gamma I(t)]e^{-c_{33}t}.\end{aligned}$$

Hence,

$$
\begin{aligned}
n(t) \;+\; & \gamma\phi(t) - e^{c_{33}t}(n(T) + \gamma\phi(T)) \\
= \; & e^{c_{33}t} \int_T^t \{(c_{11} + \gamma c_{31} - W_p - c_{33})n + (c_{12} + \gamma c_{32} - \gamma W_p)n_1 \\
+ \; & W_p(t') + \gamma I(t')\} \, e^{-c_{22}t'} dt' \\
= \; & \int_T^t \{(c_{11} + \gamma c_{31} - W_p - c_{33})n + (c_{12} + \gamma c_{32} - \gamma W_p)n_1 \\
+ \; & W_p(t') + \gamma I(t')\} \, e^{-c_{33}(t - t')} dt'.
\end{aligned}
$$

Therefore

$$
\begin{aligned}
n(t) + \gamma\phi(t) \;=\; & \int_T^t \{(c_{11} + \gamma c_{31} - W_p - c_{33})n + (c_{12} + \gamma c_{32} - \gamma W_p)n_1 \\
+ \; & W_p(t) + \gamma I(t)\} \, e^{-c_{33}(t - t')} dt' \qquad (3.2.2) \\
+ \; & e^{-c_{33}t}[n(T) + \gamma\phi(T)]
\end{aligned}
$$

Since $c_{33} < 0, n(t), n_1(t), W_p(t)$ and $I(t)$ are bounded for all t, the right hand side of (3.2.2) is bounded on $[0, +\infty)$. Therefore $n(t) + \gamma\phi(t)$ is bounded. The nonnegativity of $n(t)$ and $\phi(t)$ gives the desired result.

3.3 Stability Analysis

Suppose now that $W_p(t)$ is a positive constant, $W_p(t) = W_p$, and for simplicity, let $Sp_o = 0$. In addition, consider a system in which there is no injection signal, i.e., $I(t) = 0$. Then (3.1.5) can be simplified to the autonomous system

$$\begin{aligned}
\frac{dn}{dt} &= c_{11}n + c_{12}n_1 - \beta\sigma\gamma n\phi + W_p(1 - n - \gamma n_1) \\
\frac{dn_1}{dt} &= c_{21}n + c_{22}n_1 + \beta\sigma n\phi \\
\frac{d\phi}{dt} &= (c_{33} + \beta\sigma n)\phi \qquad (3.3.1)
\end{aligned}$$

The equilibrium points of (3.3.1) are determined by setting the derivatives equal to zero and solving the resulting algebraic system

$$\begin{aligned}
0 &= (c_{11} - W_p)n + (c_{12} - \gamma W_p)n_1 - \beta\sigma\gamma n\phi + W_p \\
0 &= c_{21}n + c_{22}n_1 + \beta\sigma n\phi \\
0 &= (c_{33} + \beta\sigma n)\phi \qquad (3.3.2)
\end{aligned}$$

The third equation in (3.3.2) implies that

$$\phi = 0 \text{ or } (c_{33} + \beta n\phi) = 0.$$

If $\phi = 0$, then

$$\begin{aligned}
(c_{11} - W_p)n + (c_{12} - \gamma W_p)n_1 + W_p &= 0 \\
c_{21}n + c_{22}n_1 &= 0 \qquad (3.3.3)
\end{aligned}$$

Then

$$n_1 = \frac{-c_{21}}{c_{22}}n.$$

Thus one of the equilibrium points of (3.3.1) is given by

$$\begin{aligned} n^1 &= \frac{-c_{22}W_p}{c_{22}(c_{11}-W_p)-c_{21}(c_{12}-\gamma W_p)} \\ n_1^1 &= -\frac{c_{21}n^1}{c_{22}} \\ \phi^1 &= 0. \end{aligned} \tag{3.3.4}$$

Similarly, if $n = -\frac{c_{33}}{\beta\sigma}$,

$$\begin{aligned} (c_{11}-W_p)\left(-\frac{c_{33}}{\beta\sigma}\right) &+ (c_{12}-\gamma W_p)n_1 - \beta\sigma\gamma\left(-\frac{c_{33}}{\beta\sigma}\right)\phi + W_p = 0 \\ c_{21}\left(-\frac{c_{33}}{\beta\sigma}\right) &+ c_{22}n_1 + \beta\sigma\left(-\frac{c_{33}}{\beta\sigma}\right)\phi = 0. \end{aligned} \tag{3.3.5}$$

Thus

$$n_1 = \frac{\beta\sigma c_{33}\phi + c_{21}c_{33}}{\beta\sigma c_{22}}$$

and hence the second equilibrium point is

$$\begin{aligned} n^2 &= -\frac{c_{33}}{\beta\sigma} \\ n_1^2 &= \frac{\beta\sigma c_{33}\phi + c_{21}c_{33}}{\beta\sigma c_{22}} \\ \phi^2 &= \frac{\beta\sigma c_{22}W_p - c_{33}[c_{22}(c_{11}-W_p)-c_{21}(c_{12}-\gamma W_p)])}{-\beta\sigma c_{33}[(c_{12}-\gamma W_p)+\gamma c_{22}]} \end{aligned} \tag{3.3.6}$$

Let $\bar{\mathbf{y}} = (\bar{n}, \bar{n}_1, \bar{\phi})$ be an equilibrium solution of (3.3.1).

Definition 1 *The equilibrium solution $\bar{\mathbf{y}}$ is stable if for each $\epsilon > 0$ there exists $\delta > 0$ such that if $\psi(t)$ is any solution of (3.3.1) having $\| \psi(t_0) - \bar{\mathbf{y}} \| < \delta$, then the solution $\psi(t)$ exists for all $t \geq t_0$ and $\| \psi(t) - \bar{\mathbf{y}} \| < \epsilon$ for $t \geq t_0$.*

Definition 2 *The equilibrium solution $\bar{\mathbf{y}}$ is asymptotically stable if it is stable and if there exists a number $\delta_0 > 0$ such that if $\psi(t)$ is any solution of (3.3.1) having $\| \psi(t_0 - \bar{\mathbf{y}} \| < \delta_0$, then $\lim_{t \to \infty} \psi(t) = \bar{\mathbf{y}}$.*[2]

The following theorem due to Perron and Poincaré [2] gives a useful stability result.

Theorem 3 *Given the system*

$$\mathbf{y}' = A\mathbf{y} + \mathbf{f}(t, \mathbf{y}). \tag{3.3.7}$$

Suppose all eigenvalues of A have negative real parts, $\mathbf{f}(t, \mathbf{y})$ and $\left(\frac{\partial \mathbf{f}}{\partial y_i}\right)(t, \mathbf{y})(i = 1, ..., n)$ are continuous in $(t, \mathbf{y})$ for $0 \leq t < \infty$, $| \mathbf{y} | < k$ where $k > 0$ is a constant and

$$\lim_{|\mathbf{y}| \to 0} \frac{| \mathbf{f}(t, \mathbf{y}) |}{| \mathbf{y} |} = 0$$

uniformly with respect to t on $0 \leq t < \infty$. Then the solution $\mathbf{y} \equiv 0$ of (3.3.7) is asymptotically stable.

The stability of the equilibrium points of (3.3.1) is investigated by linearizing about the equilibrium point.

$$\text{Let} \quad n = \bar{n} + \delta n$$

$$n_1 = \bar{n}_1 + \delta n_1$$

$$\phi = \bar{\phi} + \delta\phi$$

where $(\bar{n}, \bar{n}_1, \bar{\phi})$ is an equilibrium point of the system (3.3.1) and $(\delta n, \delta n_1, \delta\phi)$ represents a small perturbation from the equilibrium position.

Then

$$\begin{aligned}
\frac{d\delta n}{dt} &= c_{11}\delta n + c_{12}\delta n_1 - \beta\sigma\gamma\delta n\delta\phi - \beta\sigma\bar{n}\delta\phi - \beta\sigma\phi\delta n \\
&- W_p\delta n - W_p\gamma\delta n_1 + c_{11}\bar{n} + c_{12}\bar{n}_1 - \beta\sigma\gamma\bar{n}\bar{\phi} + W_p(1 - \bar{n} - \gamma\bar{n}_1) \\
\frac{d\delta n_1}{dt} &= c_{21}\delta n + c_{22}\delta n_1 + \beta\sigma\delta n\delta\phi + \beta\sigma\bar{n}\delta\phi + \beta\sigma\bar{\phi}\delta n \\
&+ c_{21}\bar{n} + c_{22}\bar{n}_1 + \beta\sigma\bar{n}\bar{\phi} \\
\frac{d\delta\phi}{dt} &= c_{31}\delta n + c_{32}\delta n_1 + c_{33}\delta\phi + \beta\sigma\delta n\delta\phi + \beta\sigma\bar{n}\delta\phi \\
&+ \beta\sigma\bar{n}\delta n + c_{33}\bar{\phi} + \beta\sigma\bar{n}\bar{\phi}
\end{aligned}$$

which reduces to

$$\begin{aligned}
\frac{d\delta n}{dt} &= (c_{11} - \beta\sigma\bar{\phi} - W_p)\delta n + (c_{12} - \gamma W_p)\delta n_1 - \beta\sigma\gamma\bar{n}\delta\phi - \beta\sigma\gamma\delta n\delta\phi \\
\frac{d\delta n_1}{dt} &= (c_{21} + \beta\sigma\bar{\phi})\delta n + c_{22}\delta n_1 + \beta\sigma\bar{n}\delta\phi + \beta\sigma\delta n\delta\phi \\
\frac{d\delta\phi}{dt} &= \beta\sigma\bar{\phi}\delta n + (c_{33} + \beta\sigma\bar{n})\delta\phi + \beta\sigma\delta n\delta\phi
\end{aligned}$$

written in matrix form

$$(\delta \mathbf{y})' = A\delta \mathbf{y} + \mathbf{g}(\delta \mathbf{y})$$

where

$$\delta \mathbf{y} = (\delta n, \delta n_1, \delta \phi)$$

and

$$A = \begin{pmatrix} c_{11} - \beta\sigma\gamma\bar{\phi} - W_p & c_{12} - \gamma W_p & -\beta\sigma\gamma\bar{n} \\ c_{21} + \beta\bar{\phi} & c_{22} & \beta\sigma\bar{n} \\ \beta\sigma\bar{\phi} & 0 & c_{33} + \beta\sigma\bar{n} \end{pmatrix}$$

The eigenvalues of the linearized system are found by solving the chracteristic equation of the matrix A which is

$$\lambda^3 + \hat{\beta}\lambda^2 + \hat{\gamma}\lambda + \hat{\sigma} = 0$$

where

$$\begin{aligned} \hat{\beta} &= -(a_{11} + a_{22} + a_{33}) \\ \hat{\gamma} &= -(a_{31}a_{13} - a_{33}a_{11} - a_{33}a_{22} - a_{11}a_{22} + a_{21}a_{12}) \\ \hat{\sigma} &= (-a_{31}a_{12}a_{23} - a_{31}a_{23}a_{13} + a_{33}a_{11}a_{22} - a_{33}a_{21}a_{12}) \end{aligned}$$

and a_{ij} is the ij^{th} entry in the matrix A.

Since the characteristic equation is cubic, the real parts of the eigenvalues will be negative if

$$\hat{\beta} > 0, \hat{\sigma} > 0, \text{ and } \hat{\beta}\hat{\gamma} - \hat{\sigma} > 0. \tag{3.3.8}$$

If, on the other hand, $\hat{\beta} < 0$ then at least one eigenvalue has a positive real part which implies that the equilibrium point is unstable.

Now consider the equilibrium point (n^1, n_1^1, ϕ^1) given in (3.3.4). Then

$$\begin{aligned} \hat{\beta} &= -(a_{11} + a_{22} + a_{33}) \\ &= -(c_{11} - W_p) - c_{22} - (c_{33} + \beta\sigma n^1) \\ &< 0 \end{aligned}$$

if $c_{33} + \beta\sigma n^1 > 0$. There, $(n^1, n_1^1, \phi;^1)$ is unstable if the condition

$$c_{33} + \beta\sigma n^1 > 0 \tag{3.3.9}$$

is satisfied.

Theorem 4 *Suppose condition (3.3.9) holds for* (n^1, n_1^1, ϕ^1). *Then the equilibrium point* (n^2, n_1^2, ϕ^2) *is asymptotically stable.*

Proof: Consider the equilibrium solution (n^2, n_1^2, ϕ^2) given by (3.3.6).

Then

$$\phi^2 = \frac{\beta\sigma c_{22} W_p - c_{33}[c_{22}(c_{11} - W_p) - c_{21}(c_{12} - \gamma W_p)]}{-\beta\sigma c_{33}[(c_{12} - \gamma W_p) + \gamma c_{22}]}$$

$$= [\beta\sigma n^1 + c_{33}] \left[\frac{n^1}{-c_{22} W_p c_{33} \beta\sigma[(c_{120}\gamma W_p) - \gamma c_{22}]} \right]$$

Now look at the quantity

$$
\begin{aligned}
c_{12} - \gamma W_p + \gamma c_{22} &= (1-\gamma)\left[\frac{1}{\tau_2} - \frac{(\gamma-1)}{\tau_{f\ell}} - \frac{1}{\tau_1}\right] - \gamma W_p - \gamma\left[\frac{\gamma-1}{\tau_{f\ell}} - \frac{1}{\tau_1}\right] \\
&= \frac{1-\gamma}{\tau_2} + \frac{(\gamma-1)^2}{\tau_{f\ell}} + \frac{\gamma}{\tau_1} - \frac{1}{\tau_1} - \gamma W_p + \frac{\gamma(\gamma-1)}{\tau_{f\ell}} - \frac{\gamma}{\tau_1} \\
&= \left[-\gamma W_p - \frac{1}{\tau_1}\right] + \left[\frac{1-\gamma}{\tau_2} + \frac{(\gamma-1)^2}{\tau_{f\ell}} + \frac{\gamma(\gamma-1)}{\tau_{f\ell}}\right] \\
&< 0
\end{aligned}
$$

since $\tau_1 << \tau_{f\ell}, \tau_2$.

Therefore

$$
\phi^2 = [\beta\sigma n^1 - c_{33}]\left[\frac{n^1}{-c_{22}W_p c_{33}\beta\sigma[(c_{12} - \gamma W_p) + \gamma c_{22}]}\right]
$$

since (3.3.9) holds, $c_{22} < 0, c_{33} < 0$ and $\beta > 0, \sigma > 0, W_p > 0$.

The coefficients $\hat{\beta}$ and $\hat{\sigma}$ of the characteristic equation are thus

$$
\begin{aligned}
\hat{\beta} &= -a_{11} + a_{22} + a_{33} \\
&= -(a_{11} + a_{22}) \\
&= -c_{11} + \beta\sigma\gamma\phi^2 + W_p - c_{22} \\
&> 0, \qquad \text{and}
\end{aligned}
$$

$$\begin{aligned}
\hat{\sigma} &= -[a_{31}a_{12}a_{23} - a_{31}a_{22}a_{13}] \\
&= -[\beta\sigma\phi^2][\beta\sigma n^2(c_{12} - \alpha W_p\gamma) + \beta\sigma\gamma n^2 c_{22}] \\
&= -(\beta\sigma)^2\phi^2[c_{12} - \gamma W_p + \gamma c_{22}] \\
&> 0.
\end{aligned}$$

Since condition (3.3.9) holds, then

$$\begin{aligned}
n^1 &= \frac{-c_{22}W_p}{c_{22}(c_{11} - W_p) - c_{21}(c_{12} - \gamma W_p} \\
&> 0.
\end{aligned}$$

This implies that $c_{22}(c_{11} - W_p) - c_{21}(c_{12} - \gamma W_p) > 0$.

Finally, consider the quantity

$$\begin{aligned}
\hat{\beta}\hat{\gamma} - \hat{\sigma} &= (a_{11} + a_{22})(a_{31}a_{13} - a_{11}a_{22} + a_{21}a_{12}) - a_{31}a_{23}a_{13} - a_{31}a_{12}a_{23} \\
&= a_{11}a_{31}a_{13} - a_{11}^2a_{22} + a_{11}a_{21}a_{12} + a_{22}a_{31}a_{13} - a_{11}a_{22}^2 + a_{22}a_{12}a_{21} \\
&\quad + a_{31}a_{23}a_{13} - a_{31}a_{12}a_{23} \\
&= (c_{11} - \beta\sigma\gamma\phi^2 - W_p)(\beta\sigma\phi^2)(-\beta\sigma\gamma n^2) - (c_{11} - \beta\sigma\gamma\phi^2 - W_p)^2c_{22} \\
&\quad + c_{22}\beta\sigma\phi^2(-\beta\sigma\gamma n^2) + (c_{11} - \beta\sigma\gamma\phi^2 - W_p)(c_{21} + \beta\sigma\phi^2)(c_{12} - \gamma W_p) \\
&\quad - (c_{11} - \beta\sigma\gamma\phi^2 - W_p)c_{22}^2 + c_{22}(c_{21} - \gamma W_p) \\
&\quad + \beta\sigma\phi^2\beta\sigma n^2(-\beta\sigma\gamma n^2) - \beta\sigma\phi^2(c_{12} - \gamma W_p)\beta\sigma n^2 \\
&= (c_{11} - \beta\sigma\gamma\phi^2 - W_p)[c_{21}(c_{12} - \gamma W_p) - c_{22}(c_{11} - W_p)] \\
&\quad + c_{22}[c_{21}(c_{12} - \gamma W_p) - c_{22}(c_{11} - W_p)] \\
&\quad + (c_{11} - W_p)\beta\sigma\phi^2[\gamma c_{22} + c_{12} - \gamma W_p] \\
&\quad - (\beta\sigma)^2(\phi^2)^2[\gamma c_{22} + c_{12} - \gamma W_p] \\
&\quad - (\beta\sigma)^2\phi^2n^2[\gamma c_{22} + c_{12} - \gamma W_p] \\
&\quad - (c_{11} - W_p)(\beta\sigma)^2\gamma\phi^2n^2 + (\beta\sigma)^3\gamma^2(\phi^2)^2n^2 \\
&\quad + c_{22}\beta\sigma\gamma\phi^2 - c_{22}\beta\sigma\phi^2\gamma W_p \\
&> 0.
\end{aligned}$$

Since $c_{11} - \beta\sigma\gamma\phi^2 - W_p < 0, c_{21}(c_{12} - \gamma W_p) - c_{22}(c_{11} - W_p) < 0, c_{12} - \gamma W_p + \gamma c_{22} < 0.$

Thus $\hat{\beta} > 0, \hat{\sigma} > 0$, and $\hat{\beta}\hat{\gamma} - \hat{\sigma} > 0$ so the linearized eigenvalues have negative real parts. Hence, the result.

In order for laser emission to occur

$$\frac{d\phi}{dt} > 0 \tag{3.3.10}$$

must be satisfied. Laser threshold [12] is characterized by steady state population inversion and lower laser population,

$$\frac{dn}{dt} = \frac{dn_1}{dt} = 0$$

as well as a very small photon density. Thus (3.3.10) is equivalent to the instability condition (3.3.9) for the first equilibrium position (3.3.3). The pumping rate necessary to exceed laser threshold can be found from (3.3.9) so that

$$\beta\sigma n^1 > -c_{33}$$

where

$$n^1 = \frac{-c_{22}W_p}{c_{22}(c_{11} - W_p) - c_{21}(c_{12} - \gamma W_p)}.$$

This implies that

$$W_p[c_{22}(1 - \beta\sigma\tau_c) - \gamma c_{21}] > c_{11}c_{22} - c_{21}c_{12}.$$

or in terms of the physical parameters

$$W_p > \frac{\tau_{fl}}{\tau_1\tau_{fl}[\beta\sigma\tau_c - 1] + \tau_1\tau_2(1 - \gamma)\beta\sigma\tau_c}. \tag{3.3.11}$$

Now consider the system (3.1.5) in which $W_p(t)$ and $I(t)$ satisfy the condition of Theorem 3.2 (i). Then the following theorem from [2] can be easily applied.

Theorem 5 *Consider the system*

$$\mathbf{y}' = (A + B(t))\mathbf{y} + \mathbf{f}(t, \mathbf{y})$$

where A and $\mathbf{f}$ *stafisfy the hypothesis of Theorem 3.3. If B(t) is continuous for* $0 \leq t < \infty$ *with* $\lim_{t\to\infty} B(t) = 0$, *then the zero solution of the system is asymptotically stable.*

Theorem 6 *Let* $W_p(t)$ *and* $I(t)$ *satisfy the conditions of Theorem 3.2(i). Then (3.1.5) is asymptotically stable.*

Proof: Let $(\bar{n}, \bar{n}_1, \bar{\phi})$ solve the system (3.1.5). Let

$$\begin{aligned} n &= N - \bar{n} \\ n_1 &= N_1 - \bar{n}_1 \\ \phi &= \Phi - \bar{\phi}. \end{aligned}$$

Assuming $\bar{n}(0) + \gamma\bar{n}_1(0) < 1$ and $n(0) + \gamma n_1(0) < 1$, the following system is obtained.

$$\begin{aligned} \frac{dN}{dt} &= (c_{11} - \beta\sigma\gamma\bar{\phi} - W_p)N + (c_{12} - \gamma W_p)N_1 - \beta\sigma\gamma\bar{n}\Phi - \beta\sigma\gamma N\bar{\Phi} \\ \frac{dN_1}{dt} &= (c_{21} + \beta\sigma\bar{\phi})N + c_{22}N_1 + \beta\sigma\bar{n}\Phi + \beta\sigma N\Phi \qquad (3.3.12) \\ \frac{d\Phi}{dt} &= (c_{31} + \beta\sigma\bar{\phi})N + c_{32}N_1 + (c_{33} + \beta\sigma\bar{n})\Phi + \beta\sigma N\Phi \end{aligned}$$

which has the trivial solution $N = N_1 = \Phi = 0$.

Consider the linear system

$$\begin{aligned} \frac{dN}{dt} &= c_{11}N + c_{12}N_1 \\ \frac{dN_1}{dt} &= c_{21}N + c_{22}N_1 \\ \frac{d\Phi}{dt} &= c_{31}N + c_{32}N_1 + c_{33}\Phi \end{aligned} \qquad (3.3.13)$$

which has the coefficient matrix

$$C = \begin{pmatrix} c_{11} & c_{12} & 0 \\ c_{21} & c_{22} & 0 \\ c_{31} & c_{32} & c_{33} \end{pmatrix}$$

The characteristic equation of the matrix C is

$$(c_{33} - \lambda)(\lambda^2 - (c_{11} + c_{22})\lambda + (c_{11}c_{22} - c_{21}c_{12})) = 0.$$

The eigenvalues of the chracteristic equation will have negative real parts provided that

$$(c_{11} + c_{22}) > 0 \quad \text{and}$$

$$c_{11}c_{22} - c_{21}c_{12} > 0.$$

The first condition is satisfied so consider

$$
\begin{aligned}
c_{11}c_{22} - c_{21}c_{12} &= \left(\frac{-1}{\tau_2} - \frac{(\gamma-1)}{\tau_{fl}}\right)\left(\frac{\gamma-1}{\tau_{fl}} - \frac{1}{\tau_1}\right) \\
&\quad - \left(\frac{1}{\tau_{fl}}\right)\left[(1-\gamma)\left(\frac{1}{\tau_2} + \frac{(\gamma-1}{\tau_{fl}} - \frac{1}{\tau_1}\right)\right] \\
&= -\frac{(\gamma-1)}{\tau_2\tau_{fl}} + \frac{1}{\tau_2\tau_1} - \frac{(\gamma-1)^2}{\tau_{fl}^2} + \frac{(\gamma-1)}{\tau_1\tau_{fl}} \\
&\quad + \frac{(\gamma-1)}{\tau_{fl}\tau_2} + \frac{(\gamma-1)^2}{\tau_{fl}^2} - \frac{(\gamma-1)}{\tau_{fl}\tau_1} \\
&= \frac{1}{\tau_2\tau_1} \\
&> 0.
\end{aligned}
$$

Therefore the eigenvalues of C have negative real parts and so the linear system (3.3.13) is asymptotically stable. Since $\bar{n}, \bar{n}_1, \bar{\phi}$, and $W_p(t)$ are nonnegative and integrable, it follows from Theorem 3.5 that $N = N_1 = \Phi = 0$ is an asymptotically stable solution to the nonlinear system (3.3.12).

3.4 Numerical Analysis

In this section, the numerical solution to the system (3.1.5) subject to initial conditions (3.1.6) are discussed. In particular, the system is assumed initially to be quiescent, i.e. $n(0) = n_1(0) = \phi(0) = 0$.

The initial value problem was solved numerically on a DEC VAX 11/750 using a Runge-Kutta Fehlberg (RKF) algorithm and on a CYBER CY173 using a backward difference method [13]. Material parameters for Titanium-doped Sapphire that were used in the calculations are given in Table 3.1. Experimental parameters that are typical of a Ti:Sapphire laser system are listed in Table 3.2.

Other parameters to be considered are the cavity lifetime τ_c and the spontaneous emission parameter Sp_0. The cavity lifetime for the ring cavity discussed in Section 2 was computed by

$$\tau_c = \frac{2L}{c \cdot \tau_{\text{norm}}}[2\alpha\ell - \ell_m - \ell n[R_1 R_2 R_3 T_s^4]]^{-1}.$$

Variations in τ_c were assumed to correspond to changes in the mirror reflectivities or cavity length so the effects on the numerical solution caused by changes in τ_c were studied. The spontaneous emission parameter Sp_0 ws computed by

$$Sp_0 = \left[\left(1+\frac{r}{\ell}\right) - \sqrt{1+\left(\frac{r}{\ell}\right)^2}\right]\left[8\pi c \tau_{\text{norm}} n^2 \sigma \frac{\Delta\lambda}{\lambda^4}\tau_{f\ell}\right].$$

The model (3.1.5) allows for the introduction of an injection signal to the system. The injection signal, when present, was assumed to be a Gaussian distribution given by

$$I(t) = I \cdot f(t, t_I, \tau_I) \tag{3.4.1}$$

where

Table 3.1 Material Parameters for Titanium-Doped Sapphire

$g_2 = 2.0$

$g_1 = 3.0$

$n- = 1.76$

$\tau_{fl} = 3870.0ns$

$\tau_1 = 1.0ns$

$\tau_2 = 3000.0ns$

$\sigma = 3.0 \times 10^{19} cm^2$

$\sigma_{ab} = 6.8 \times 10^{-20} cm^2$

$\lambda = 780nm$

$\Delta\lambda = 1nm$

$\alpha = .02cm^{-1}$

Table 3.2 Experimental Parameters for Ti:Sapphire System

Crystal Parameters

$\ell = 2.5cm$

$r = .05cm^{-1}$

$n_T = 1.2 \times 10^{-19} cm^{-3}$

Cavity Parameters

$L = 120cm$

$\ell_m = 0.0$

$R_1 = .4$

$R_2 = .9$

$R_3 = .9$

$$I = \left[\frac{E_I}{\left(\frac{h_c}{\lambda_I}\right)}\right]\left[\frac{1}{\tau_I}\right]\left[\frac{1}{\pi r^2 \ell}\right]\left[\frac{1}{n_T}\right]$$

and the function f is defined by

$$f(t, t_0, \tau) = 2\sqrt{\frac{\ell n 2}{\pi}} \exp\left[\frac{-(\ell n 2)(t - t_0)^2}{\left(\frac{1}{2}\tau\right)^2}\right].$$

In the definition for I,

E_I = energy of pulse (μJ)

λ_I = wavelength of the injected signal (cm)

t_I = center of injection pulse (ns)

τ_I = width of injection pulse (ns).

Variations in I were assumed to correspond to variations in the energy of the injected signal. Some typical values of the injection parameters are given in Table 3.3.

Two pumping schemes were considered. In the case of a constant pump pulse,

$$\begin{aligned} W_p(t) &= W_p \\ &= \eta\left[\frac{E_p}{\left(\frac{h_c}{\lambda_p}\right)}\right]\left[\frac{1}{\tau_p}\right]\left[\frac{1 - e^{-2(\frac{r}{r_p})^2}}{\pi r^2 \ell}\right]\left[\frac{1 - e^{-\alpha_p \ell}}{N_T}\right] \end{aligned} \qquad (3.4.2)$$

Table 3.3 Injection Pulse Parameters

$E_I = 10\mu J$

$t_I = 60$ ns

$\tau_I = 20$ ns

Table 3.4 Pump Pulse Parameters

$E_p = 10$ mJ

$r_p = .05$ cm

$\eta = 1.0$

$\lambda_p = 532.0$ nm

$t_p = 30$ ns

$\tau_p = 10$ ns

where

η = branching ratio

E_p = pumping energy (mJ)

λ_p = pump wavelength (cm)

α_p = absorption coefficient (cm^{-1}) given by $n_T\sigma_{ab}$

τ_p = length of pump pulse (ns)

r_p = pump beam radius (cm)

Typical values for the pump parameters are given in Table 3.4. Changes in the value of W_p were assumed to correspond to changes in the pumping energy. Effects on the numerical solution caused by changes in W_p were studied.

The second pumping scheme considered was a Gaussian distribution for the pump pulse, given by

$$W_p(t) = W_p \cdot f(t, t_p, \tau_p)$$

where W_p is as described above and

$$t_p = \text{center of the pump pulse (ns)}$$

All numerical computations performed on the VAX computer were in double precison. For relatively low values of W_p, the RKF algorithm was used, but for large values of the parameter the backward difference method on the CYBER computer was employed.

The normalized population inversion and photon concentration are plotted in Figs. 3.1 and 3.2 as a function of time for a system in which the pumping rate

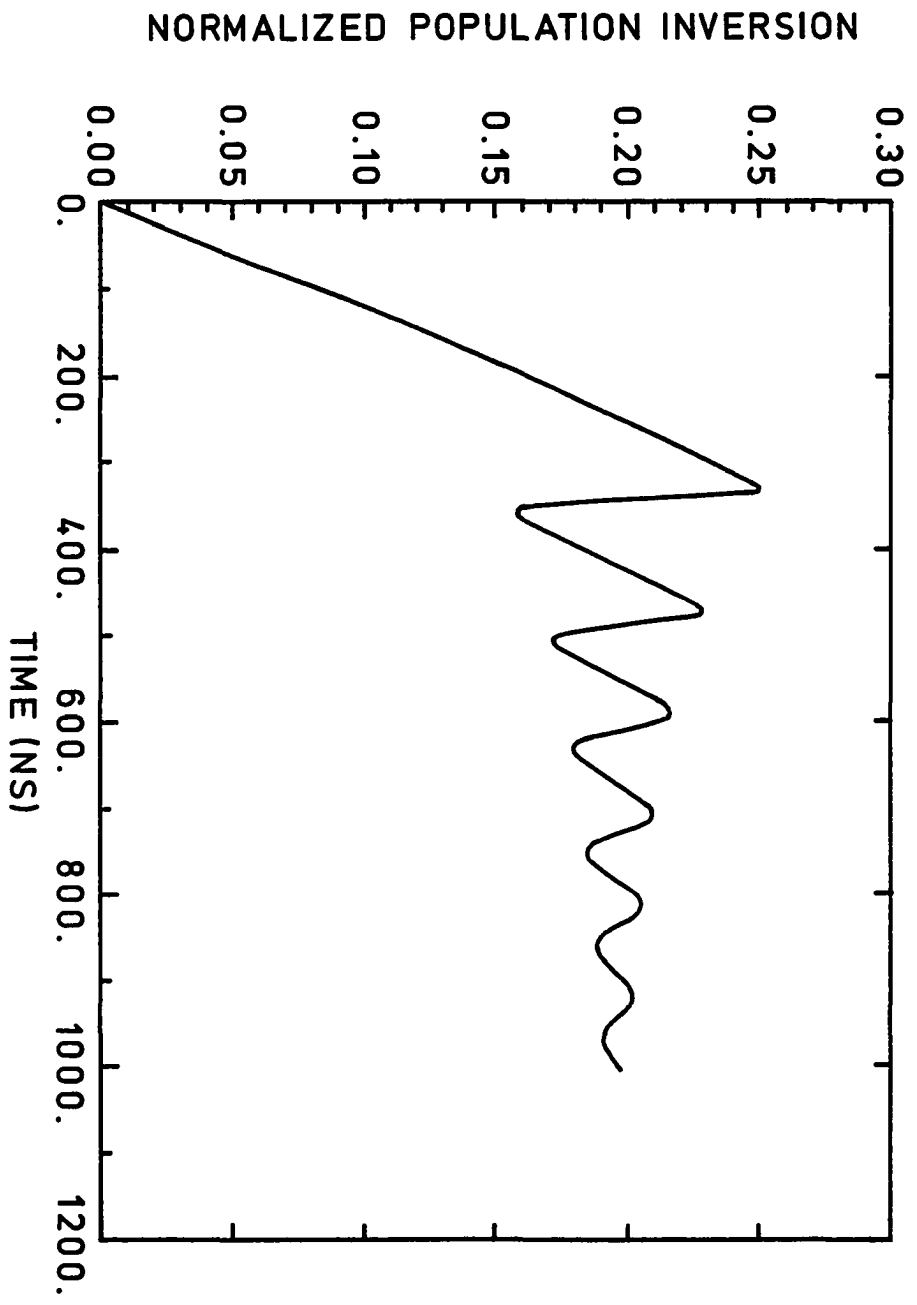

Figure 3.1 Computed curve showing the evolution of the inverted population concentration for an end-pumped laser with constant pumping rate. The population concentration is normalized to the doping concentration in the crystal. Here, $w_p = .001 ns^{-1}$ and $\tau_c = 1.0 ns$

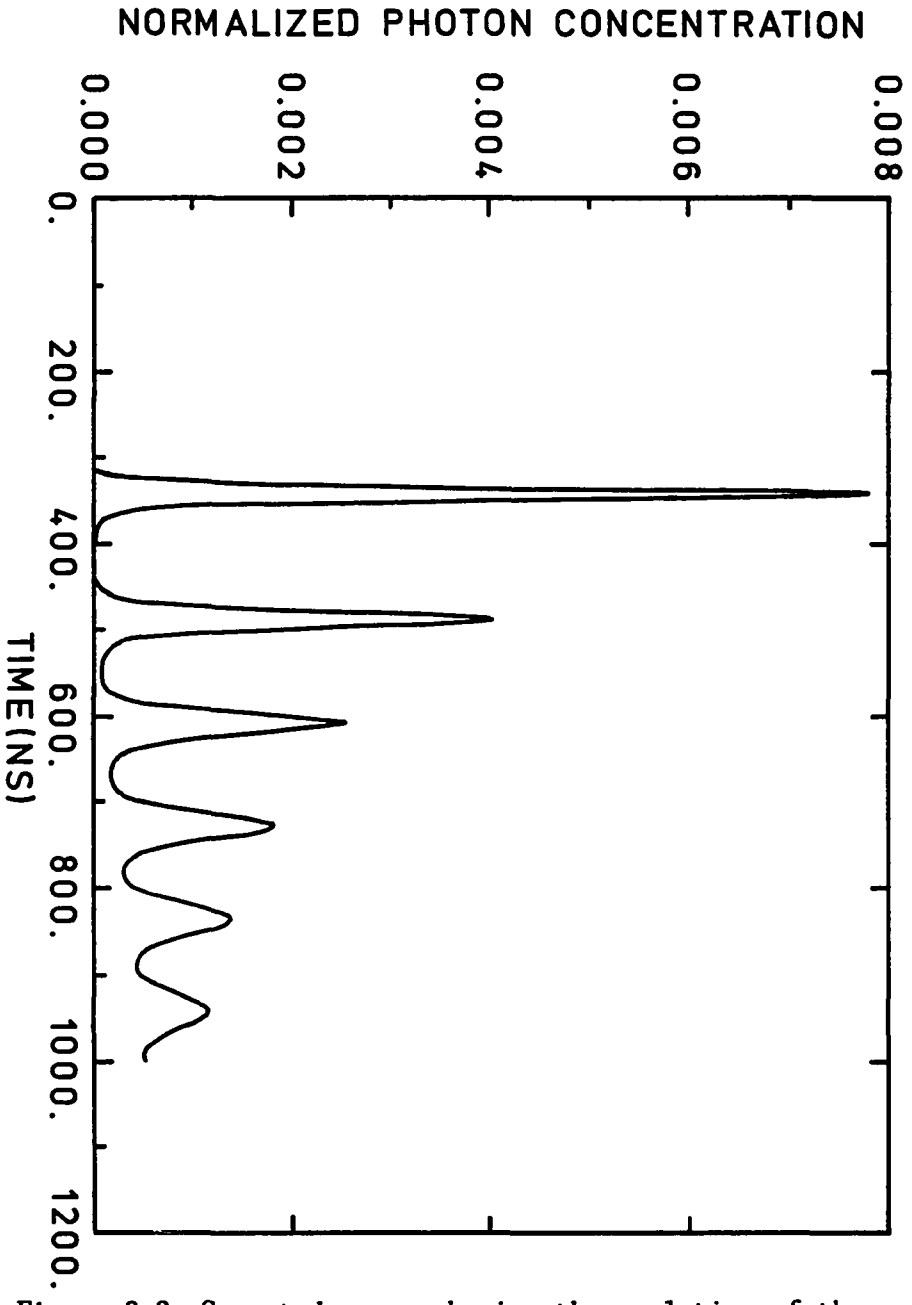

Figure 3.2 Computed curve showing the evolution of the normalized photon concentration for the parameter values W_p=.001ns^{-1} and τ_c=1.0ns

is constant, $W_p = .001ns^{-1}, I = 0$, and $\tau_c = 1.0$ ns. Initially, the number of upper energy electrons is zero and the photon concentration is zero. At $t = 0$, the pump is turned on and the population inversion increases. The increase continues until the photons in the pump beam are absorbed. During this time the photon concentration has been steadily increasing (but not visibly on the graph). Up to this point the dynamics have been dominated by the linear part of the rate equations. As the photon concentration becomes significant, the nonlinear term $(n \cdot \phi)$ begins to dominate the dynamics. At this point there is a rapid increase in the photon concentration along with a corresponding decrease in the population inversion. In this particular case, relaxation oscillations are present in the solution. As time passes, the oscillations die out as the system appproaches its asymptotically stable equilibrium solution. In a laser system, this relaxation process is known as spiking and for some laser applications it is desirable to supress the modulations in the output [12]. If τ_c is changed to 5.0 ns, the numerical solutions (Figs. 3.3 and 3.4) predict that the oscillations die out more quickly.

A study of the nature of the eigenvalues of the system (3.1.5) linearized about the equilibrium solution provides a means of predicting values of the parameters that lead to relaxation oscillations.

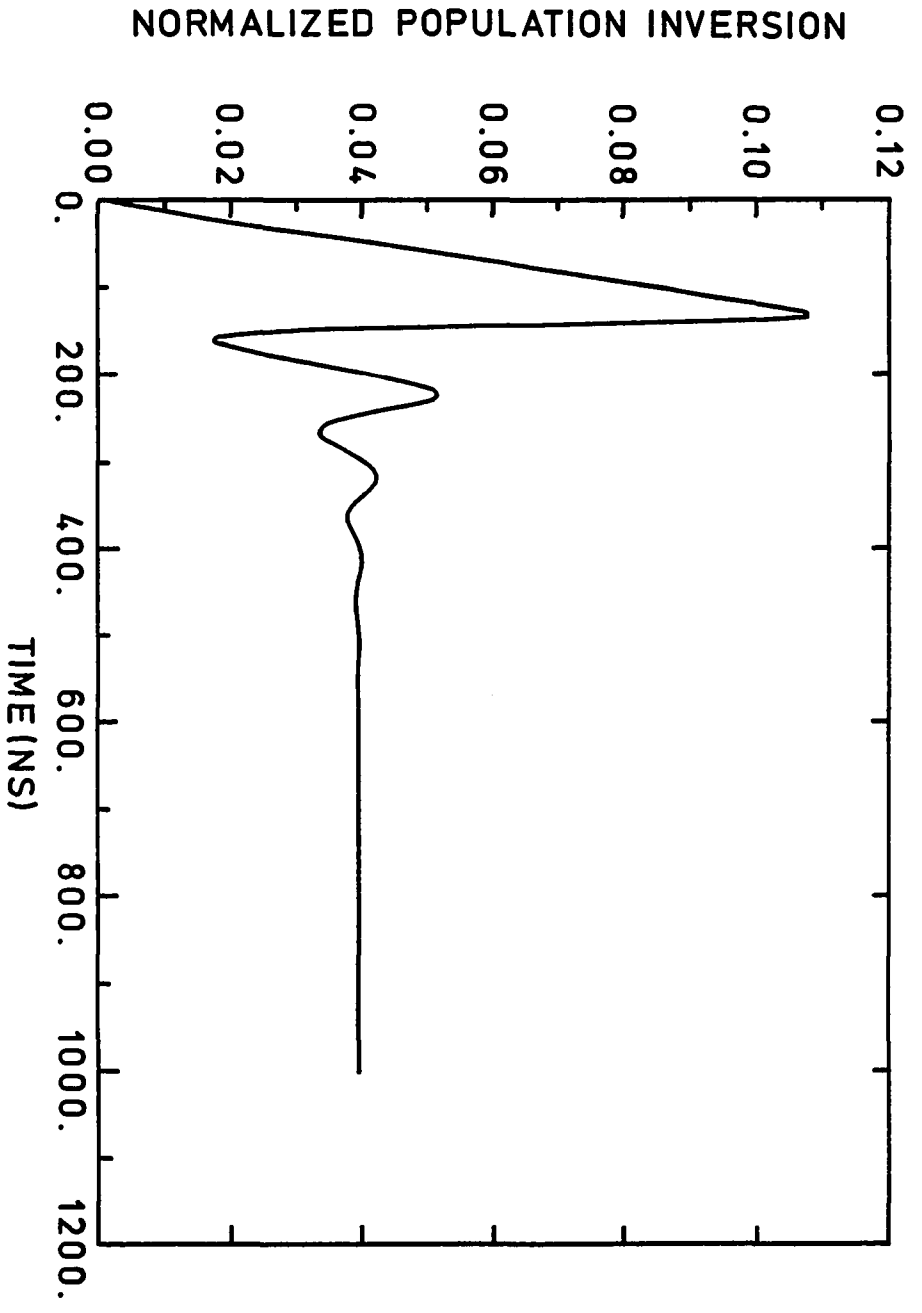

Figure 3.3 Curve showing the effect on the normalized population inversion of holding W_p constant at .001ns^{-1} while increasing τ_c to 5.0ns

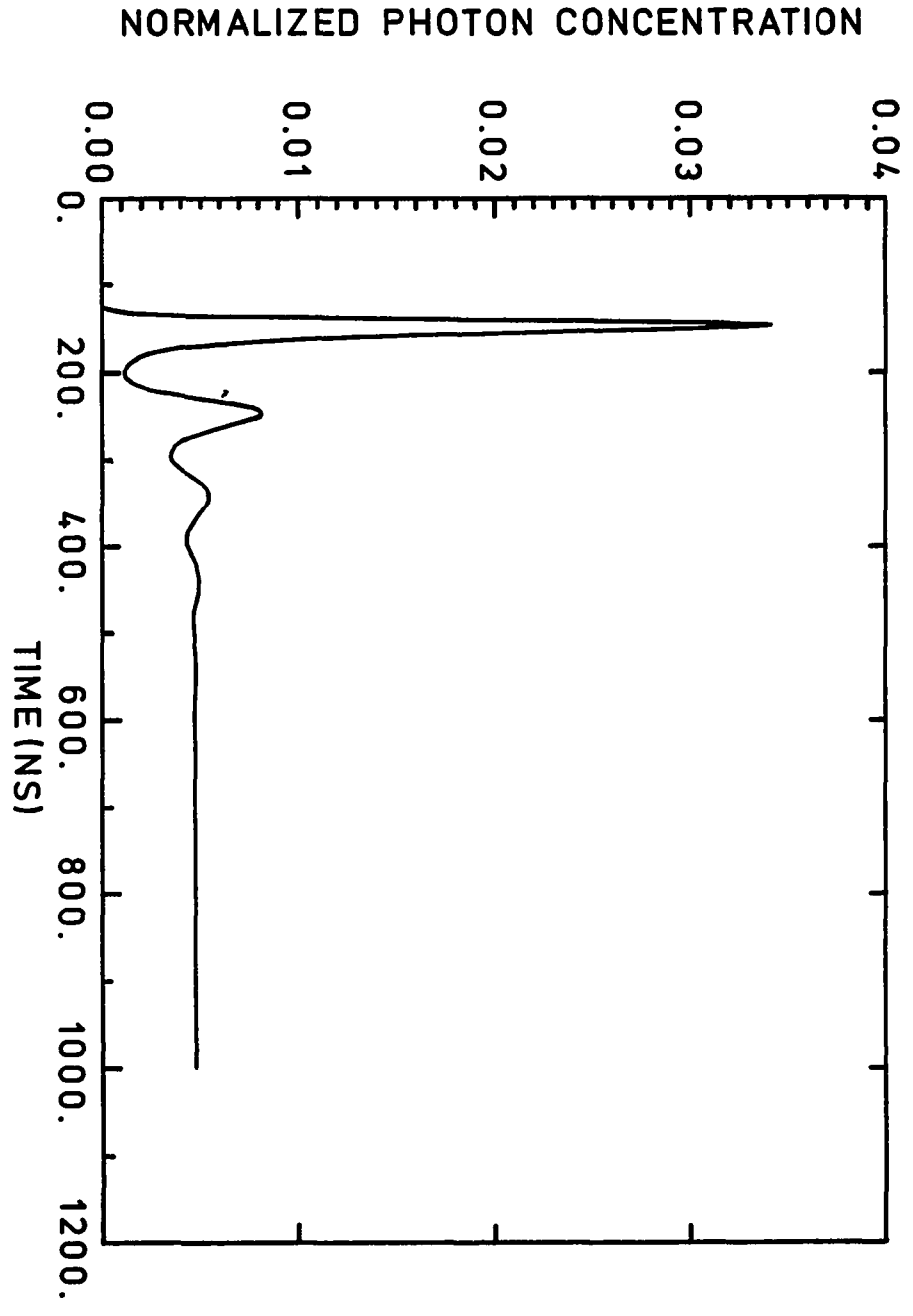

Figure 3.4 The normalized photon concentration for parameter values W_p=.001ns^{-1} and τ_c=5.0ns

The characteristic equation for the coefficient matrix is cubic,

$$\lambda^3 + \hat{\beta}\lambda^2 + \hat{\gamma}\lambda + \hat{\sigma} = 0 \qquad (3.4.3)$$

where

$$\begin{aligned}
\hat{\beta} &= -[a_{11} + a_{22} + a_{33}] \\
\hat{\gamma} &= -[a_{23}a_{32} + a_{21}a_{12} + a_{31}a_{13} - a_{11}a_{22} - a_{33}a_{11} - a_{23}a_{32}] \\
\hat{\sigma} &= -[a_{11}a_{22}a_{33} - a_{11}a_{23}a_{32} - a_{21}a_{12}a_{33} + a_{21}a_{32}a_{13} + a_{31}a_{1}a_{23} - a_{31}a_{13}a_{12}]
\end{aligned}$$

and

$$\begin{aligned}
a_{11} &= c_{11} - \beta\sigma\gamma\phi_0 - W_p \quad & a_{12} &= c_{12} - \gamma W_p \quad & a_{13} &= -\beta\sigma\gamma n_0 \\
a_{21} &= c_{21} + \beta\sigma\phi_0 \quad & a_{22} &= c_{22} \quad & a_{23} &= \beta\sigma n_0 \\
a_{31} &= c_{31} + \beta\sigma\phi_0 \quad & a_{32} &= c_{32} \quad & a_{33} &= c_{33} + \beta\sigma n_0
\end{aligned}$$

where (n^0, n_1^0, ϕ^0) is an equilibrium solution.

Making the transformation

$$\lambda = \xi - \frac{\hat{\beta}}{3}$$

equation (3.4.3) becomes

$$\xi^3 + \rho\xi + q = 0$$

where

$$P = \hat{\gamma} - \frac{1}{3}\hat{\beta}^2$$
$$q = \hat{\sigma} - \frac{\hat{\gamma}\hat{\beta}}{3} + \frac{2\hat{\beta}^3}{27}.$$

The cubic discriminant is defined

$$D = -4p^3 - 27q^3.$$

If $D < 0$, then there is one real and two complex roots to equation (3.4). If $D \geq 0$, then all roots of (3.4.3) are real and if $D = 0$, then there is multiplicity of the roots.

The computer code given in Appendix I determines the nature of the eigenvalues of the linearized system using the cubic discriminant as well as the stability properties by using the criteria (3.3.8). Figure 3.5 is a plot of the cubic discriminant as a function of τ_c holding W_p constant, $W_p = .001ns^{-1}$. The plot predicts oscillations in the solutions will occur for an approximate range $.5 \leq \tau_c \leq 28.6$. After τ_c exceeds 28.6ns the oscillations should not be present in the solutions. Figs. 3.6 and 3.7 give the numerical solution for the population inversion and photon concentration, respectively, for $\tau_c = 30ns$. Figs. 3.8, 3.9 Figs. 3.8, 3.9 and 3.10 give the phase portraits for $\tau_c = 1.0ns, \tau_c = 5.0ns$, and $\tau_c = 30ns$ which display the asymptotic behavior of the system.

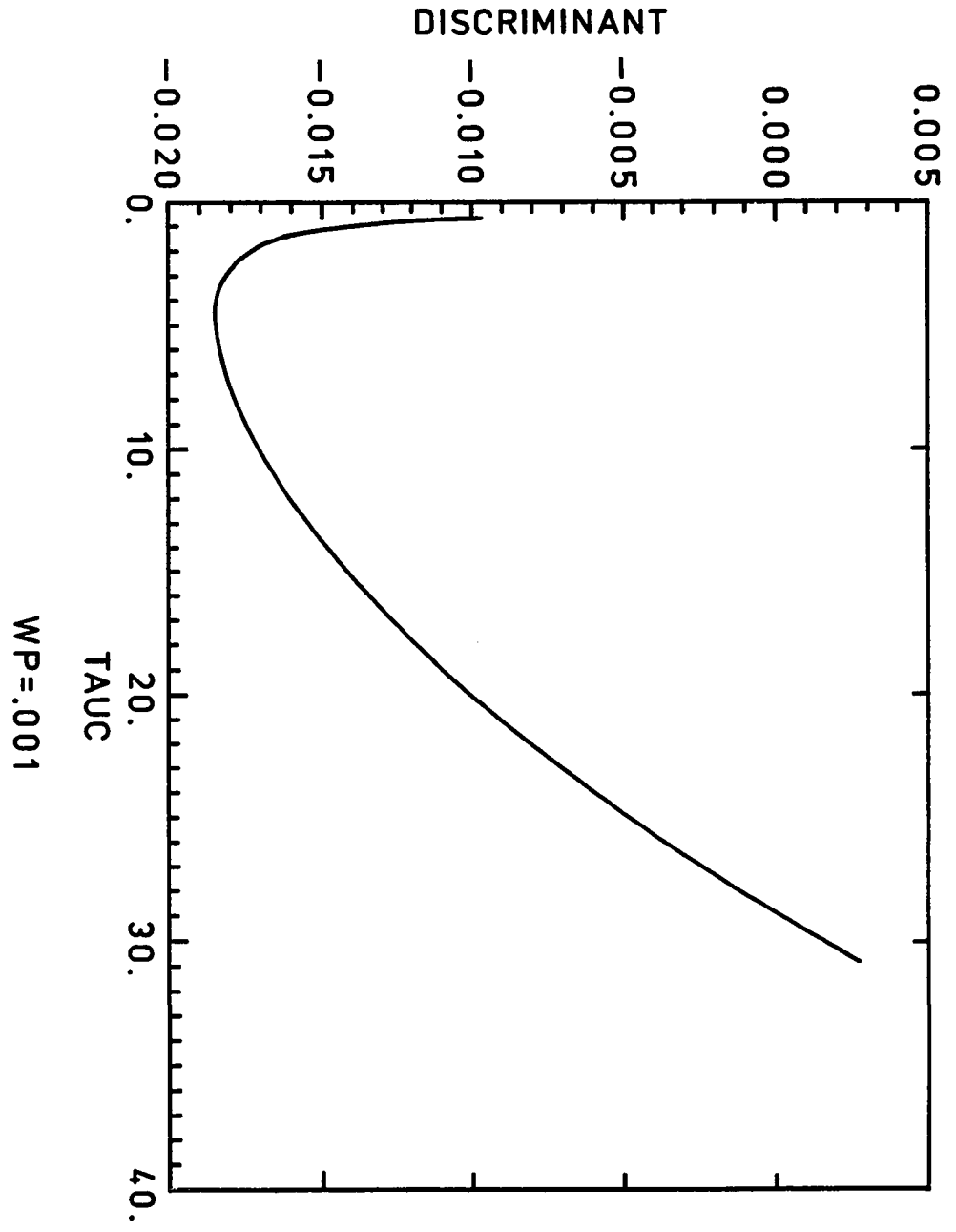

Figure 3.5 The discriminant of the cubic characteristic equation for the linearized eigenvalues computed for W_p=.001ns^{-1} as a function of τ_c

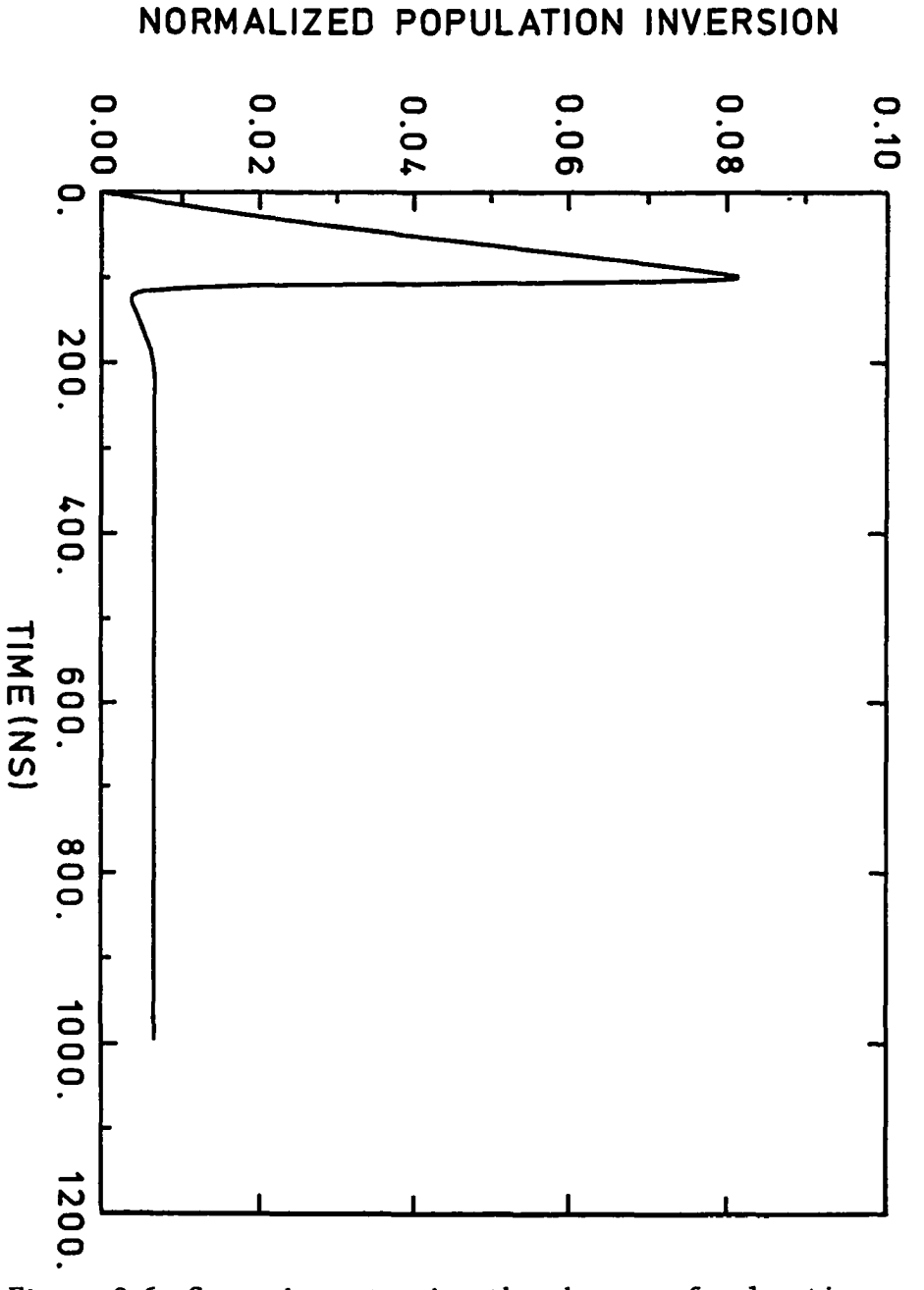

Figure 3.6 Curve demonstrating the absence of relaxation oscillations in the normalized population inversion for the parameter values $W_p = .001 ns^{-1}$ and $\tau_c = 30.0 ns$

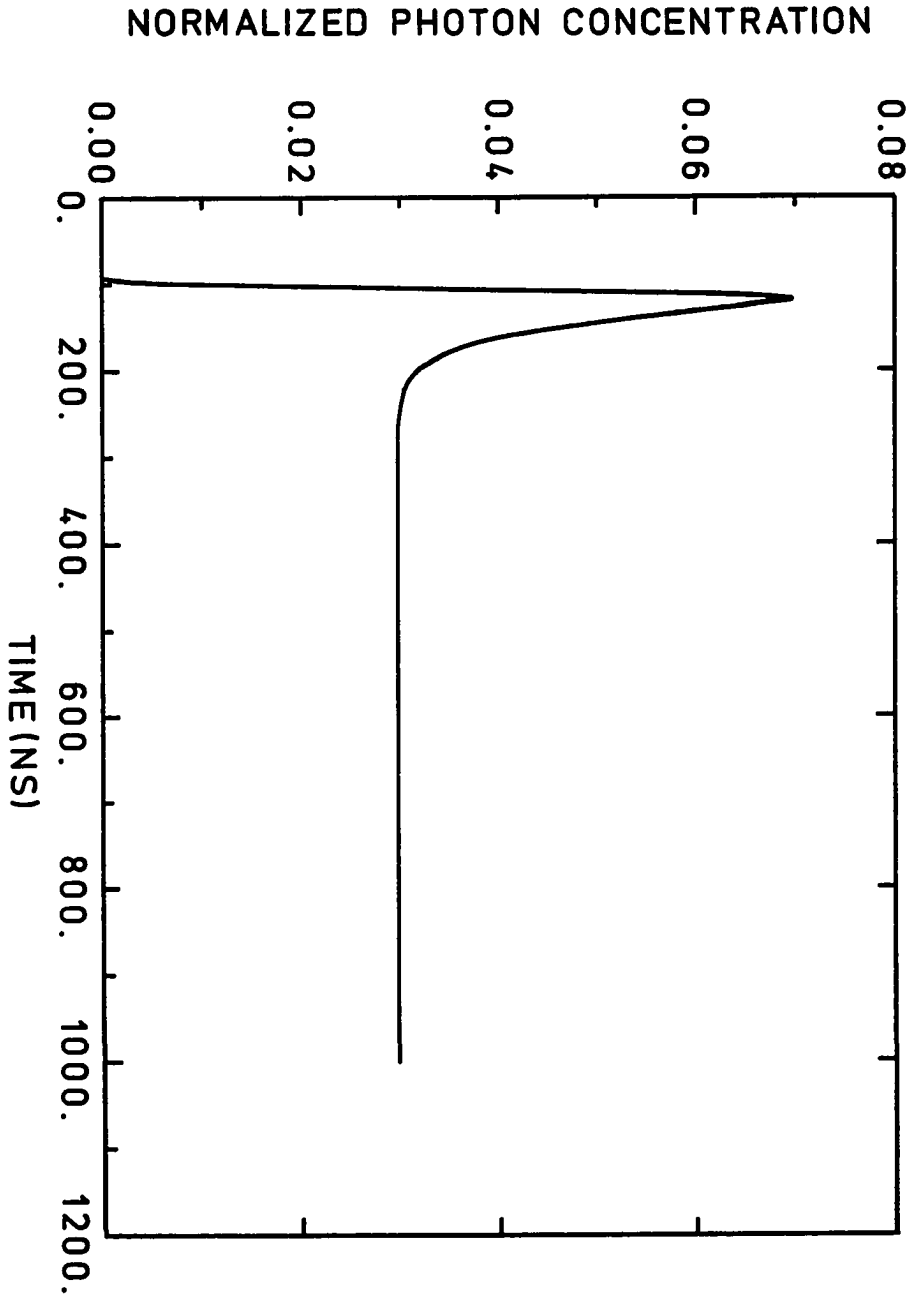

Figure 3.7 The normalized photon concentration computed for the value $W_p = .001 ns^{-1}$ and $\tau_c = 30.0 ns$

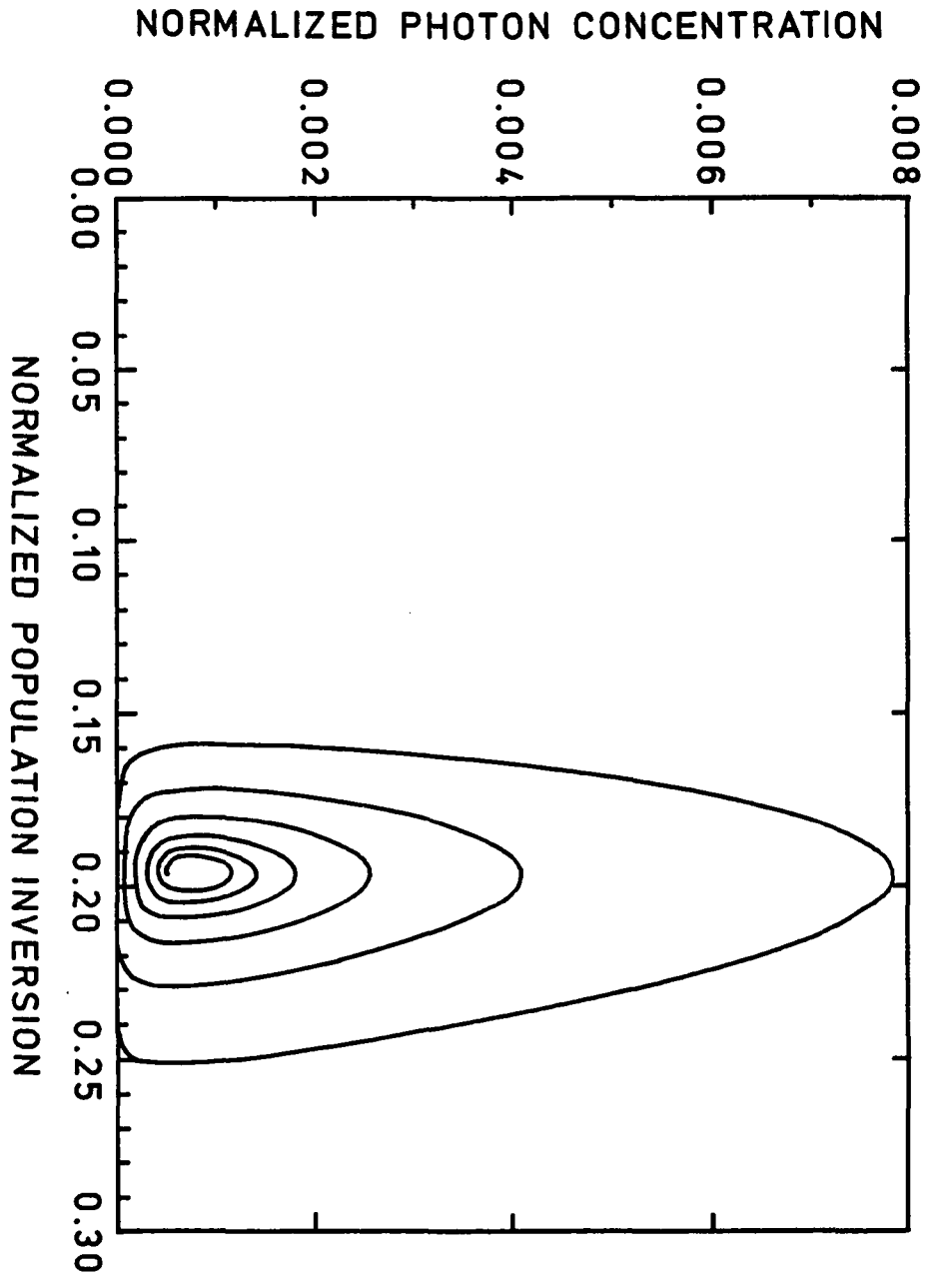

Figure 3.8 Phase plane portrait showing the asymptotic behavior of the system for the parameter values W_p=.001ns^{-1} and τ_c=1.0ns

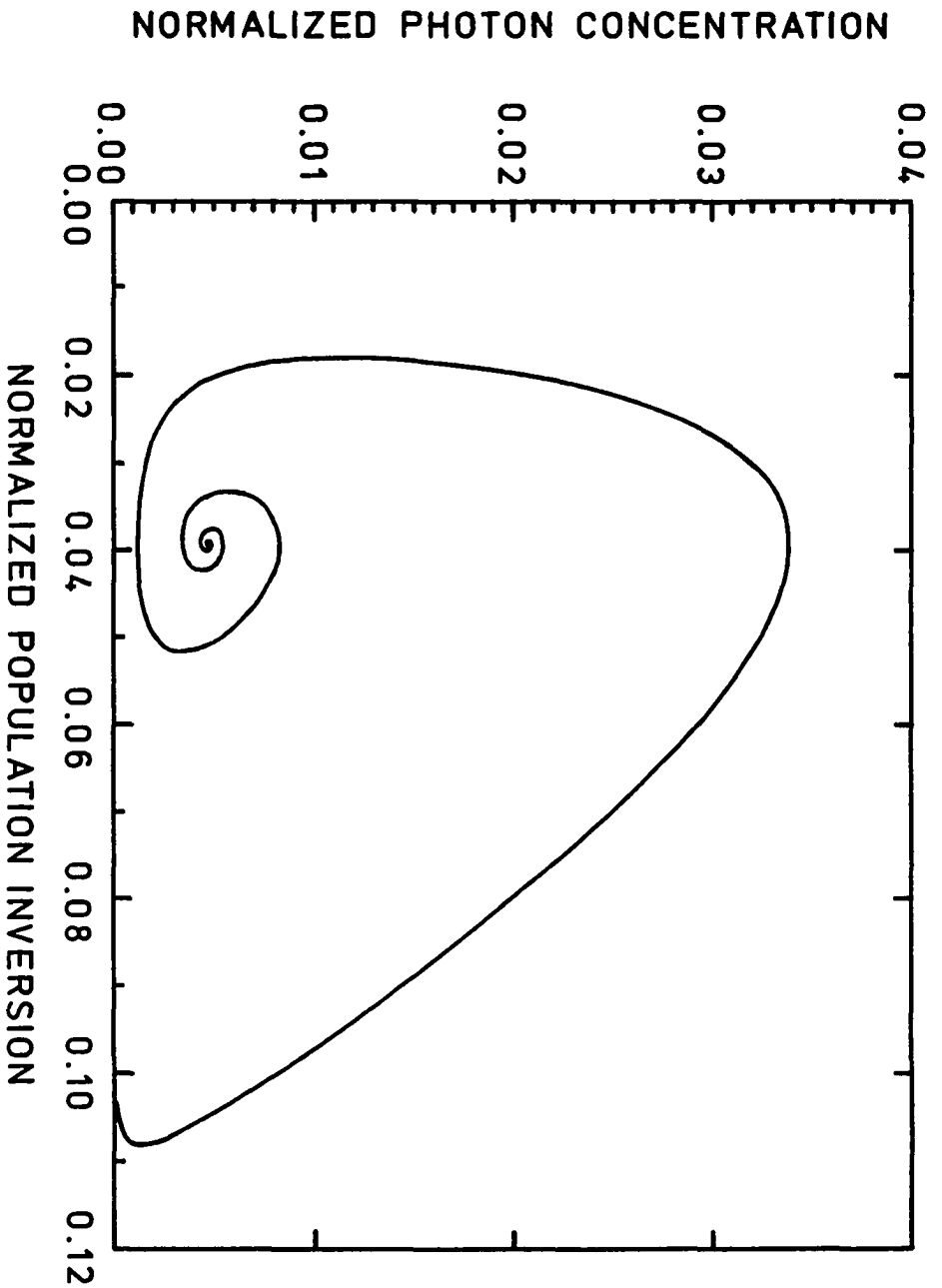

Figure 3.9 Phase plane portrait emphasizing the reduction in oscillaotry behavior for the system in which $W_p = .001 ns^{-1}$ and $\tau_c = 5.0 ns$

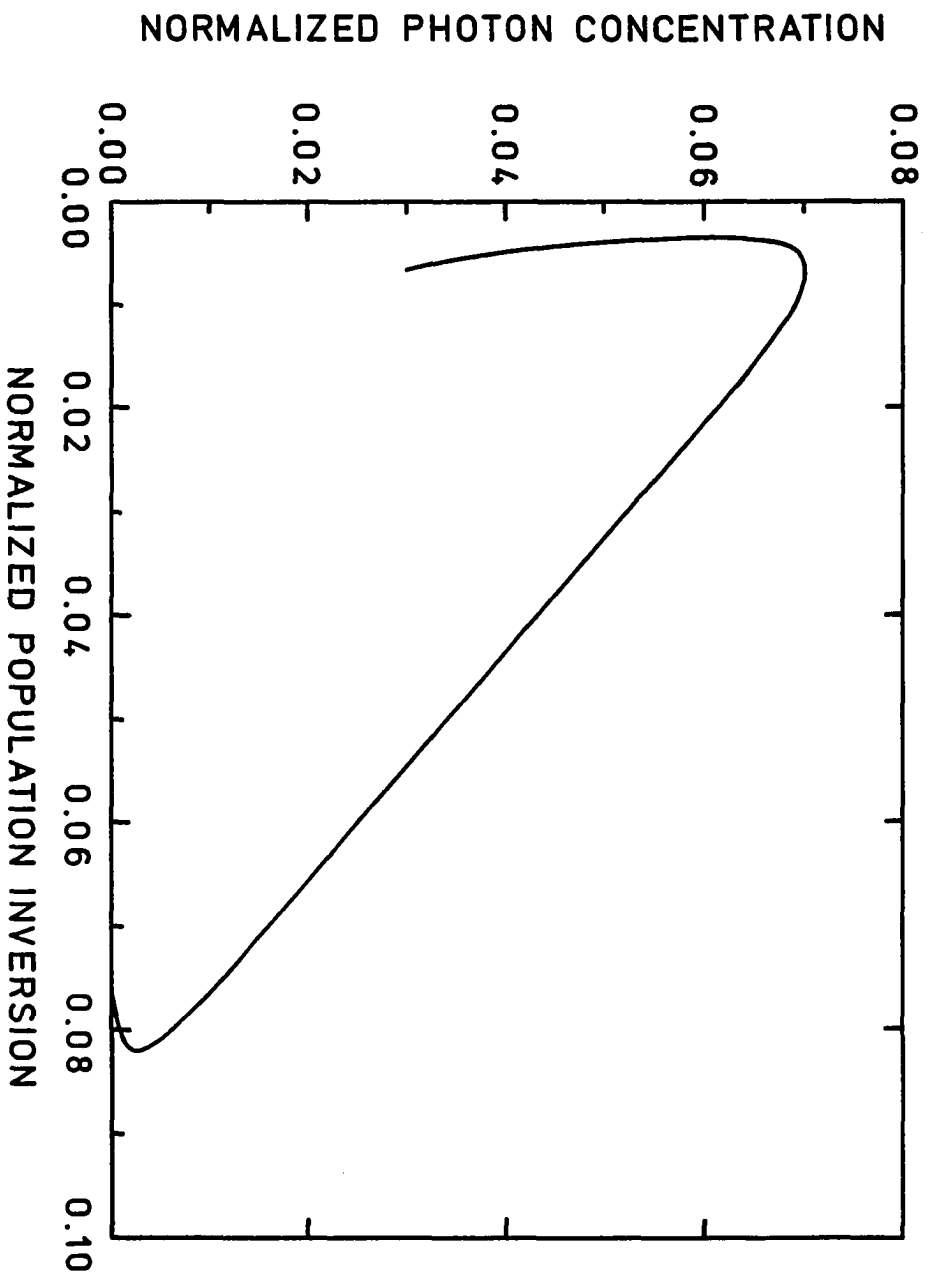

Figure 3.10 Phase plane portrait demonstrating the absence of oscillations for the system in which W_p to .01ns^{-1} and τ_c=30.0ns

A similar study was conducted with τ_c held constant and varying W_p. Figure 3.11 displays the cubic discriminant for $\tau_c = 5.0ns$ and $.005ns^{-1} \leq W_p \leq 0.1ns^{-1}$. Oscillations are predicted for an approximate range $.005^{-1} \leq W_p \leq .04ns^{-1}$. Figs. 3.12-3.15 give the computer results for $\tau_c = 5.0ns$ and $W_p = .01ns^{-1}$ and $W_p = .1ns^{-1}$, respectively. Phase portraits are given in Figs. 3.16 and 3.17.

Figure 3.18 shows a typical computation for a system in which the pump pulse has a Gaussian time dependence and no injection signal is present. In this case $W_p = .01ns^{-1}$. Initially, the system is in a quiescent state and at $t = 0$, the pump is turned on. The population inversion follows the leading edge of the pump pulse and increases until the active ions have absorbed the photons in the pump beam. When the photon concentration in the active medium is sufficiently large, there is a rapid decrease in the population inversion and stimulated emission occurs. In this case the pump is negligible after the laser pulse so there is no further growth of excited state ions and the system approaches the quiescent state once again. This type of dynamic behavior of the solutions is predicted by Theorem 3.5 for the case of an integrable time dependence of the pump pulse.

The value of W_p was varied from $.05ns^{-1}$ to $1.0ns^{-1}$ by factors of two. It is evident from Figure 3.19 that the larger the value of W_p, the earlier stimulated

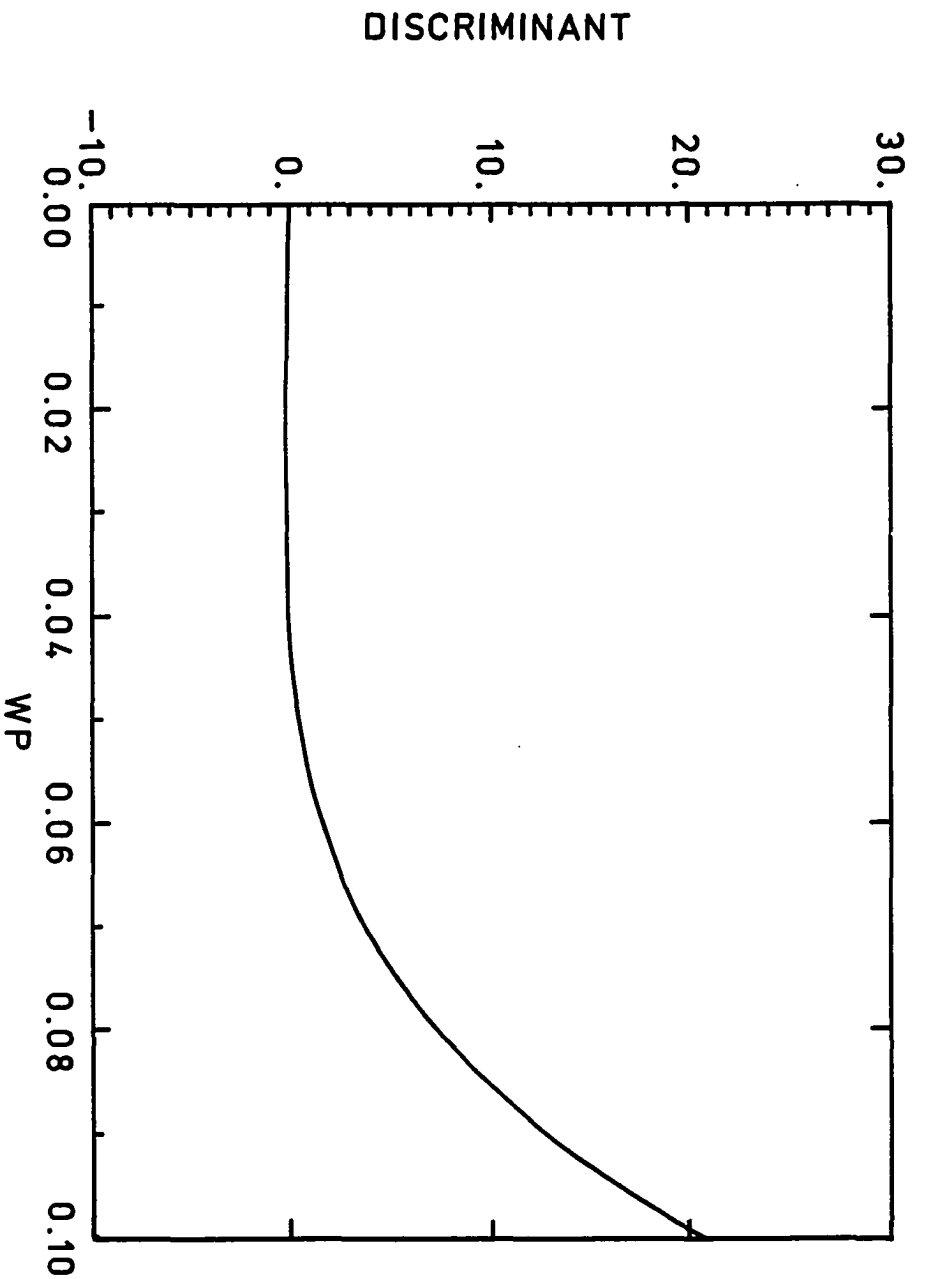

Figure 3.11 The cubic discriminant of a system in which τ_c is fixed at 5.0ns as a functin of W_p

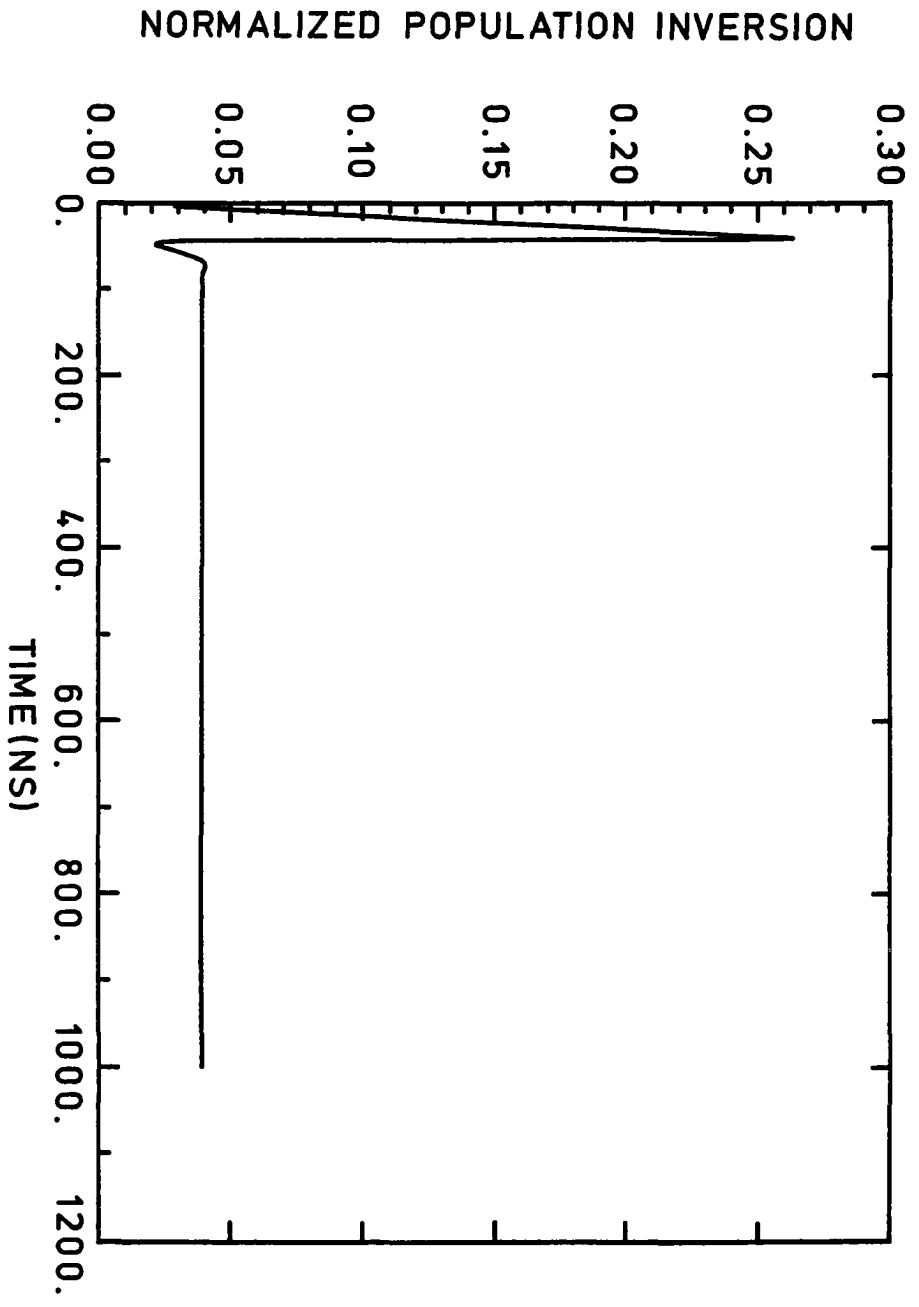

Figure 3.12 The reduction in oscillatory behavior in the normalized population inversion by increasing W_p to .01ns^{-1}. τ_c is fixed at 5.0ns

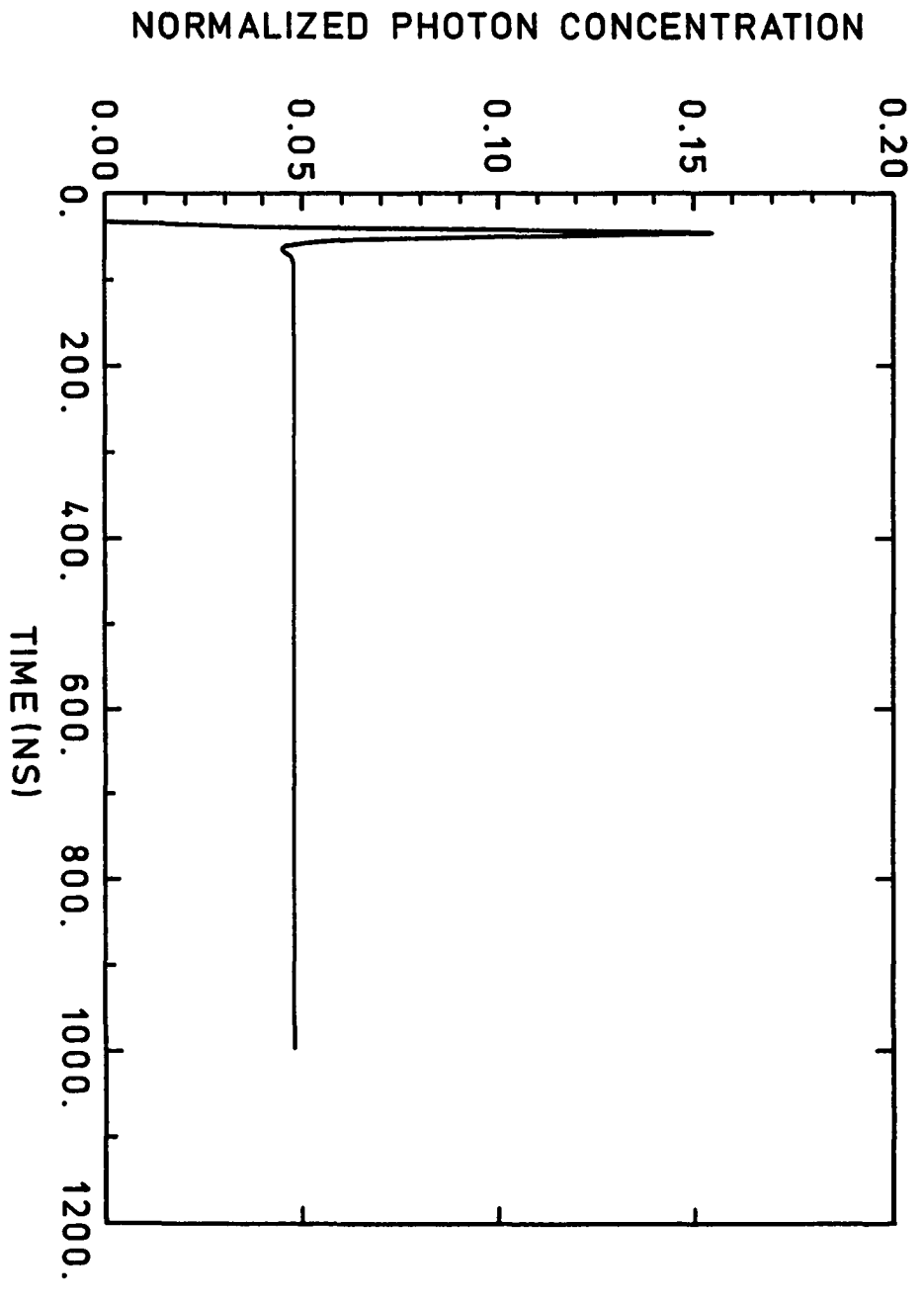

Figure 3.13 The evolution of the normalized photon concentration for the system in which τ_c=5.0ons and W_p=.01ns^{-1}

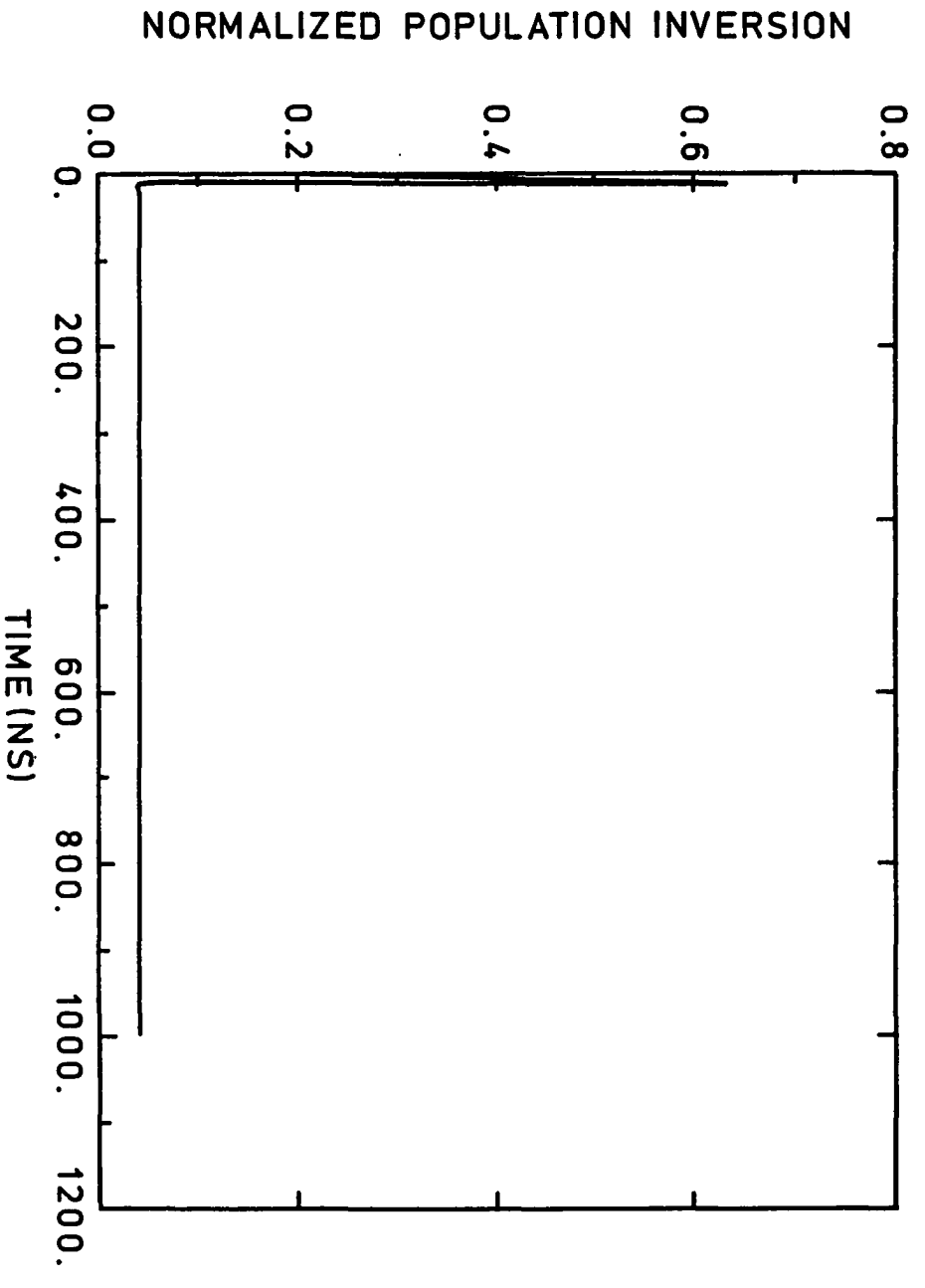

Figure 3.14 Computed curve showing the absence of oscillations in the normalized population inversion for the parameter values τ_c=5.0ns and W_p=.1ns^{-1}

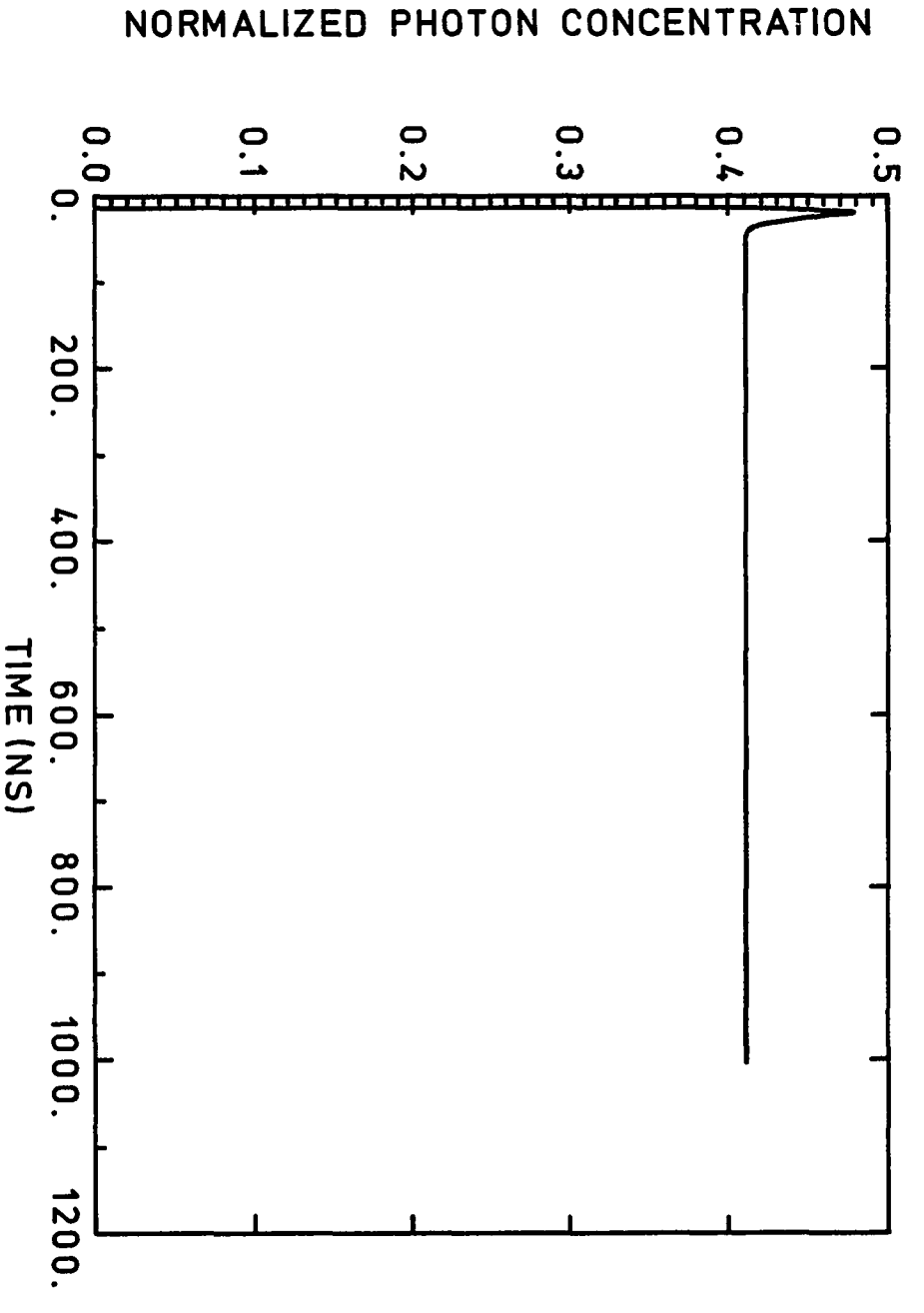

Figure 3.15 The normalized photon concentration for system in which τ_c=5.0ns and W_p=.1ns^{-1}

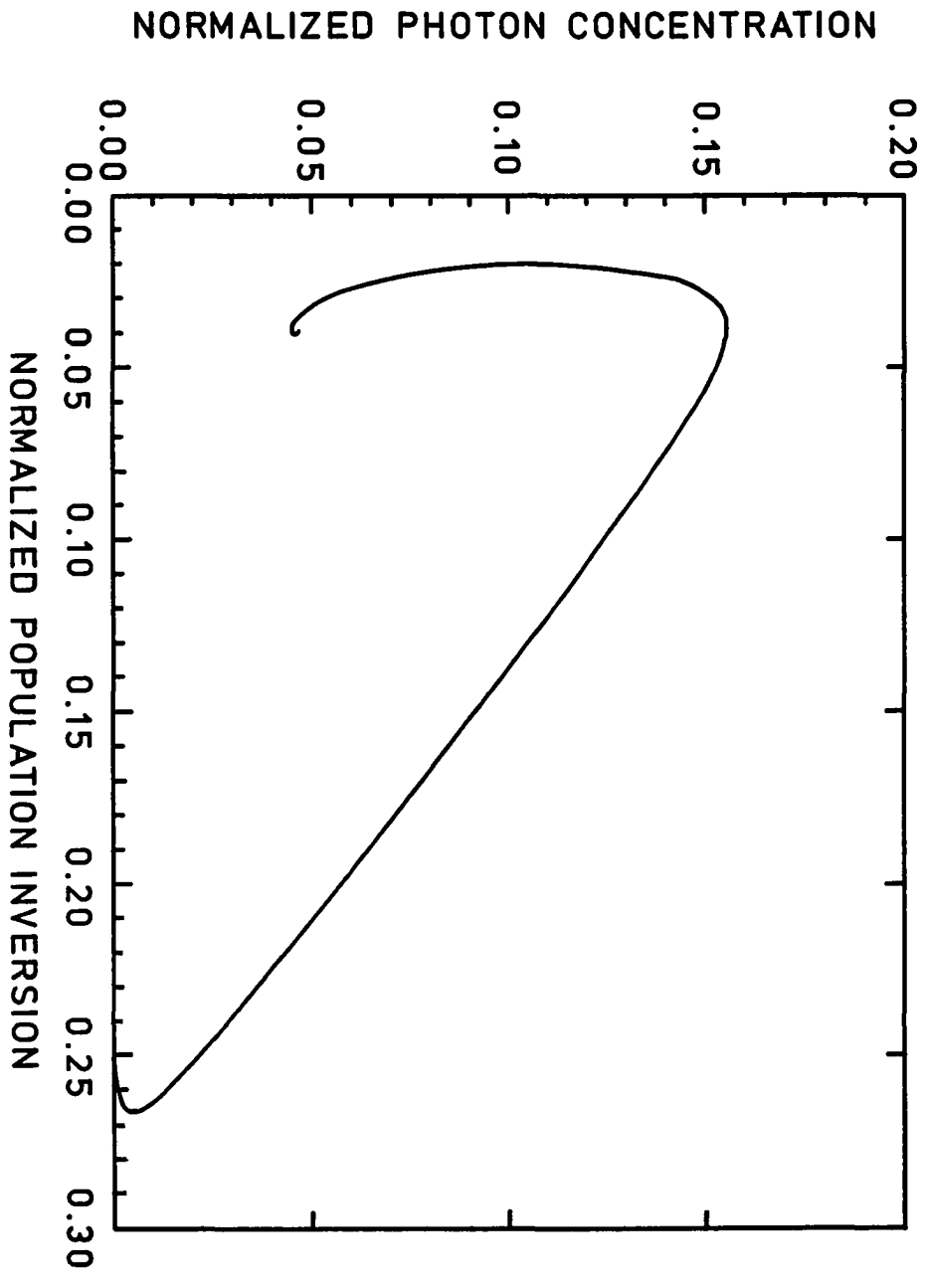

Figure 3.16 Phase plane portrait for type system in which τ_c=5.0ns and W_p=.01ns^{1}

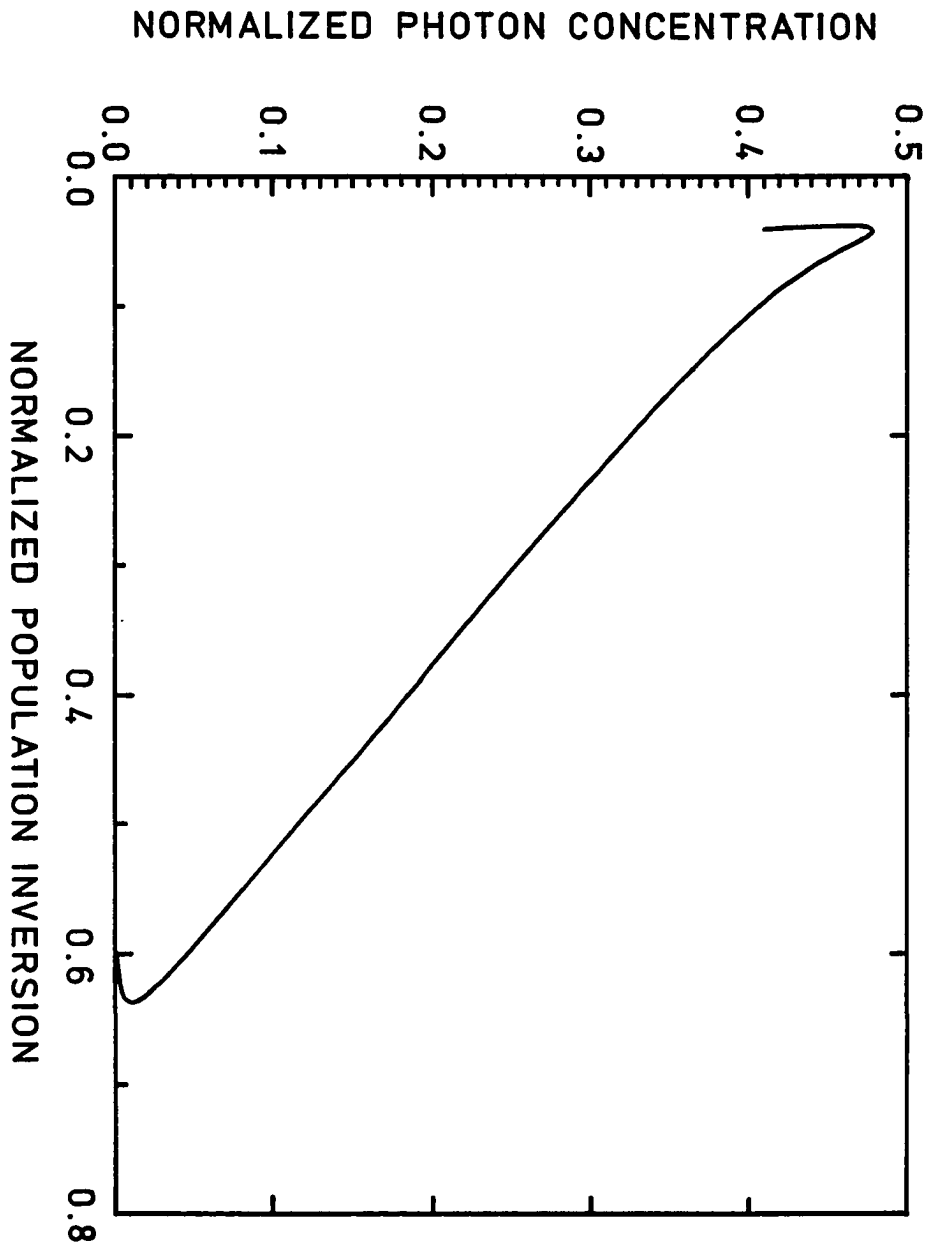

Figure 3.17 Phase plane portrait for the system in which τ_c=5.0ns and W_p=.1ns^{-1}

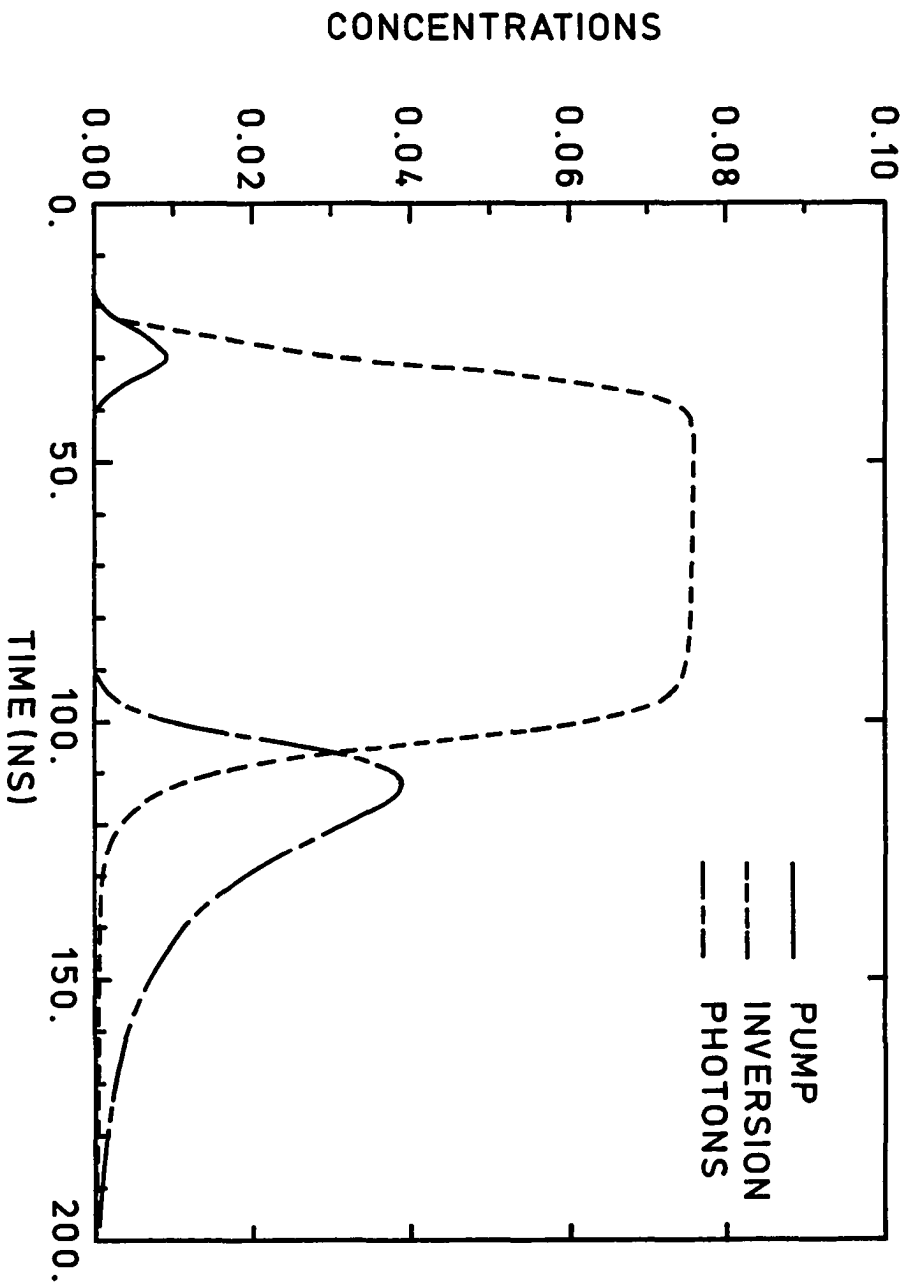

Figure 3.18 Typical computation for Gaussian pump pulse. Here, $W_p = .01 ns^{-1}$

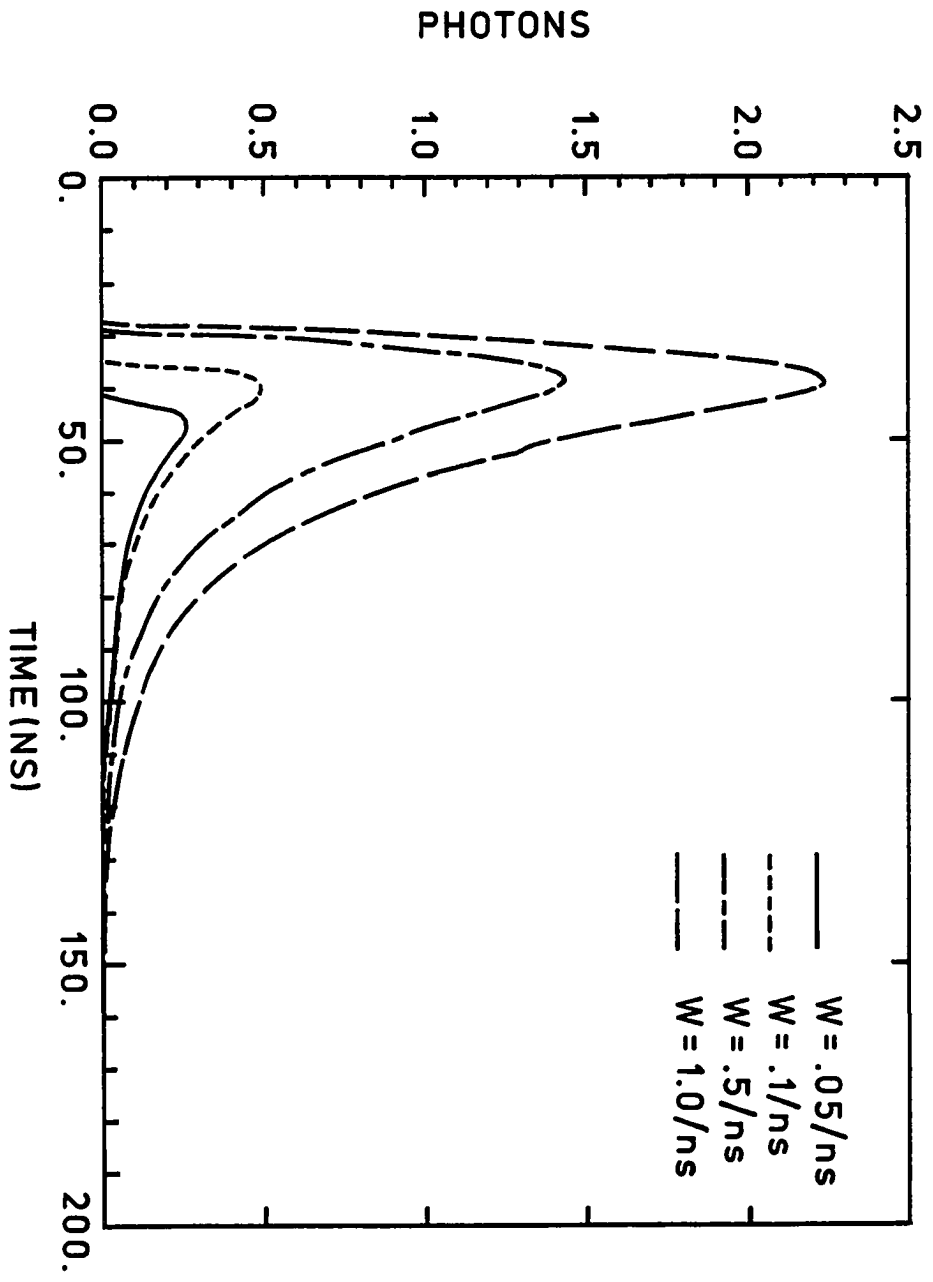

Figure 3.19 Curves showing the effect of increasing the intensity of the pump beam. The strength of the output pulse increases with pump energy

emission will occur and the stronger it will be. The efficiency of the RKF algorithm was studied for the different pumping rates. The algorithm required 822 evaluations of the derivatives for the case when $W_p = .01ns^{-1}$ but as W_p was increased, the number of derivative evaluations increased significantly to 1944 for $W_p = .1ns^{-1}$ and 6612 evaluations for $W_p = 1.0ns^{-1}$. The growth in the number of derivative evaluations as a function of pumping rate is shown in Figure. 3.20.

For larger values of W_p, the RKF algorithm required an unreasonable number of iterations. In excess of 67000 derivative evaluations for the case of $W_p = 500ns^{-1}$ were required to compute solutions from $t = 0$ to $t = 44ns$. A backward difference method significantly improved computing effort, requiring 17000 derivative evaluations and 3700 Jacobean evaluations to compute solutions over the interval $0 \leq t \leq 200ns$ (Figure 3.21). For high values of W_p, the system of differential equations becomes stiff, resulting in considerable effort to compute solutions.

The effect of introduction of an injected signal into the system was studied by varying the value of I. Figure 3.22 shows the results of varying I from $1.0ns^{-1}$ to $1.0 \times 10^{-4}ns^{-1}$ to $1.0 \times 10^{-6}ns^{-1}$. It is clear from the plot that the presence of an injected beam speeds up the onset of the stimulated emission. The time at which the peak of the photon concentration occured as a function of increasing injection strength is displayed in Fig. 3.23 The efficiency of the RKF algorithm did not appear to be adversely affected by increasing the value of I. The solutions

required no more than 846 derivative evaluations for these cases.

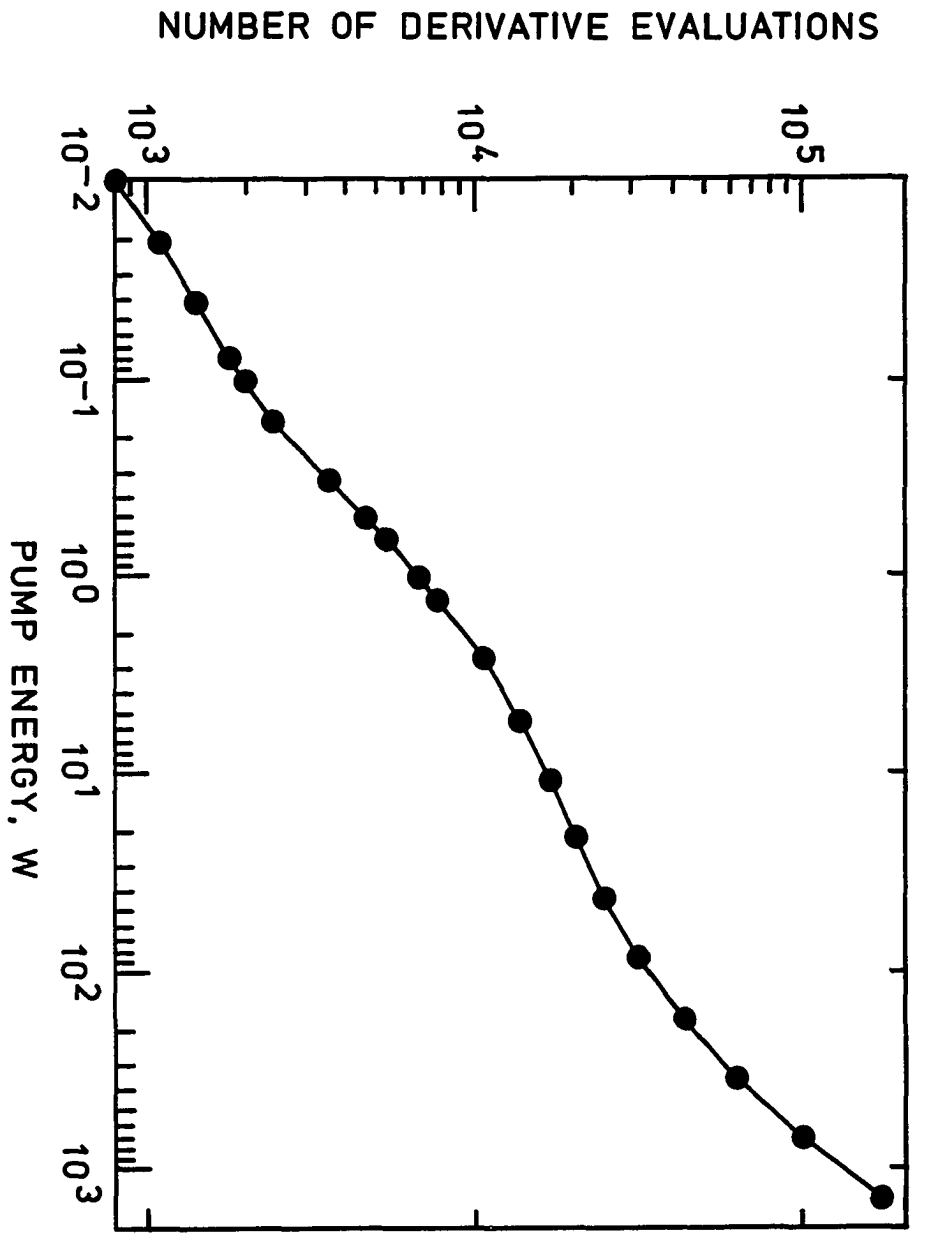

Figure 3.20 Stiffening of the equations with increasing pump energy displayed in terms of the number of derivative evaluations required in the Runge_kutta-Fehlberg algorithm

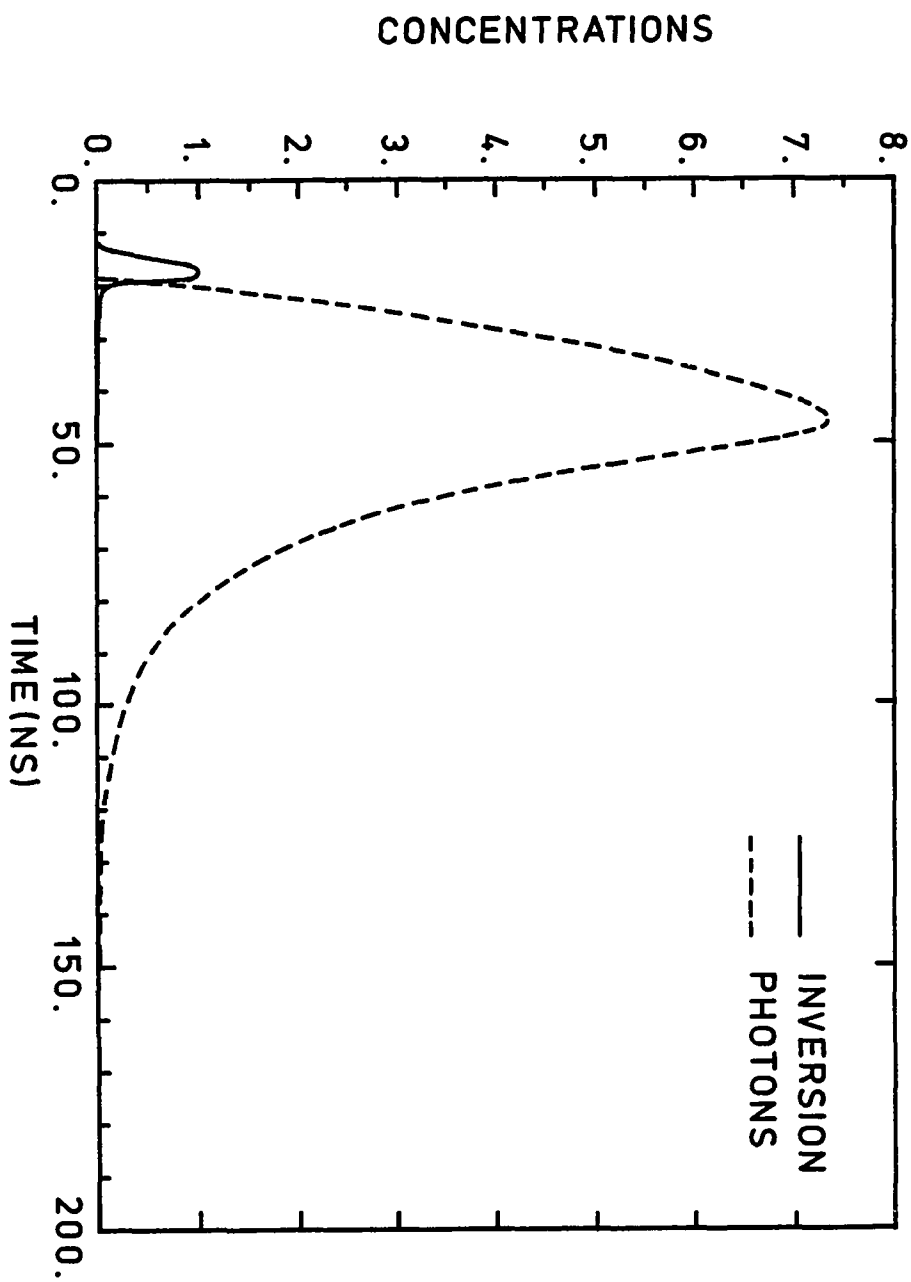

Figure 3.21 Extreme values of pump energy computed using a backward difference algorithm on the CYBER CY173

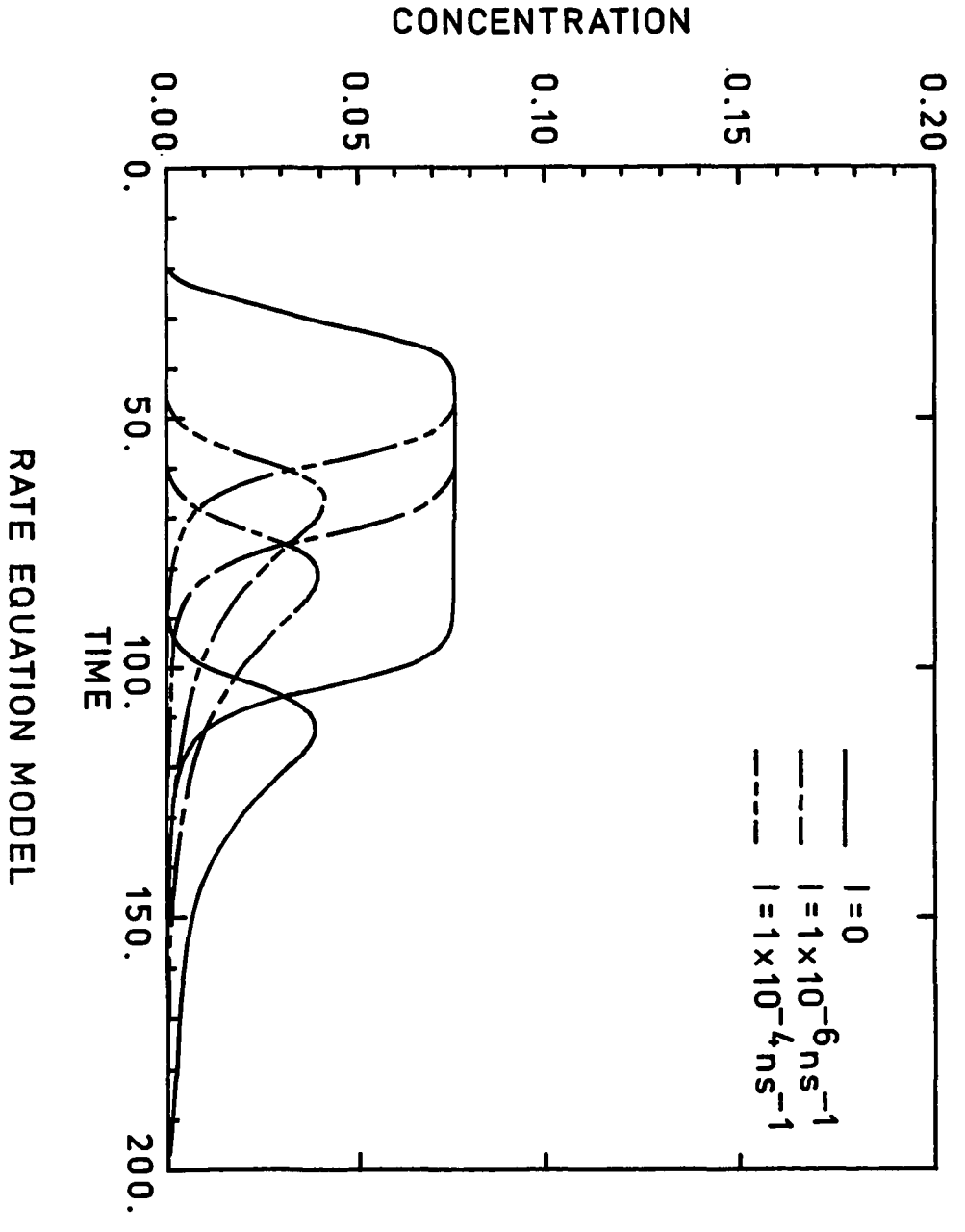

Figure 3.22 Curves showing the variations in the population inversion and photon concentration resulting from varying the injection energy. Increasing the strength of the injection pulse speeds up the onset of stimulated emission

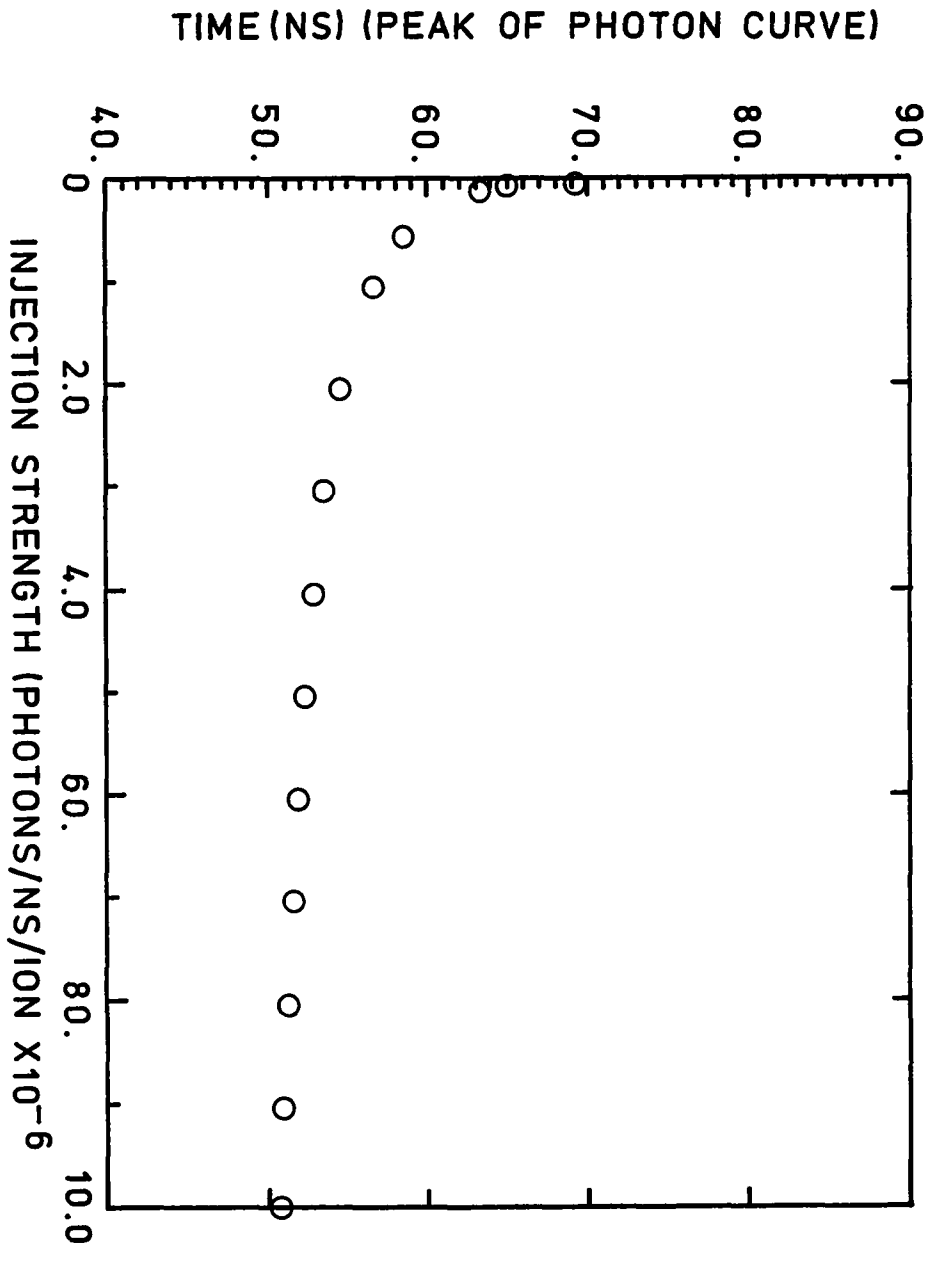

Figure 3.23 Data showing the decrease in time required for the photon pulse to reach its peak as a function of increased injection strength

Chapter 4

Analysis of the Spatial and Temporal Model

4.1 The Spatial and Temporal Model

In this chapter the model of the spatial and temporal dynamics in a ring laser cavity is considered. The model consists of the system of partial differential equations (2.4.1) and (2.4.3) together with the initial conditions (2.5.1), (2.5.2) and boundary conditions (2.5.4). Qualitative properties of the solutions are analyzed and the numerical procedure for generating approximate solutions is developed. The well-posedness of the problem is not addressed.

It is assumed that the emission cross section, $\sigma(\lambda)$, tends to zero sufficiently fast so that the integral

$$\int_0^\infty \sigma(\lambda)\Phi(x,t;\lambda)d\lambda \tag{4.1.1}$$

exists for $0 \leq x \leq \ell$ and all t In order to study the system of equations, the significant part of the emission spectrum of Ti:Sapphire is divided into m intervals,

each having length $\Delta\lambda$. Then the integral in (4.1.1) is approximated by

$$\begin{aligned}\int_0^\infty \sigma(\lambda)\Phi(x,t;\lambda)d\lambda &\sim \int_{\lambda_0}^{\lambda_m} \sigma(\lambda)\Phi(x,t;\lambda)d\lambda \\ &\approx \sum_{j=1}^{m} \frac{1}{2}\left[\sigma(\lambda_{j-1}) + \sigma(\lambda_j)\right]\Phi(x,t;\bar{\lambda}_j)\Delta\lambda\end{aligned}$$

where $\bar{\lambda}_i = \frac{1}{2}[\lambda_{i-1} + \lambda_i]$ for $i = 1,...,m$. Then the model is modified to

$$\begin{aligned}\frac{\partial n(x,t)}{\partial t} &= c_{11}N(x,t) + c_{12}N_1(x,t) - \gamma\beta N(x,t)\sum_{i=1}^{m}\sigma_i\Phi(x,t;\bar{\lambda}_i)\Delta\lambda \\ &+ W(x,t)\left[\frac{n_T}{n_{\text{norm}}} - \gamma N_1(x,t) + N(x,t)\right]\end{aligned}$$

$$\frac{\partial n(x,t)}{\partial t} = c_{21}N(x,t) + c_{22}N_1(x,t) - \gamma\beta N(x,t)\sum_{i=1}^{m}\sigma_i\Phi(x,t;\bar{\lambda}_i)\Delta\lambda$$

$$\begin{aligned}\frac{1}{v\cdot\tau_{\text{norm}}}\frac{\partial\phi_\pm(x,t;\bar{\lambda}_i)}{\partial t} \pm \frac{\partial\phi_\pm(x,t;\bar{\lambda}_i)}{\partial x} &= \frac{1}{v\cdot\tau_{\text{norm}}}\left[f_\pm(x,t;\bar{\lambda}_i)[N(x,t) + (\gamma-1)N_1(x,t)\right] \\ &+ \left[n_{\text{norm}}\sigma_i N(x,t) - \alpha_i\right]\phi_\pm(x,t;\bar{\lambda}_i)\end{aligned}$$

for $0 \le x \le \ell$ and $i = 1,...,m$.

Here

$$\begin{aligned}\Phi(x,t;\bar{\lambda}_j) &= \phi_+(x,;\bar{\lambda}_j) + \phi_-(x,;\bar{\lambda}_j) \text{for each } j \\ \sigma_i &= \frac{1}{2}[\sigma(\lambda_{i-1}) + \sigma(\lambda_i)] \qquad i = 1,...,m \\ \alpha_i &= \frac{1}{2}[\alpha(\lambda_{i-1} + \alpha(\lambda_i)] \qquad j = 1,...,m, \text{ and} \\ f_\pm(x,\bar{\lambda}_i)[N(x,t) + (\gamma-1)N_1(x,t)] &= S_\pm(x,t;\bar{\lambda}_i) \text{ for each } i.\end{aligned}$$

In the remainder of the cavity,

$$\frac{1}{c \cdot \tau_{\text{norm}}} \frac{\partial \Phi_{\pm}(x,t;\bar{\lambda}_i)}{\partial t} \pm \frac{\partial \Phi_{\pm}(x,t;\bar{\lambda}_i)}{\partial x} = 0 \quad \text{for} \quad i = 1,...,m \tag{4.1.2}$$

describe the development of the photon density.

Let $\mathbf{u} = (N, N_1, W, \phi_{+_1}, \phi_{+_2}, ..., \phi_{+_m} \phi_{-_1} \phi_{-_2} .... \phi_m)^T$ be the $2m+3$ dimensional column vector that contains the dependent variables in the active medium, $0 \leq x \leq \ell$. Here $\phi_{\pm_i} = \phi_{\pm}(x,t;\lambda_i)$ for $i = 1,...,m$ and $0 \leq x \leq \ell$. Then the system (4.1.1) along with (2.4.2) can be written in matrix form

$$u_t + Au_x - B = 0 \tag{4.1.3}$$

where A is the diagonal matrix whose elements are $0, 0, \underbrace{v \cot \tau_{\text{norm}}, ..., v \cdot \tau_{\text{norm}}}, \underbrace{-v \cdot \tau_{\text{norm}}, ..., -v \cdot \tau_{\text{norm}}}$ and B is the column vector whose elements are given by the right hand sides of the equations in (4.1.1) and (2.4.2). The matrix A does not depend on u, so the system of partial differential equations is semilinear. Since A is diagonal and hence symmetric, the system is symmetric hyperbolic and A has a full set of $2m + 3$ characteristic values, ξ_j, $j = 1, 2, ..., 2m + 3$ [8]. Each equation is of the form

$$\frac{\partial u_j}{\partial t} + \xi_j \frac{\partial u_j}{\partial x} = b_j \quad , \quad j = 1, 2, ..., 2m + 3.$$

The $2m + 3$ solutions of

$$\det(A - \xi I) = 0$$

where $\xi = \dfrac{dx}{dt}$ define the characteristic directions of (4.1.3) at the point (x, y)[11]. Thus if s is a parameter along a characteristic curve, then u_j must satisfy the ordinary differential equation

$$\frac{du_j}{ds} = b_j$$

for each j along the characteristic.

A number of qualitative properties for the solutions of (4.1.3) can be determined by investigating the solutions along their respective characteristics. In addition, integrating along the characteristics provides a natural approach to solving the initial and boundary value problem numerically. The qualitative results and numerical analysis of the system are discussed in sections 4.2 and 4.3, respectively.

4.2 Some Qualitative Results

In the active region, $0 \leq x \leq \ell$, consider equations (4.1.1) for the laser dynamics and (2.4.2) for the pump pulse. Without loss of generality, assume that $n_{\text{norm}} = n_T$ and recall that

$$c_{11} = -\left(\frac{1}{\tau_2} + \frac{\gamma - 1}{\tau_{f\ell}}\right) \quad c_{12} = (1 - \gamma)\left[\frac{1}{\tau_2} + \frac{\gamma - 1}{\tau_{f\ell}} - \frac{1}{\tau_1}\right]$$
$$c_{21} = \frac{1}{\tau_{f\ell}} \qquad c_{22} = \frac{\gamma - 1}{\tau_{f\ell}} - \frac{1}{\tau_1}.$$

Assume that the physical parameters satisfy

$$\begin{aligned} 0 < \sigma_j, \alpha_j &< \infty \qquad j = 1, ..., m \\ f_{\pm}(x, \lambda_j) &> 0 \quad 0 \leq x \leq \ell \qquad j = 1, ..., m \\ \gamma &> 1 \\ 0 < \tau_1 << \tau_2 &< \tau_{f\ell} \\ \sigma_{ab}, \beta &> 0. \end{aligned} \tag{4.2.1}$$

The initial conditions are assumed to satisfy

$$\begin{aligned} & N(x,0) \geq 0 \\ & N_1(x,0) \geq 0 \\ & \phi_{\pm}(x,0;\lambda_j) \geq 0 \qquad j = 1, ..., m \\ & W(0,x) > 0 \end{aligned} \tag{4.2.2}$$

for $0 \leq x \leq \ell$ and

$$\Phi_{\pm}(x,0;\lambda_j) \geq 0 \qquad j = 1, ..., m$$

for $\ell \leq x \leq L$. The boundary conditions obey

$$\begin{aligned}
\phi_+(0^+,t;\lambda_j) &= A_1\Phi_+(L^-,t;\lambda_j) \qquad 0 < A_1 \leq 1 \\
\Phi_-(L^-,t;\lambda_j) &= A_2\phi_-(0^+,t;\lambda_j) \qquad 0 < A_2 \leq 1 \\
\Phi_+(\ell^+,t;\lambda_j) &= A_3\phi_+(\ell^-,t;\lambda_j) \qquad 0 < A_3 \leq 1 \\
\phi_-(\ell^-,t;\lambda_j) &= A_4\Phi_-(\ell^+,t;\lambda_j) \qquad 0 < A_3 \leq 1 \qquad (4.2.3)
\end{aligned}$$

for $t \geq 0$ and $j = 1,...,m$.

Lemma 1 *Let* $W(0,t) > 0$ *for* $0 \leq t < \infty$ *and*

$W(x,0) > 0$ for $0 \leq x \leq \ell$. Then for any x, $0 \leq x \leq \ell$,

$W(x,t) > 0, \quad 0 \leq t < \infty.$

Proof: $W(x,t)$ satisfies the partial differential equation

$$\frac{\partial W}{\partial t} + v \cdot \tau_{\text{norm}} \frac{\partial W}{\partial x} = -c[1 - \gamma N_1 - N]W, \text{ where } c > 0. \qquad (4.2.4)$$

If s is a parameter along a characteristic, i.e. $x = x(s)$ and $t = t(s)$ where $\frac{dt}{ds} = 1$ and $\frac{dx}{ds} = v \cdot \tau_{\text{norm}}$, then W satisfies the ordinary differential equation

$$\frac{dW}{ds} = -c[1 - \gamma N_1 - N]W$$

along the characteristics.

Then

$$W(s) = W(s_0)\exp\{-c\int_{s_0}^{s}[1 - \gamma N_1(x(\tau),t(\tau)) - N(x(\tau),t(\tau))]d\tau\}$$

where

$$W(s_0) = W(x(s_0), t(s_0))$$

and $(x(s_0), t(s_0))$ is a point on the initial line or on the boundary.

Therefore, since $W(s_0) > 0$ it follows that $W(s) > 0$ for all s. Then $W(x,t) > 0$ for all $t \geq 0$ and $0 \leq x \leq \ell$, which was to be proved.

The following results can now be shown.

Theorem 7 *Given the system of partial differential equations defined by (4.1.1) and (4.2.5) along with initial and boundary conditions given in (4.2.2), (4.2.3) and (4.2.4). If the physical parameters also satisfy (4.2.1), then*

(i) if $N(x,0) + \gamma N_1(x,0) < 1$ *for* $0 \leq x \leq \ell$, *then* $N(x,t) + \gamma N_1(x,t) < 1$ *for all* $t \geq 0$ *and* $0 \leq x \leq \ell$.

(ii) if $N(x,0) + \gamma N_1(x,0) \geq 1$ *for* $0 \leq x \leq \ell$, *then there exists* T *such that* $N(x,t) + \gamma N_1(x,t) < 1$ *for all* $t > T$ *and* $0 \leq x \leq \ell$.

(iii) $N(x,t) \geq 0, N_1(x,t) \geq 0$ *for all* $t \geq 0$ *and* $0 \leq x \leq \ell$ *and*

$\phi_{\pm}(x,t;\lambda_j) \geq 0$ *for* $j = 1,2,...,m$ *and* $t \geq 0, \quad 0 \leq x \leq \ell$.

Proof: (i) Suppose $N(x,0) + \gamma N_1(x,0) < 1, \quad 0 \leq x \leq \ell$. Then for each x, $N(x,t) + \gamma N_1(x,t) < 1$ for t close to zero.

Suppose there exists $X \leq \ell$ and T such that

$$N(X,T) + \gamma N_1(X,T) = 1$$

and $N(x,t) + \gamma N_1(x,t) < 1$ for $0 \leq t < T$ and $0 \leq x \leq \ell$.

Then, along the characteristic $x = X$, $\dfrac{\partial(N+\gamma N_1)}{\partial t} = \dfrac{d(N+\gamma N_1)}{dt}$ and so, at (T,X),

$$\begin{aligned} \frac{d}{dt}(N+\gamma N_1) &= (c_1+\gamma c_{21})N + (c_{12}+\gamma c_{22})N_1 \\ &\geq 0. \end{aligned}$$

Suppose $N(X,T) \geq 0$ and $N_1(X,T) \geq 0$. Since $N(X,T) + \gamma N_1(X,T) = 1, N(X,T)$ and $N_1(X,T)$ are not both zero. Now, $c_{11} + \gamma c_{21} < 0$ and $c_{12} + \gamma c_{22} < 0$, so it follows that at (T,X),

$$\frac{d}{dt}(N+\gamma N_1) < 0,$$

which contradicts

$$N(X,t) + \gamma N_1(X,t) < 1 \text{ for } 0 \leq t < T.$$

Now suppose that $N_1(X,t) < 0$. From the initial condition, $N_1(x,0) \geq 0$ for $0 \leq x \leq \ell$, so consider the two cases

$$\text{a)} N_1(x,0) > 0 \text{ for } 0 \leq x \leq \ell \text{ and}$$

$$\text{b)} N_1(x,0) = 0 \text{ for some } x,\ 0 \leq x \leq \ell.$$

a) If $N_1(x,0) > 0$, then for each x

$N_1(x,t) > 0$ for t sufficiently close to zero. Then there exists a point (X_1, T_1), $T_1 < T$, $X_1 \leq X$ such that $N_1(X_1, T_1) = 0$ and $N_1(x,t) > 0$ for $0 \leq x \leq \ell$ and $0 \leq t < T_1$.

Then, at (X_1, T_1),

$$\frac{dN_1}{dt} = \left[c_{21} + \beta \sum_{j=1}^{m} \sigma(\lambda_j)[\phi_{+j} + \phi_{-j}]\Delta\lambda \right] N \leq 0.$$

Suppose that $N(X_1, T_1) < 0$ and

$$\left[c_{21} + \beta \sum_{j=1}^{m} \sigma(\lambda_j)[\phi_{+j} + \phi_{-j}]\Delta\lambda \right] |_{(X_1,T_1)} \geq 0.$$

Then, since $N(X_1, 0) \geq 0$, there exists $T_2 < T_1$ such that $N(X_1, T_2) = 0$ and $N(X_1, t) \geq 0$ for $0 \leq t < T_2$.

So, at (T_2, X_1)

$$\frac{dN}{dt} = c_{12}N_1 + W[1 - \gamma N_1] > 0$$

since $c_{12} > 0$, $N_1(X_1, T_2) > 0$, $W(X_1, T_2 > 0$ and $1 - \gamma N_1(X_1, T_2) > 0$ which contradicts $N(X_1, t) \geq 0$ for $0 \leq t < T_2$. So $N(X_1, T_1) > 0$.

Suppose there exists a point $(\hat{X}, \hat{T})$ with $\hat{T} < T_1$ and $\hat{X} \leq X_1$ such that $N(\hat{x}, \hat{T}) < 0$. Then since $N(\hat{X}, 0) \geq 0$ there exists $\tilde{T} < \hat{T}$ such that $N(\hat{x}, \tilde{T}) = 0$ for and $N(\hat{X}, t) \geq 0$ for $0 \leq t < \tilde{T}$.

Then, at $(\hat{X}, \tilde{T})$, $\frac{dN}{dt} > 0$. So by similar argument, $N(\hat{X}, \hat{T}) \geq 0$. It follows that $N(x,t) \geq 0$ on the rectangle $[0, \ell] \times [0, T_1)$.

On the rectangle $[0,\ell] \times (0,T), N_1 > 0, N \geq 0$ and $N + \gamma N_1 < 1$, so now consider the case where

$$c_{21} + \beta \sum_{j=1}^{m} \sigma(\lambda_j)[\phi_+(X_1, T_1; \lambda_j) + \phi_-(X_1, T_1; \lambda_j)]\Delta\lambda \leq 0. \qquad (4.2.5)$$

Since $c_{21} > 0$, $\beta > 0$, $\sigma(\lambda_j) > 0$ and $\Delta\lambda > 0$ for $j = 1, ..., m$, (4.2.5) can be true only if for some j,

$$\phi_+(X_1, T_1; \lambda_j) < 0 \text{ or } \phi_-(X_1, T_1; \lambda_j) < 0.$$

Suppose $\phi_+(X_1, T_1; \lambda_j) < 0$.. Then there exists $\hat{T} < T_1$ and $\hat{X} < X_1$ such that $\phi_+(\hat{X}, \hat{T}, \lambda_j) = 0$ and $\phi_+(x, t; \lambda_j) < 0$ for $\hat{T} < t \leq T_1$ and $\hat{X} < X \leq X_1$. Then if s is a parameter along the characteristic through $(\hat{X}, \hat{T})$, at $(\hat{X}, \hat{T})$

$$\frac{d\phi_{+j}}{ds} = f(\hat{X}_j \lambda_j)[N + (\gamma - 1)N_1] > 0$$

since $f(\hat{X}; \lambda_j) > 0, N(\hat{X}, \hat{T}) \geq 0, (\gamma - 1)N_1(\hat{X}, \hat{T}) > 0$ which contradicts $\phi_+(x, t; \lambda_j) < 0$ for $\hat{T} < t \leq T_1$ and $\hat{X} < X \leq x_1$. Therefore, $\phi_+(X_1, T_1; \lambda_j) \geq 0$.

Now suppose $\phi_-(X_1, T_1, \lambda_j) < 0$. Then there exists $(\hat{X}, \hat{T})$, with $\hat{T} < T_1$ and $\hat{X} > X_1$ such that

$\phi_-(\hat{X}, \hat{T}; \lambda_j) = 0$ and $\phi_-(x, t; \lambda_j) < 0$ for $\hat{T} < t \leq T_1$ and $X_1 \leq x < \hat{X}$. Then at $(\hat{X}, \hat{T})$,

$$\frac{d\phi_{-j}}{ds} = f_-(\hat{X}, \lambda_j)[N + (\gamma - 1)N_1] > 0,$$

where s is a parameter along the characteristic through $(\hat{X}, \hat{T})$. This contradicts $\phi_-(x, t; \lambda_j) < 0$ for $\hat{T} < t \leq t_1$ and $\hat{X} < t \leq X_1$.

Therefore, $\phi_-(X_1, T; \lambda_j) \geq 0$.

Suppose now that $N(X_1, T_1) = 0$. Then, at (X_1, T_1),

$$\begin{aligned} \frac{dN}{dt} &= W > 0 \\ \frac{dN_1}{dt} &= 0. \end{aligned}$$

Then look at

$$\begin{aligned} \frac{d^2N_1}{dt}(x,t) &= c_{21}\frac{dN}{dt}(x,t) + c_{22}\frac{dN_1}{dt}(x,t) \\ &+ \beta\left[\frac{dN}{dt}(x,t)\sum_{j=1}^{m}\sigma(\lambda_j)[\phi_{+_j} + \phi_{-_j}]\Delta\lambda\right. \\ &+ \left. N(x,t)\sum_{j=1}^{m}\frac{d}{dt}[\phi_{+_j} + \phi_{-_j}]\Delta\lambda.\right] \end{aligned}$$

At (X_1, T_1)

$$\frac{d^2N_1}{dt} = c_{21}W + \beta W\sum_{j=1}^{m}\sigma(\lambda_j)[\phi_{+_j} + \phi_{-_j}]\Delta\lambda > 0$$

since

$c_{21} > 0$, $W(X_1, T_1) > 0, \beta > 0$, $\sum_{j=1}^{m}\sigma(\lambda_j)[\phi_+(X_1, T_1, \lambda_j) + \phi_-(X_1, T_1, \lambda_j)]\Delta\lambda \geq 0$.

This contradicts $N_1(X_1, t) \geq 0$ for $0 \leq t \leq T_1$. Therefore, $N_1(X, T) \geq 0$.

Suppose that $N(X, T) < 0$. Then there exists $\hat{T} < T$ such that $N(X, \hat{T}) = 0$ and $N(X, t) \geq 0$ for $0 \leq t < \hat{T}$. At $(X, \hat{T})$,

$$\frac{dN}{dt} - c_{21}N_1 + W[1 - \gamma N_1] > 0$$

which contradicts the fact that $N(X,t) \geq 0$ for $0 \leq t \leq \hat{T}$.

Therefore $N(X,T) \geq 0$.

At least one of $N_1(X,T)$ and $N(X,T)$ is strictly positive, so suppose $N_1(X,T) > 0$ and $N(X,T) = 0$. Then, at (X,T),

$$\frac{d(N+\gamma N_1)}{dt} = (c_{12} + \gamma c_{22})N_1 < 0$$

since $c_{12} + \gamma c_{22} < 0$.

Likewise, if $N(X,T) > 0$ and $N_1(X,T) = 0$

$$\frac{d(N+\gamma N_1)}{dt} = (c_{11} + \gamma c_{21})N < 0$$

since $c_{11} + \gamma c_{21} < 0$.

In either case,

$$\frac{d(N+\gamma N_1)}{dt} < 0$$

which is a contradiction to $N(X,t) + \gamma N_1(X,t) < 1$ for $0 \leq t < T$.

Therefore,

$N(x,t) + \gamma N_1(x,t) < 1$ for $0 \leq t < \infty$ and $0 \leq x \leq \ell$

when $N(x,0) + \gamma N_1(x,0) < 1$ and $N_1(x,0) > 0$ for $0 \leq x \leq \ell$.

(b) Now suppose $N_1(x,0) = 0$ for some x, $0 \leq x \leq \ell$.

Then

$$\begin{aligned} \frac{dN_1(x,0)}{dt} &= N(x,0)[c_{21} + \beta \sum_{j=1}^{m} \sigma(\lambda_j)[\phi_+(x,0;\lambda_j) + \phi_-(x,0;\lambda_j)]\Delta\lambda \\ &\geq 0 \end{aligned}$$

since $c_{21} > 0$, $\beta > 0$, $\sigma(\lambda_j) > 0$ for $j = 1, ..., m$ and $\Delta\lambda > 0$.

Since $c_{21} + \beta\sum_{j=1}^{m}\sigma(\lambda_j)[\phi_+(x,0;\lambda_j) + \phi_-(x,0;\lambda_j)]\Delta\lambda > 0$, it follows that

$$\frac{dN_1(x,0)}{dt} = 0 \quad \text{if and only if} \quad N(x,0) = 0.$$

Now, if $N(x,0) = 0$, then

$$\frac{dN_1(x,0)}{dt} = 0 \quad \text{and}$$

$$\frac{d^2N_1}{dt^2} = c_{21}W + \beta W\sum_{j=1}^{m}\sigma(\lambda_j)[\phi_+(x,0;\lambda_j) + \phi_-(x,0;\lambda_j)]\Delta\lambda > 0$$

In addition, it is clear that $\frac{dN_1}{dt} > 0$ at $(x,0)$ if $N(x,0) > 0$.

Therefore, if $N_1(x,0) = 0$, then $N_1(x,t) > 0$ for t close to zero. Then the arguments in the previous case can be used to obtain the desired result.

(ii) The proof of (i) shows that if $N(x,0) + \gamma N_1(x,0) = 1$ for $0 \le x \le \ell$, then $N(x,t) + \gamma N_1(x,t) < 1$ for all $t > 0$ and $0 \le x \le \ell$.

Suppose for some x, $N(x,0) + \gamma N_1(x,0) > 1$. Then for some t close to zero

$$\begin{aligned}\frac{d}{dt}[N + \gamma N_1] &= (c_{11} + \gamma c_{21})N + (c_{12} + \gamma c_{22})N_1 \\ &< 0\end{aligned}$$

since $c_{11} + \gamma c_{21} < 0$, $c_{12} + \gamma c_{22} < 0$, and $N(x,0) + \gamma N_1(x,0) > 1$ implies that at least one of $N(x,0) + \gamma N_1(x,)$ is strictly positive.

Now suppose there exists $\xi \geq 1$ since that $N(x,t) + \gamma N_1(x,t) \geq \xi \geq 1$ for all t. Then

$$\begin{aligned} \frac{d(N+\gamma N_1)}{dt} &= (c_{11}+\gamma c_{21})(N+\gamma N_1) + (c_{12}+\gamma c_{22} - \gamma(c_{11}+\gamma c_{21}))N_1 \\ &\leq (c_{11}+\gamma c_{21})\xi \end{aligned}$$

since $c_{12} + \gamma c_{22} - \gamma(c_{11} + \gamma c_{21}) < 0$ and $c_{11} + \gamma c_{21} < 0$.

Integrating along the characteristic,

$$N(x,t) + \gamma N_1(x,t) - [N(x,0) + \gamma N_1(x,0)] \leq (c_{11} + \gamma c_{21})\xi t$$

so

$$N(x,t) + \gamma N_1(x,t) \leq (c_{11} + \gamma c_{21})\xi t + [N(x,0) + \gamma N_1(x,0)].$$

Thus

$$\lim_{t\to\infty}[N(x,t) + \gamma N_1(x,t)] = -\infty$$

which contradicts $N(x,t) + \gamma N_1(x,t) \geq \xi \geq 1$ for all t.

Hence, there exists T such that $N(x,T) + \gamma N_1(x,T) = 1$ and $N(x,t) + \gamma N_1(x,t) < 1$ for t close T. The proof of (i) can now be used to establish the desired result.

(iii) The arguments in (i) show that N and N_1 are nonnegative whenever $N + \gamma N_1 < 1$. Therefore if $N(x,t) + \gamma N_1(x,t) < 1$ for $0 \leq x \leq \ell$, it follows that $N(x,t) \geq 0$ and $N_1(x,t) \geq 0$ for all t and $0 \leq x \leq \ell$.

Suppose there exists (X,T) such that $N(x,t) \geq 0$ and $N_1(x,t) \geq 0$ for $0 \leq x \leq X$ and $0 \leq t \leq T$ and also $\phi_+(X,T;\lambda_j) < 0$ for some j. Then there exists (X_1,T) such that

$$\phi_+(X_1,T_1;\lambda_j) = 0 \quad \text{and}$$

$$\phi_+(x,t;\lambda_j) < 0 \quad \text{for} \quad T_1 < t < T \quad \text{and} \quad x_1 < x < X.$$

If s in a parameter along the characteristic through (X_1,T_1), at (X_1,T_1),

$$\frac{d\phi_{+j}}{ds} = f_+(X_1;\lambda_j)[N + (\gamma - 1)N_1] \geq 0$$

which is a contradiction. Therefore

$$\phi_+(x,t;\lambda_j) \geq 0 \text{ for } j = 1,...,.,0 \leq x \leq \ell, \text{ and } 0 \leq t < \infty.$$

Similarly, if there exist (X,T) such that $\phi_-(X,T;\lambda_j) < 0$ for some j, then there exists (X_1,T_1) such that

$$\phi_-(X_1,T_1;\lambda_j) = 0 \quad \text{and}$$

$$\phi_-(X_1,T_1;\lambda_j) < 0 \text{ for } T_1 < t < T \text{ and } X < x < X_1.$$

Then if s is a parameter along the characteristic through (X_1,T_1), at (X_1,T_1),

$$\frac{d\phi_{-j}}{ds} = f_-(X_i;\lambda_j)[N + (\gamma - 1)N_1] \geq 0$$

which is a contradiction. Therefore $\phi_-(x,t;\lambda) \geq 0$ for $0 \leq x \leq \ell$ and all t.

Finally, suppose that

$N(x,0) + \gamma N_1(x,0) > 1$ for some x. Then choose T so that $N(x,T) + \gamma N_1(x,T) = 1$ and $N(x,t) + \gamma N_1(x,t) > 1$ for $0 \leq t < T$. Suppose there exists T_1 such that $N(x,T_1) < 0$. Then choose $T_2 < T_1 < T$ such that $N(x,T_2) = 0$ and $N(x,t) \geq 0$ for $0 \leq t \leq T_2$. Then, at (x,T_2),

$$\frac{dN}{dt} = c_{12}N_1 > 0$$

since $c_{12} > 0$ and $N_1(x,T_2) > 0$, which is a contradiction. Therefore $N(x,t) \geq 0$ for all t.

Now, if there exists T_1 such that $N_1(x,T_1) < 0$, then choose $T_2 < T_1 < T$ such that $N_1(x,T_2) = 0$ and $N_1(x,t) \geq 0$ for $0 \leq t \leq T_2$. Then, at (x,T_2),

$$\frac{dN_1}{dt} = N[c_{21} + \beta \sum_{j=1}^{m} \sigma(\lambda_j)][\phi_{+_j} + \phi_{-_j}]\Delta\lambda > 0$$

since $N(x,T_2) > 0$ and $c_{21} + \beta \sum_{j=1}^{m} \sigma(\lambda_j)][\phi_{+_j} + \phi_{-_j}]\Delta\lambda > 0$. Therefore, by similar reasoning, $N_1(x,t) \geq 0$ for all t.

The following corollary can now be proved.

Corollary 1 *Let W be as in Lemma 4.1. If $W(0,t)$ is an integrable function of t, then for fixed x, $0 \leq x \leq \ell$, $W(x,t)$ is an integrable function of t.*

Proof: Fix $x = \hat{x}, 0 \leq \hat{x} \leq \ell$. Then $W(\hat{x},t)$ is a continuous function of t.

Let T be such that $N(\hat{x},T) + \gamma N_1(\hat{x},T) < 1$ for $t > T$. If $T > \dfrac{1}{v \cdot \tau_{\text{norm}}}\hat{x}$, then consider the integral

$$\int_0^t W(\hat{x},\tau)d\tau = \int_0^{\frac{1}{v\cdot\tau_{\text{norm}}}\hat{x}} W(\hat{X},\tau)d\tau + \int_{\frac{1}{v\cdot\tau_{\text{norm}}}\hat{x}}^{T} W(\hat{x},\tau)d\tau + \int_T^t W(\hat{x},\tau)d\tau.$$

Otherwise consider

$$\int_0^t W(\hat{x},\tau)d\tau = \int_0^{\frac{1}{v\cdot\tau_{\text{norm}}}\hat{x}} W(\hat{x},\tau)d\tau + \int_{\frac{1}{v\cdot\tau_{\text{norm}}}\hat{x}}^{t} W(\hat{x},\tau)d\tau.$$

By continuity $\int_0^{\frac{1}{v\cdot\tau_{\text{norm}}}\hat{x}} W(\hat{x},\tau)d\tau$ and $\int_{\frac{1}{v\cdot\tau_{\text{norm}}}\hat{x}}^{T} W(\hat{x},\tau)d\tau$ exist.

So look at $\int_{\frac{1}{v\cdot\tau_{\text{norm}}}\hat{x}}^{t} W(\hat{x},\tau)d\tau$. By the lemma, $W(x) = W(s_0)\exp[-c\int_{s_0}^{s}[1-\gamma N_1 - N]d\tau]$ where s is a parameter along the characteristic through $(\hat{x},t)$ and s_0 is a parameter along the boundary. Since every characteristic to the right of the line $x = (v\cdot\tau_{\text{norm}})t$ intersects the t axis, choose $s_0 = t_0$. Then $\frac{dt}{ds} = 1$ implies $t - t_0 = s - s_0$ so that $t = s$ and $\frac{dx}{ds} = v\cdot\tau_{\text{norm}}$ implies $x - x_0 = v\cdot\tau_{\text{norm}}(s - s_0)$ so that $x = v\cdot\tau_{\text{norm}}(t - t_0)$ since $x_0 = 0$. Therefore $t_0 = t - \frac{1}{v\cdot\tau_{\text{norm}}}\hat{x}$ and so it follows that

$$\begin{aligned} W(t,\hat{x}) &= W(0,t_0)\exp[-c\int_{t_0}^{t}[1-\gamma N_1 - N]d\tau] \\ &= W(0,t_0)\exp[-c\int_{t-\frac{1}{v\cdot\tau_{\text{norm}}}\hat{x}}^{t}[1-\gamma N_1 - N]d\tau] \end{aligned}$$

Since $0 < 1-\gamma N_1 - N \leq 1$ for $t \geq T$ and $0 \leq x \leq \ell$, it follows that for $t \geq T$

$$\exp\left[-c\int_{t-\frac{1}{v\cdot\tau_{\text{norm}}}\hat{x}}^{t}[1-\gamma N_1 - N]d\tau\right] < 1.$$

Therefore, if $T < \frac{1}{v \cdot \tau_{norm}} \hat{x}$

$$\int_0^t W(\hat{x},\tau)d\tau = \int_0^{\frac{1}{v\cdot\tau_{norm}}\hat{x}} W(\hat{x},\tau)d\tau + \int_{\frac{1}{v\cdot\tau_{norm}}\hat{x}}^t W(\hat{x},\tau)d\tau$$

$$\leq \int_0^{\frac{1}{v\cdot\tau_{norm}}\hat{x}} W(\hat{x},\tau)d\tau + \int_{\frac{1}{v\cdot\tau_{norm}}\hat{x}}^t W(0,\tau)d\tau$$

and so $W(\hat{x},t)$ is an integrable function of t.

On the other hand, if $T > \frac{1}{v \cdot \tau_{norm}} \hat{x}$

$$\int_0^t W(\hat{x},\tau)d\tau = \int_0^{\frac{1}{v\cdot\tau_{norm}}\hat{x}} W(\hat{x},\tau)d\tau + \int_{\frac{1}{v\cdot\tau_{norm}}\hat{x}}^T W(\hat{x},\tau)d\tau, + \int_T^t w(\hat{x},\tau)d\tau$$

$$\leq \int_0^{\frac{1}{v\cdot\tau_{norm}}\hat{x}} W(\hat{x},\tau)d\tau + \int_{\frac{1}{v\cdot\tau_{norm}}\hat{x}}^T W(\hat{x},\tau)d\tau, + \int_{\frac{1}{v\cdot\tau_{norm}}\hat{x}}^t W(\hat{x},\tau)d\tau$$

which again implies that $W(\hat{x},t)$ is an integrable function of t.

Theorem (4.2) gives a general qualitative result for the populations N and N_1 provided that $W(0,t)$ is an integrable function of t.

Theorem 8 *Let the conditions in (4.4.2) hold and let* $N(x,0) + \gamma N_1(x,0) < 1$ *for* $0 \leq x \leq \ell$. *In addition, let* $W(0,t)$ *be an integrable function of* t. *Then for fixed* x, $0 \leq x \leq \ell$, $N(x,t)$ *and* $N_1(x,t)$ *are integrable functions of* t.

Proof: Since $N(x,0) + \gamma N_1(x,0) < 1$ for $0 \leq x \leq \ell$, then for fixed $x = \hat{x}$,

$$\begin{aligned}\frac{d(N+\gamma N_1)}{dt} &= (c_{11}+\gamma c_{21})N + (c_{12}+\gamma c_{22})N_1 + W[1-\gamma N_1 - N] \\ &= (c_{11}+\gamma c_{21})(N+\gamma N_1) - \gamma(c_{11}\gamma c_{21})N_1 + (c_{12}+\gamma c_{22})N_1 \\ &\quad +W[1-\gamma N_1 - N] \\ &\leq (c_{11}+\gamma c_{21})(N+\gamma N_1) + W[1-\gamma N_1 - N]\end{aligned}$$

since $c_{12} - \gamma c_{22} - \gamma(c_{22}+\gamma c_{21}) < 0$ and $N_1(\hat{x},t) \geq 0$.

Therefore,

$$\frac{d(N+\gamma N_1)}{dt} \leq (c_{11}+\gamma c_{21}-W)(N+\gamma N_1) + W.$$

Then

$$\begin{aligned}e^{\int_0^t [W-c_{11}-\gamma c_{21}]d\tau}\frac{d(N+\gamma N_1)}{dt} &- e^{\int_0^t [W-c_{11}-\gamma c_{21}]d\tau}[c_{11}+\gamma c_{21}-W](N+\gamma N_1) \\ &\leq e^{\int_0^t [W-c_{11}-\gamma c_{21}]d\tau} W(\hat{x},t),\end{aligned}$$

or

$$\frac{d}{dt}\left[e^{\int_0^t [W-c_{11}-\gamma c_{21}]d\tau}(N+\gamma N_1)\right] \leq e^{\int_0^t [W-c_{11}-\gamma c_{21}]d\tau} W(\hat{x},t).$$

So

$$e^{\int_0^t [W-c_{11}-\gamma c_{21}]d\tau}[N+\gamma N_1] - [N(\hat{x},0)+\gamma N_1(\hat{x},0)] \leq \int_0^t e^{\int_0^\tau [W-c_{11}-\gamma c_{21}]d\tau'} W(\hat{x},\tau)d\tau,$$

and thus

$$
\begin{aligned}
N+\gamma N_1 &\leq e^{\int_0^t [c_{11}-\gamma c_{21}-W]dr} \int_0^t e^{\int_0^\tau [W-c_{11}-\gamma c_{21}]dr'} W(\hat{x},\tau)d\tau \\
&+ e^{\int_0^t [c_{11}-\gamma c_{21}-W]dr}[N(\hat{x},0)+\gamma N_1(\hat{x},0)] \\
&= \int_0^t e^{\int_0^t [c_{11}-\gamma c_{21}-W]dr'} W(\hat{x},\tau)d\tau \\
&+ e^{\int_0^t [c_{11}-\gamma c_{21}-W]dr}[N(\hat{x},0)+\gamma N_1(\hat{x},0)]
\end{aligned}
$$

Now, $W(\hat{x},t) \geq 0$ so $e^{-\int_\tau^t W dr} \leq 1$ so

$$
\begin{aligned}
N+\gamma N_1 &\leq \int_0^t e^{\int_\tau^t [c_{11}+\gamma c_{21}]dr'} W(\hat{x},\tau)d\tau + e^{\int_0^t [c_{11}+\gamma c_{21}]dr}[N(\hat{x},0)+\gamma N_1(\hat{x},0)] \\
&= \int_0^t e^{(c_{11}-\gamma c_{21})(t-\tau)} W(\hat{x},\tau)d\tau + e^{(c_{11}+\gamma c_{21})t}[N(\hat{x},0)+\gamma N_1(\hat{x},0)].
\end{aligned}
$$

So now,

$$
\begin{aligned}
\int_0^{t'} [N(\hat{x},t)+\gamma N_1(\hat{x},t)]dt &\leq \int_0^{t'} \int_0^t e^{(c_{11}+\gamma c_{21})(t-\tau)} W(\hat{x},\tau)d\tau dt \\
&+ \int_0^{t'} e^{(c_{11}-\gamma c_{21})t}[N(\hat{x},0)+\gamma N_1(\hat{x},0)]dt \\
&= \int_0^{t'} W(\hat{x},\tau) \int_\tau^{t'} e^{(c_{11}-\gamma c_{21})(t-\tau)} dt d\tau \\
&+ [N(\hat{x},0)+\gamma N_1(\hat{x},0)] \left[\frac{e^{(c_{11}+\gamma c_{21})t'}-1}{c_{11}+\gamma c_{21}}\right] \\
&= \int_0^{t'} W(\hat{x},\tau) \left[\frac{e^{(c_{11}-\gamma c_{21})(t'-1)}-1}{c_{11}+\gamma c_{21}}\right] d\tau \\
&+ [N(\hat{x},0)+\gamma N_1(\hat{x},0)] \left[\frac{e^{(c_{11}-\gamma c_{21})t'}-1}{c_{11}+\gamma c_{21}}\right]
\end{aligned}
$$

Since $c_{11}+\gamma c_{21} < 0$ and $W(\hat{x},t)$ is an integrable function of t, it follows that $[N+\gamma N_1](\hat{x},t)$ is an integrable function of t. Both N and N_1 are nonnegative

so $N(\hat{x},t)$ and $N_1(\hat{x},t)$ are integrable function of t. Therefore, for fixed x, $0 \leq x \leq \ell$, $N(x,t)$ and $N_1(x,t)$ are integrable functions of t.

4.3 Numerical Analysis

The spatial and temporal model presents a number of problems which must be considered in choosing a numerical scheme for solving the system. The laser dynamics in the active region, taken to be $0 \leq x \leq \ell$, and the rest of the cavity, $\ell \leq x \leq L$, are represented by two different sets of partial differential equationr which are coupled via boundary conditions at $x = 0$ (which corresponds to $x = L$) and at $x = \ell$. In addition, the solutions must satisfy other conditions that describe the optical environment of the active medium. For example, in the simple ring cavity, the effects of the mirrors must be taken into account. It is expected that the dynamic variables will evolve in a similar way, qualitatively, as those in the spatially averaged version, so there may be regions where the time deviatives are large and in order to capture the correct behavior of the solutions, small time steps and large amounts of computer time may be needed. In this section the discretization of the problem as well as an effective algorithm for the numerical solution of the initial and boundary value problem are given. Results obtained from this algorithm are compared to those obtained from a stable finite difference algorithm. Effects on the solutions of changes in the pump pulse and injection seeding are presented.

The numerical computations were done in double precision on a DEC VAX

11/750. The emission spectrum of Ti:Sapphire from 650 to 950 nm was divided into 24 intervals of length $\Delta\lambda = 12.5$ nm. The physical parameters used were the same as for the spatially averaged version of the model and so typical values are given in Tables 3.1 and 3.2.

The pump pulse at the boundary $x = 0$ is assumed to obey a specified temporal dependence and as in Chapter 3, the cases of a Gaussian pump profile as well as a constant pump pulse are considered. For the Gaussian pump pulse,

$$W(0,t) = W_p \cdot f(t, t_p, \tau_p)$$

where

$$W_p = \eta \left[\left(\frac{E_p}{\left(\frac{hc}{\lambda_p}\right)} \right) \right] \left[\frac{1}{\tau_p} \right] \left[\frac{\sigma_{ab}}{\pi r_P^2} \right]$$

and

$$f(t, t_p, \tau_p) = \sqrt{\frac{\ell n 2}{\pi}} \exp\left((-\ell n 2) \left[\frac{(t - t_0}{\frac{1}{2}\tau_p} \right]^2 \right).$$

For the constant pump case

$$W(0,t) = W_p.$$

In each of the above expressions, the parameters are as defined previously.

The model also allows for the introduction of an injected signal. Injection seeding is accomplished by a reverse wave supressor mirror external to the ring cavity [3,6] (Fig. 4.1). The contribution to the photon concentration by injection seeding is incorporated into the boundary condition at the output coupler, $x = L_1$ and given by

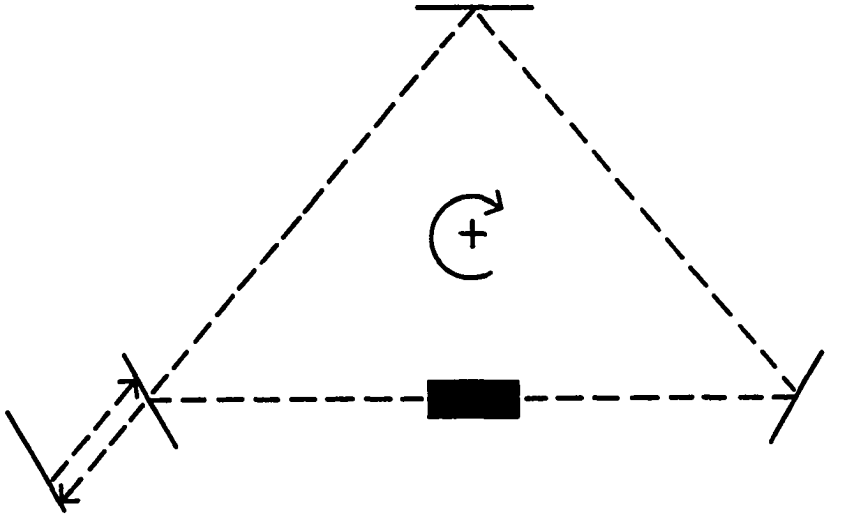

Figure 4.1 Schematic of a ring laser cavity which allows for injection seeding. A fraction of the laser output is reintroduced into the system thrugh the output mirror.

$$\Phi_+(L_1,t;\lambda_j) = \Phi_+(L_1,t;\lambda_j) + R_I\Phi_-^{\text{out}}(t;\lambda_j)$$

where R_I is the reflectively of the external mirror and $\Phi_-^{\text{out}}(t;\lambda_j)$ is the fraction of the reverse wave which is transmitted through the output mirror.

The numerical procedure used to solve the initial and boundary value problem is motivated by the "method of characteristics" [8,11] and exploits the particularly simple form that the characteristics of the system enjoy. Since the characteristics do not depend on the solution and in fact are known in advance to be three families of lines in the $x-t$ plane, the system of partial differential equations can be reduced to a system of ordinary differential equations along the relevant characteristics in a suitable small region. For example, assume that initial conditions (Fig. 4.2) are specified along a segment of the x- axis and that the point $P(\xi,\eta)$ is a point in a small vicinity of the x- axis. The solutions at $P(\xi,\eta)$ are found by integrating each ordinary differential equation along the appropriate characteristic and applying the initial conditions.

By introducing a lattice of mesh points that coincide with points of intersection of the charcateristic lines, at each lattice point the system of partial differential equations together with the initial and boundary conditions is reduced to an initial value problem with the corresponding system of ordinary differential equations along the characteristics.

Consider the ring cavity configuration in Fig. 4.1 For simplicity, the effect of the second and third mirrors are incorporated into the boundary conditions

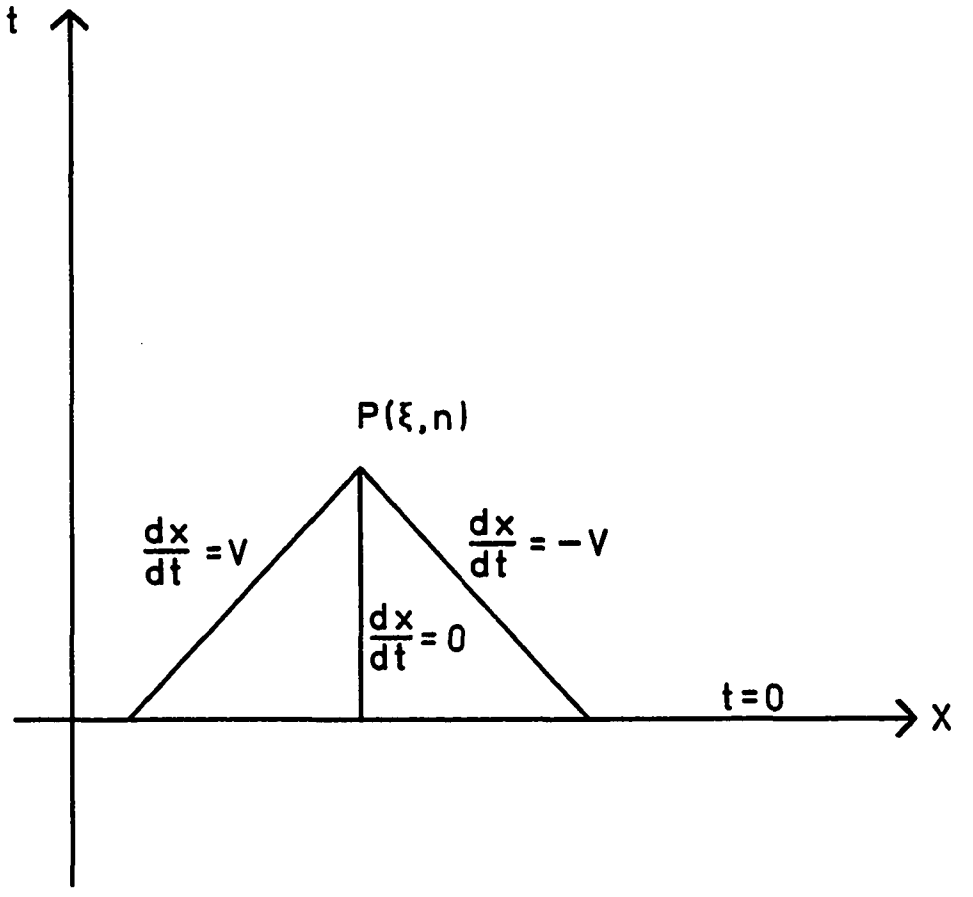

Figure 4.2 Determination of solutions at a point $P(\xi,\eta)$ of the partial differential equations by integration along the relevant characteristics.

of ϕ_+ at $x = 0$ and for ϕ_- at the location of the first mirror, $x = L_1$. As in the figure, it is assumed that the cavity is equilateral, however, the assumption is without loss of generality.

Let M be the number of spatial increments in the crystal. Then the length of each increment is given by $\Delta x_{cr} = \frac{\ell}{M}$. The time increment will be the length of time necessary for a photon to travel a distance of Δx_{cr}. Thus

$$\Delta t = \frac{1}{v} \Delta x_{cr}$$

which implies that

$$\Delta x_{\text{cav}} = c\Delta t.$$

It is assumed for convenience that the locations of the first mirror and edge of the crystal at $x = L$ coincide with spatial grid points. To approximate this situaiton, let M_1 be the number of spatial increments between the edge of the crystal $x = \ell$ and the mirror at $x = L_1$, defined by

$$M_1 = \text{ nearest integer } \left\{ \frac{L_1 - \ell}{\Delta x_{\text{cav}}} \right\}.$$

Also, let M_2 be the number of spatial increments between the first mirror at $x = L_1$ and the edge of the crystal at $x = L$, defined by

$$M_2 = \text{ nearest integer } \left\{ \frac{L - L_1}{\Delta x_{\text{cav}}} \right\}.$$

Then $M_T = M + M_1 + M_2$ defines the number of spatial increments in the cavity.

Now consider the discrete functions N_s^r, N_{1s}^r, W_s^r, and $\phi_{\pm j_s}^r$ defined by

$$
\begin{aligned}
N_s^r &= N(x_r, t_s) \\
N_{1s}^r &= N_1(x_r, t_s) \\
W_s^r &= W(x_r, t_s) \\
\phi_{\pm js}^r &= \phi_\pm(x_r, t_s; \lambda_j) \qquad j = 1, ..., m
\end{aligned}
$$

for $r = 0, 1, ..., M$ and $s = 0, 1, ...$, which correspond to the solution in the active region at the mesh points. Corresponding to the solutions at the mesh point in the rest of the cavity, the discrete function $\Phi_{\pm js}^r$, $j = 1, ..., m$ are defined similarly for $r = M, M+1, ..., M_T$ and $s = 0, 1, ...$

In terms of the discrete functions, the initial conditions are

$$
\begin{aligned}
&N_o^r = N_{10}^r = 0 \quad r = 0, 1, ..., M \\
&\Phi_{\pm j0}^r = 0 \qquad r = 0, 1, ..., M \\
&\Phi_{\pm j0}^r = 0 \qquad r = M+1, ..., M_T \qquad j = 1, ..., m. \qquad (4.3.1)
\end{aligned}
$$

The boundary conditions at $x = 0$ and $x = L$ become

$$
\begin{aligned}
\phi_{+js}^0 &= T_s R_2 R_3 \Phi_{+js}^{M_T} \\
\phi_{-js}^0 &= T_s \phi_{-js}^0 \ , \qquad (4.3.2)
\end{aligned}
$$

at the edge of the crystal $x = \ell$,

$$\Phi^{M}_{+j_s} = T_s \phi^{M}_{+j_s}$$

$$\phi^{M}_{-j_s} = T_s \Phi^{M}_{-j_s} \quad , \tag{4.3.3}$$

and at the location of the first mirror $x = L_1$

$$\phi^{M_1+1}_{+j_s} = R_1 \Phi^{M_1}_{+j_s} + R_I T_1 \Phi^{M_1+1}_{-j_s-1}$$

$$\Phi^{M_1-1}_{-j_s} = R_1 R_2 R_3 \Phi^{M_1}_{-j_s} \quad j = 1, ..., M \tag{4.3.4}$$

where R_1, R_2, R_3, R_I, and T_1 are as previously defined and $s = 1, 2, ...,$.

The discrete pump function has initial and boundary conditions given by

$W^0_s = W_P \cdot f(t_s, t_p, \tau_p)$ for $s = 0, 1, ...,$,where $W_p$and$f(t, t_p, \tau_p)$are as specified before

or

$$W^0_s = W_p.$$

The homogeneous equations in the region $x = \ell$ to $x = L$ are particularly easy to integrate, for if t is the independent variable along a characteristic,

$$\frac{d\Phi_{\pm}(x(t), t; \lambda_j)}{dt} = 0$$

which implies that

$$\Phi^{r+1}_{+j_{s+1}} = \Phi^{r}_{+j_s} \tag{4.3.5}$$

for $r = M, ..., M_1 - 1$ and $r = M_1 + 1, ..., M_T$

and

$$\Phi^{r-1}_{-js+1} = \Phi^{r}_{-js} \tag{4.3.6}$$

for $r = M_T, M_T - 1, ..., M_1 + 1$ and $r = M_1 - 1, M_1 - 2, ..., M$.

Note that

$\Phi^{M_1+1}_{+js}$ and $\Phi^{M_1-1}_{-js}$ are specified by (4.3.4).

The nonlinear ordinary differential equations along the characteristics in the active region must be itegrated by an approximate method. Euler's Method is a first order accurate [as in 7] procedure that can be implemented in the following way. For the population equations, integration is along the vertical lines $x = x_r$, so that

$$\begin{aligned} N^r_{s+1} &= N^r_s + \Delta t \left[\frac{dN(x_r, t_s)}{dt}\right] \\ N^r_{1s+1} &= N^r_{1s} + \Delta t \left[\frac{dN_1(x_r, t_s)}{dt}\right] \quad , \quad r = 0, ..., M \\ \text{and } s &= 0, 1, ..., \end{aligned} \tag{4.3.7}$$

The functions W and ϕ_+ are integrated along the lines parallel to $t = \frac{1}{v}x$, so

$$\begin{aligned} W^r_{s+1} &= W^r_s + \Delta t \left[\frac{dW(x_r, t_s)}{dt}\right] \\ \phi^{r+1}_{s+1} &= \phi^r_s + \Delta t \left[\frac{d\phi_+(x_r, t_s; \lambda_j)}{dt}\right] \quad , \quad r = 0, ..., M \\ \text{and } s &= 0, 1, ..., \end{aligned} \tag{4.3.8}$$

Similarly, ϕ_- is integrated along the lines parallel to $t = \frac{-1}{v}x$, so

$$\phi^{r-1}_{-js+1} = \phi^{r+1}_{-js} + \Delta t \left[\frac{d\phi_-(x_r, t_s; \lambda_j)}{dt}\right] \quad r = M, ..., 1 \text{ and } s = 0, 1, ..., .$$

For illustrative purposes, the pump energy was taken to be large, $E_p = 200mJ$ and no injection present in the system.

Figures 4.3-4.6 display the time evolution of the numerical solution at the first interior grid point in the crystal using M=5. If M is increased by a factor of two, the qualitative behavior of the solutions is basically unchanged as shown by Figs 4.7-4.10, but quantitatively the solutions are slightly different. While increased accuracy is expected from a smaller step size, it is at the expense of tremendously increased computational effort necessary to calculate the solutions.

The accuracy of Euler's method can be improved to second order by implementing the Modified Euler Method [as in 7] in the following way. The values of the discrete functions are predicted at the new grid points by the Euler relations (4.3.7)- (4.3.8). Then an improved estimate is obtained by iteration using the relations

$$\begin{aligned}
\bar{N}^r_{s+1} &= N^r_s + \Delta t \left[\frac{1}{2}\left[\frac{dN(x_r, t_{s+1})}{dt} + \frac{dN(x_r, t_s)}{dt}\right]\right] \\
\bar{N}^r_{1_{s+1}} &= N^r_{1_s} + \Delta t \left[\frac{1}{2}\left[\frac{dN_1(x_r, t_{s+1})}{dt} + \frac{dN(x_r, t_s)}{dt}\right]\right] \\
W^{r+1}_{s+1} &= W^r_s + \Delta t \left[\frac{1}{2}\left[\frac{dW(x_{r+1}, t_{s+1})}{dt} + \frac{dW(x_r, t_s)}{dt}\right]\right] \qquad (4.3.9) \\
\phi_{+_j} \begin{matrix} r+1 \\ s+1 \end{matrix} &= \phi^r_s + \Delta t \left[\frac{1}{2}\left[\frac{d\phi_+(x_{r+1}, t_{s+1}; \lambda_j)}{dt} + \frac{d\phi_-(x_r, t_s; \lambda_j)}{dt}\right]\right] \\
\phi_{-_j} \begin{matrix} r-1 \\ s+1 \end{matrix} &= \phi^r_{-j} + \Delta t \left[\frac{1}{2}\left[\frac{d\phi_-(x_{r-1}, t_{s+1}; \lambda_j)}{dt} + \frac{d\phi_-(x_r, t_s; \lambda_j)}{dt}\right]\right]
\end{aligned}$$

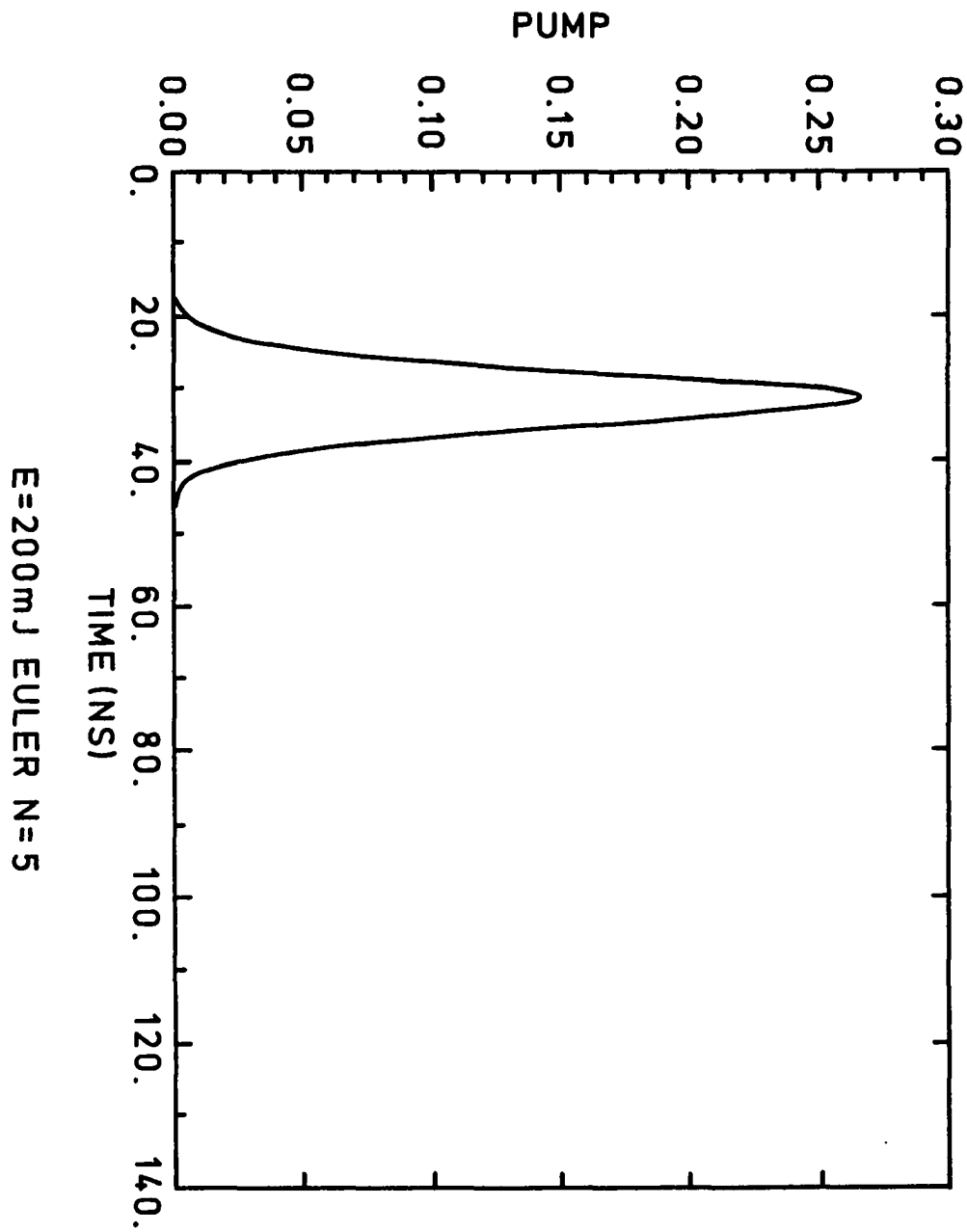

Figure 4.3 The computed pump pulse (E_p=200mJ) using Euler's Method for integration with M=5. The plot displays the results at the first interior grid point.

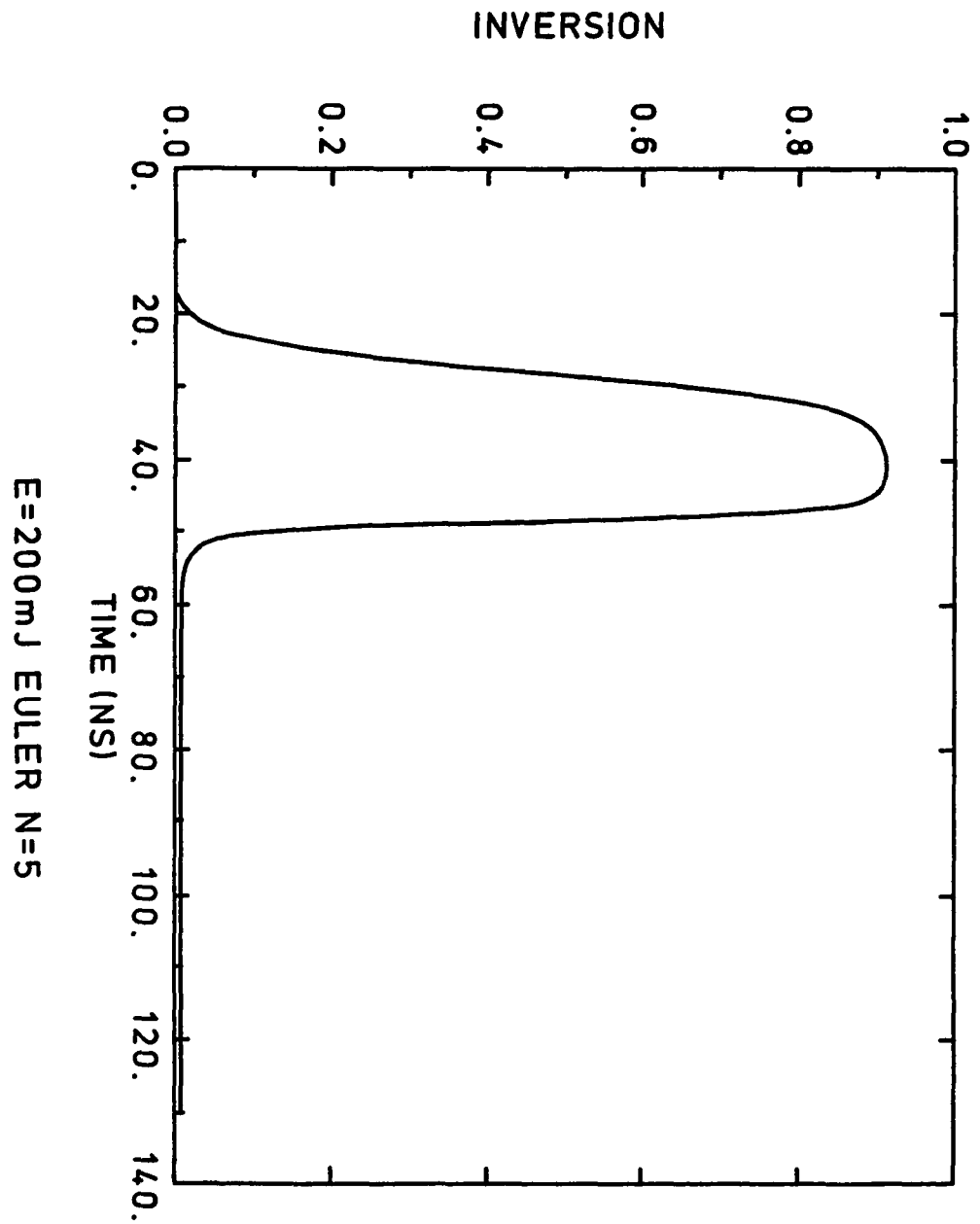

Figure 4.4 The computed population inversion at the first interior grid point. E_p=200 mJ.

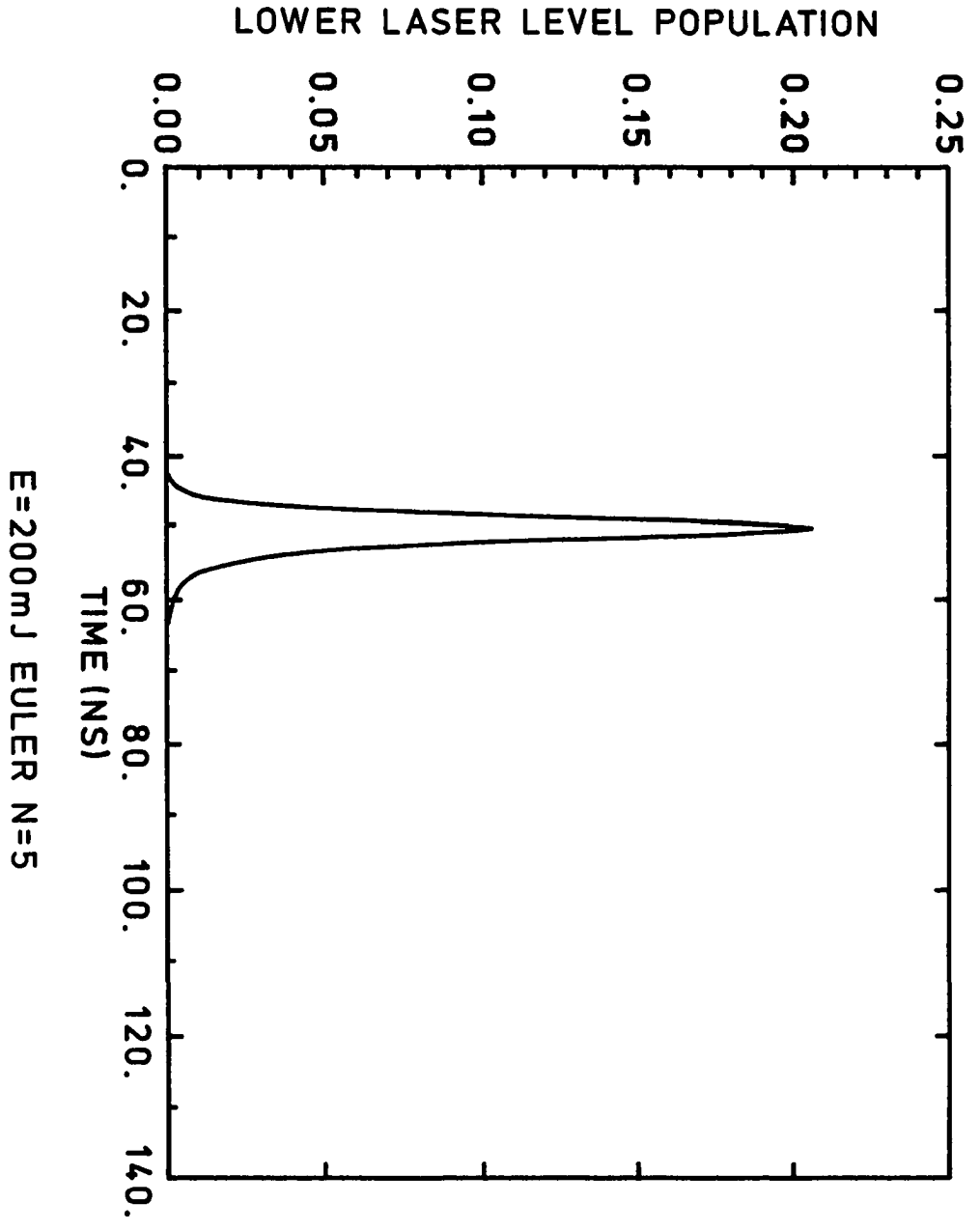

Figure 4.5 The computed lower laser lavel polulation at the first interior grid point. E_p=200 mJ.

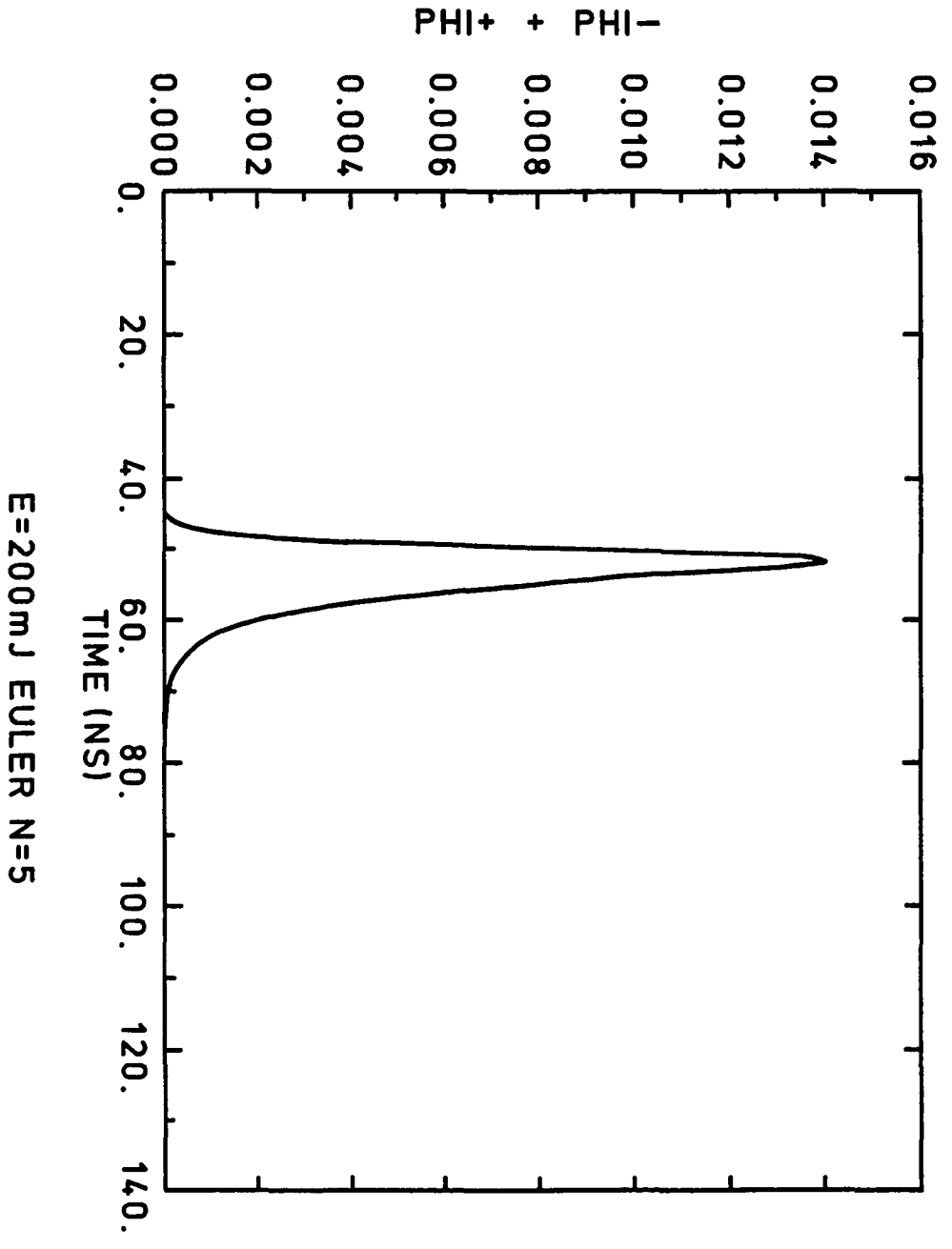

Figure 4.6 The computed total photon concentration at the first grid point. E_p=200 mJ.

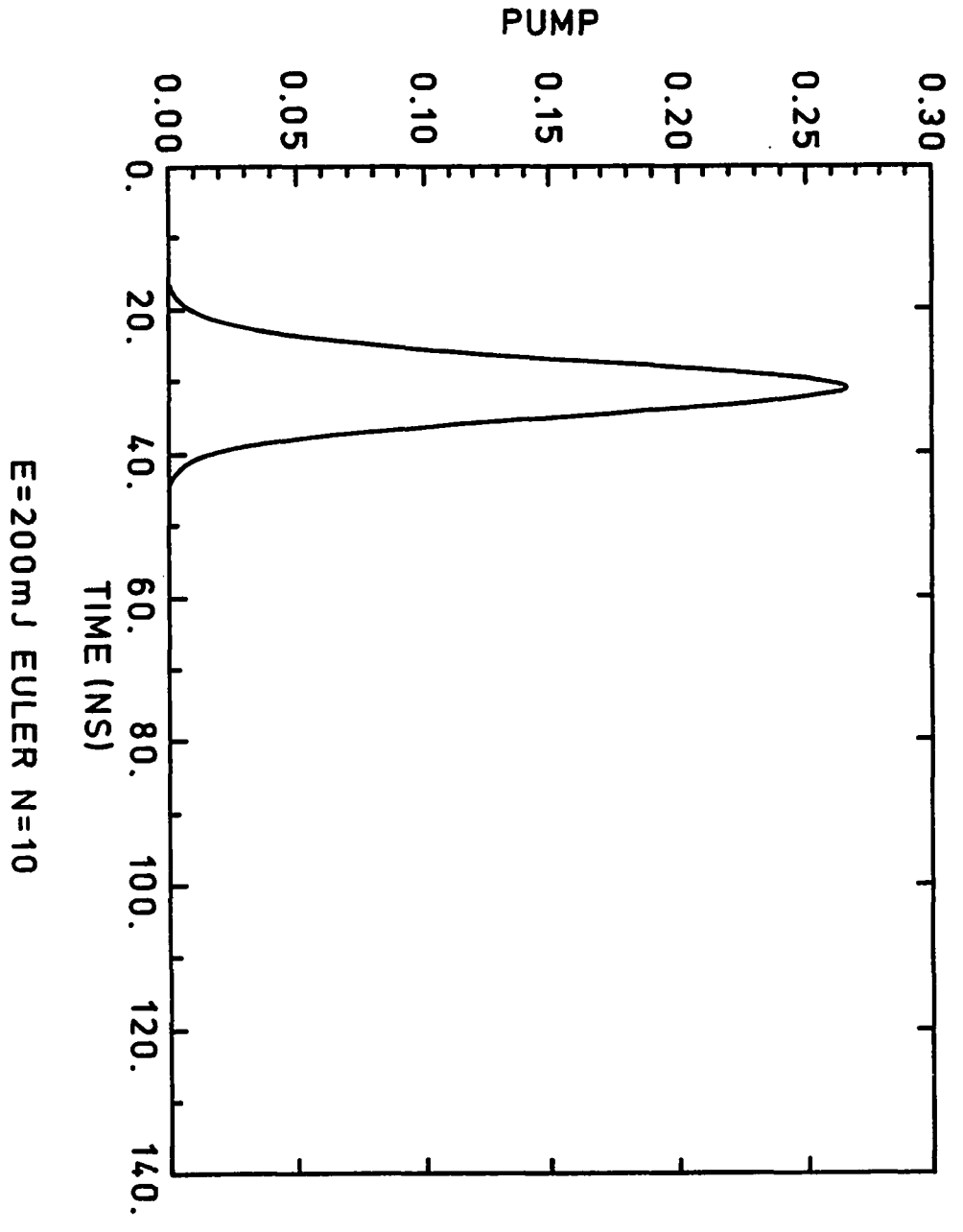

Figure 4.7 The computed pump pulse (E_p=200 MJ) using Euler's Method for integration with M=10. The plot displays the results at the second interior grid point.

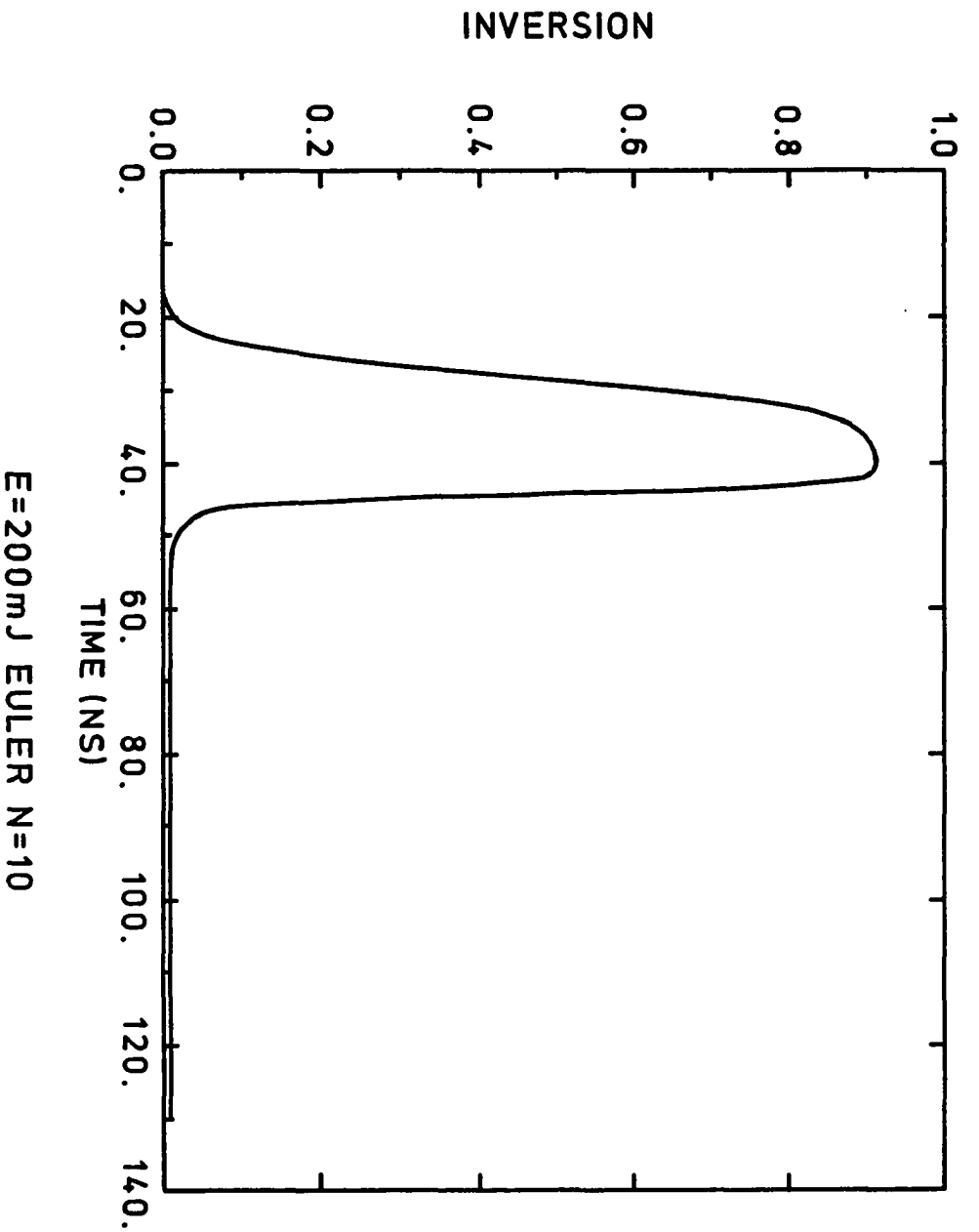

Figure 4.8 The computed population inversion at the second inter grid point. E_p=200 mJ.

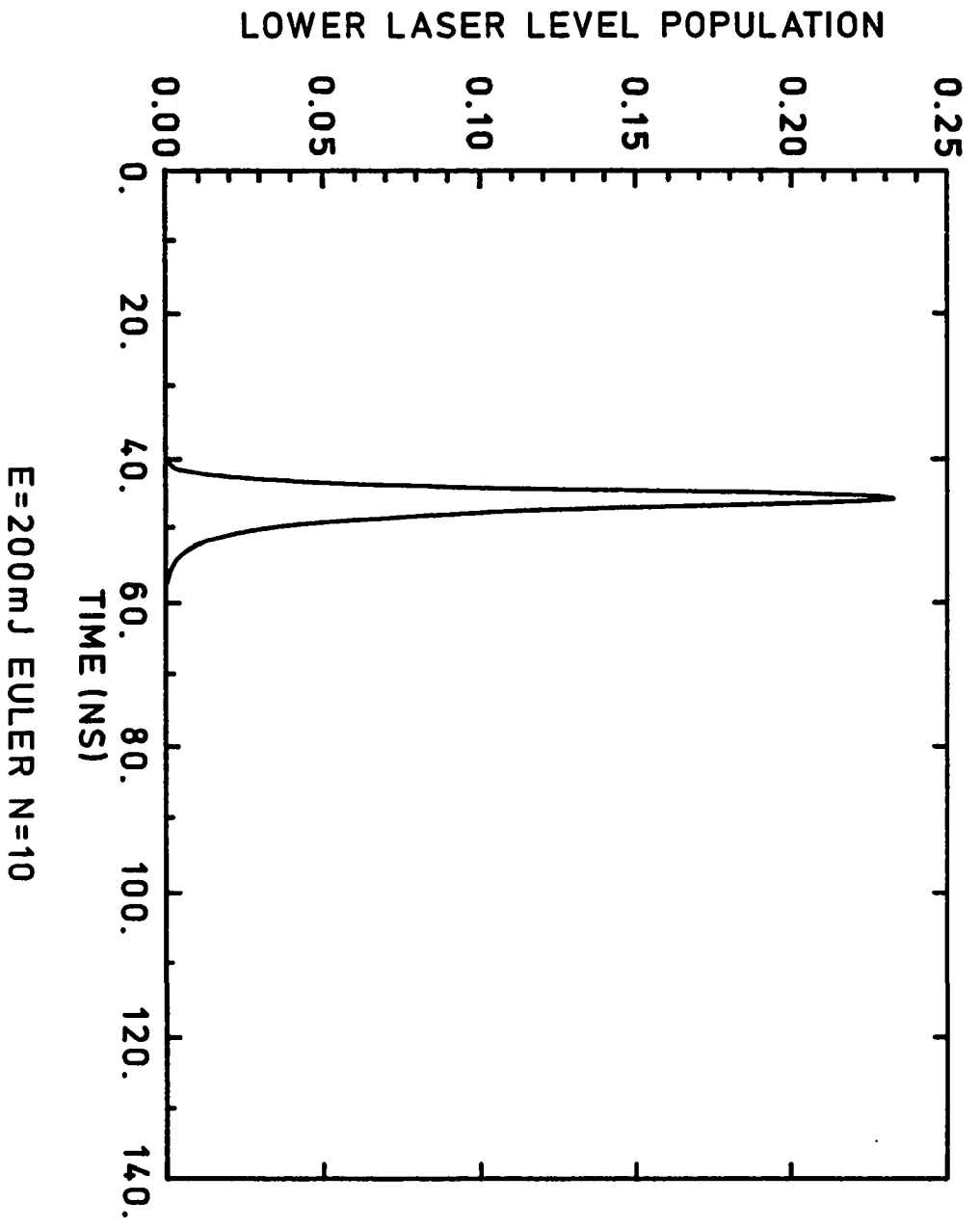

Figure 4.9 The computed lower laser level concentration at the second interior grid point. E_p=200 mJ.

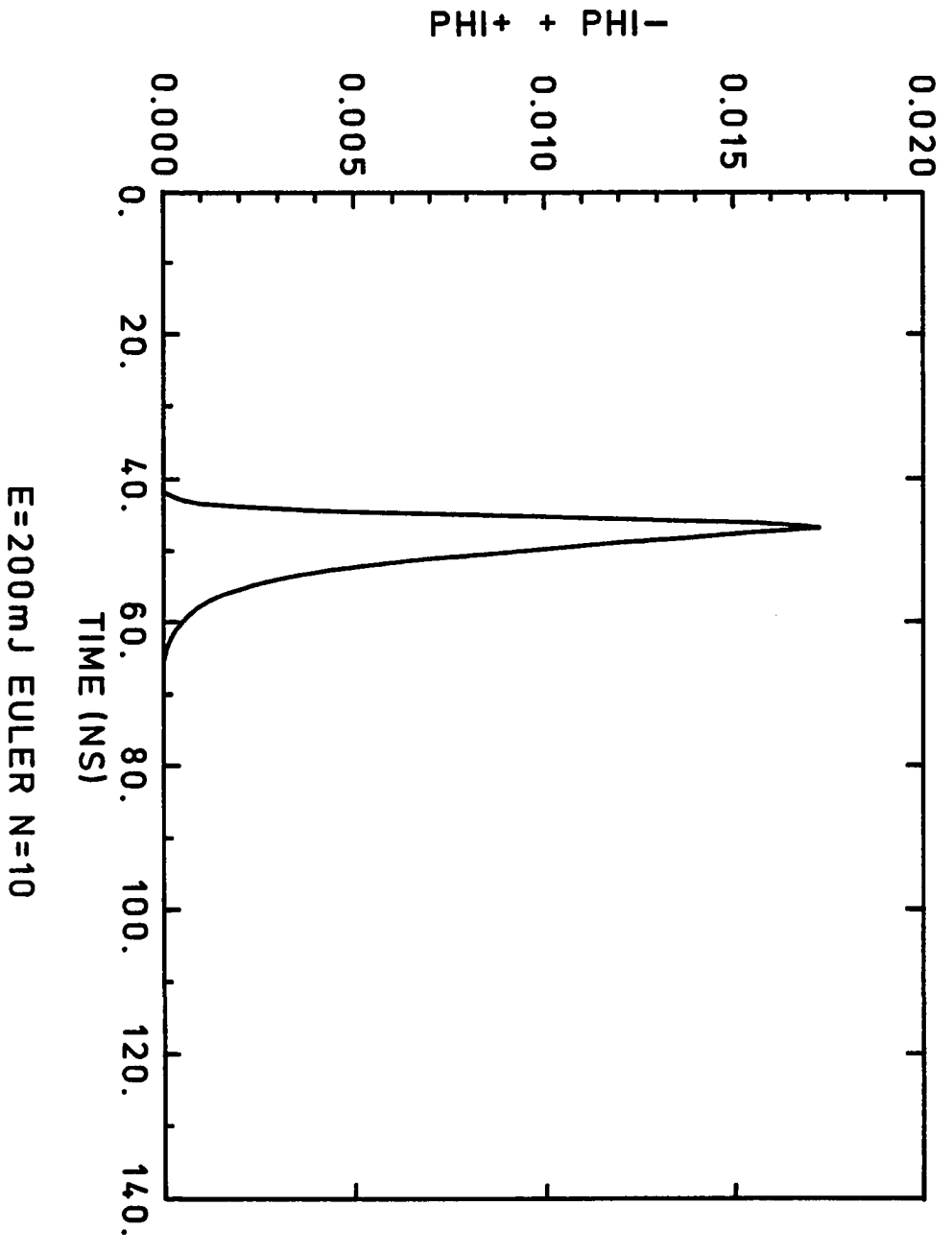

Figure 4.10 The computed total photon concentration at the secon interior grid point. E_p=200 mJ.

Figure 4.11 is a plot of the computed solution for the population inversion at the first interior grid point using one iteration of the Modified Euler procedure. By using two iterations, a significant improvment over Euler's method with the same number of grid points in the crystal is shown by comparing Fig. 4.11 and Fig. 4.12 . In fact, doubling the number of grid points in the Modified Euler procedure with two iterations does not significantly change the solution quantitatively as is evident from Fig. 4.13. While the calculated solutions are shown for the population inversion, the same comparison applies to the other dynamic variables.

While the Modified Euler Method with two iterations requires more computational effort than Euler's Method alone, it was necessary to increase the number of spatial increments in the crystal to M=20 in order to achieve comparable accuracy with M=5 in the Modified Euler scheme. Therefore, using the Modified Euler Method with a smaller number of mesh points is more efficient than using Euler's Method with four times the number of mesh points.

To verify the results obtained by using the method of characteristics, a stable first order finite difference approximation [11] was employed. Figs. 4.14-4.15 display the results for the population inversion for $M = 10$ and $M = 50$ at corresponding grid points in the crystal. The qualitative behavior for the latter case ($M = 50$) compares favorably to the results obtained by the method of chracteristics but the computer time required to compute the first order solutions was several times greater than with the Modified Euler Method. The Modified

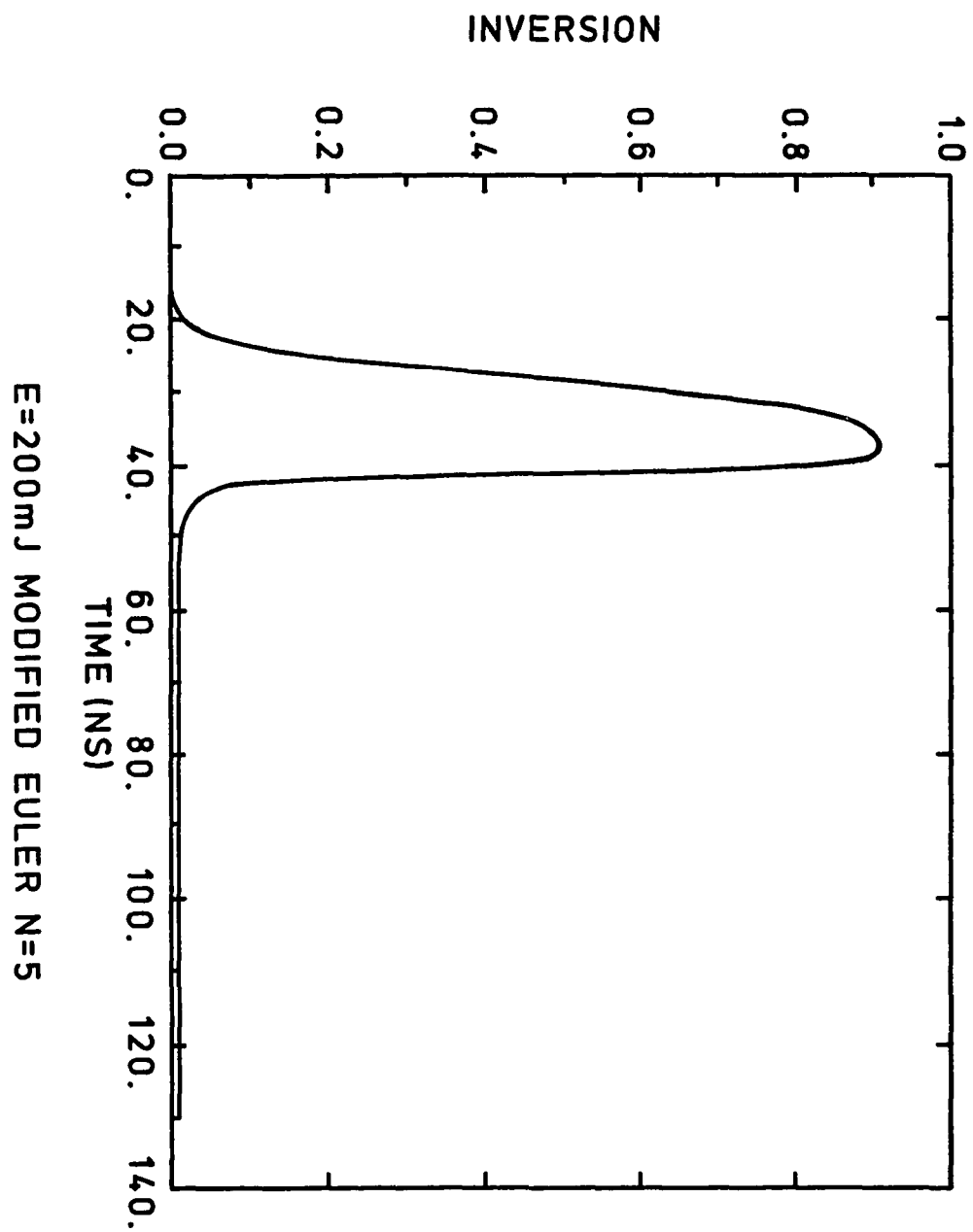

Figure 4.11 Curve demonstrating the improvement in accuracy in the computed population inversion using one iteration of the Modified Euler Method for integration. Results are shown for M=5 at the first intrerior grid point with E_p=2300 mJ.

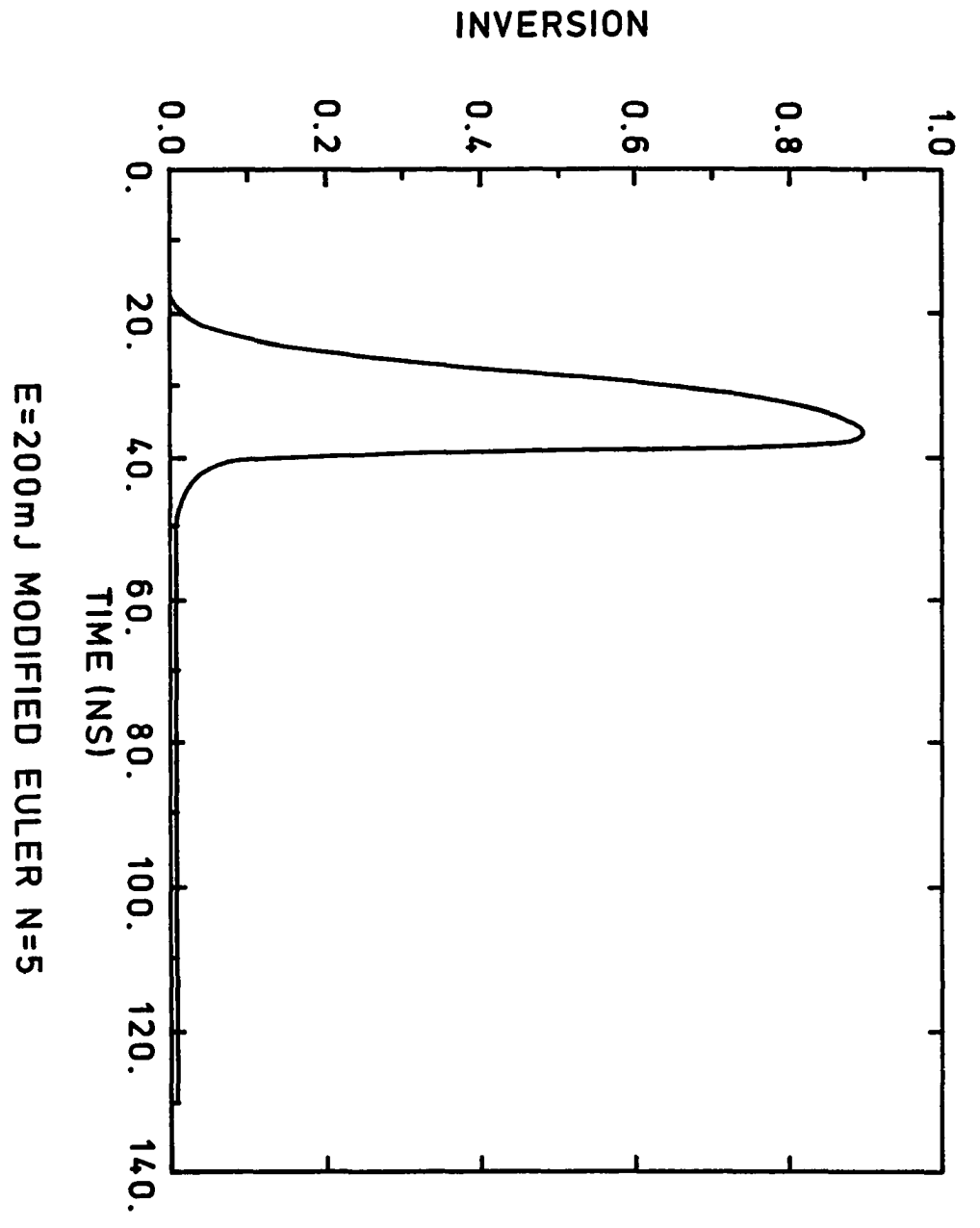

Figure 4.12 Further improvement in accuracy in the computed population inversion using two iterations of the Modified Euler scheme. Results are shown for M=5 at the firs interior grid point with E_p=200 mJ.

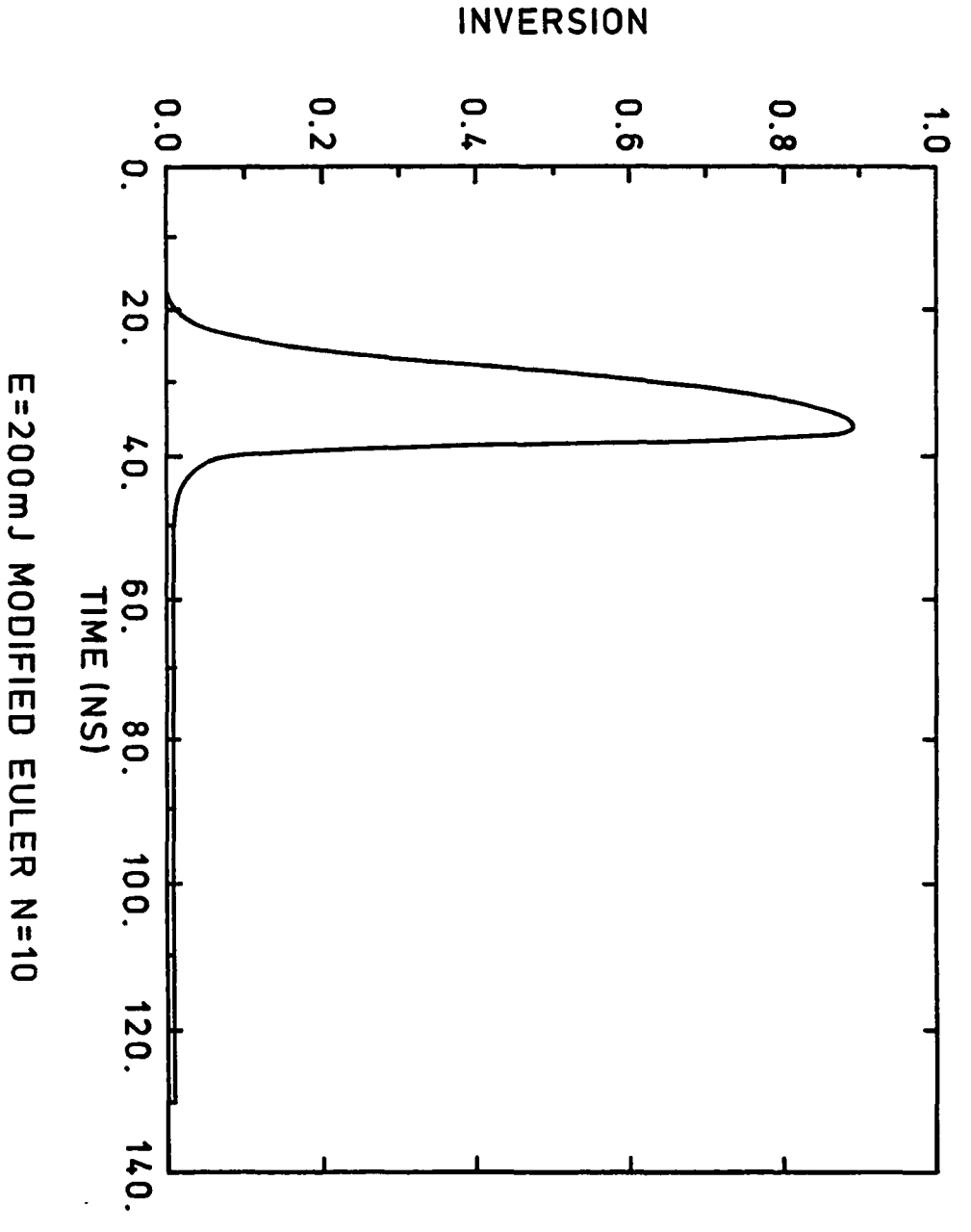

Figure 4.13 Computed population inversion using two iterations of the Modified Euler Method with M=10. Results are shown at the second interior grid point with E=200 mJ. No significant improvement over the case with M=5 is demonstrated.

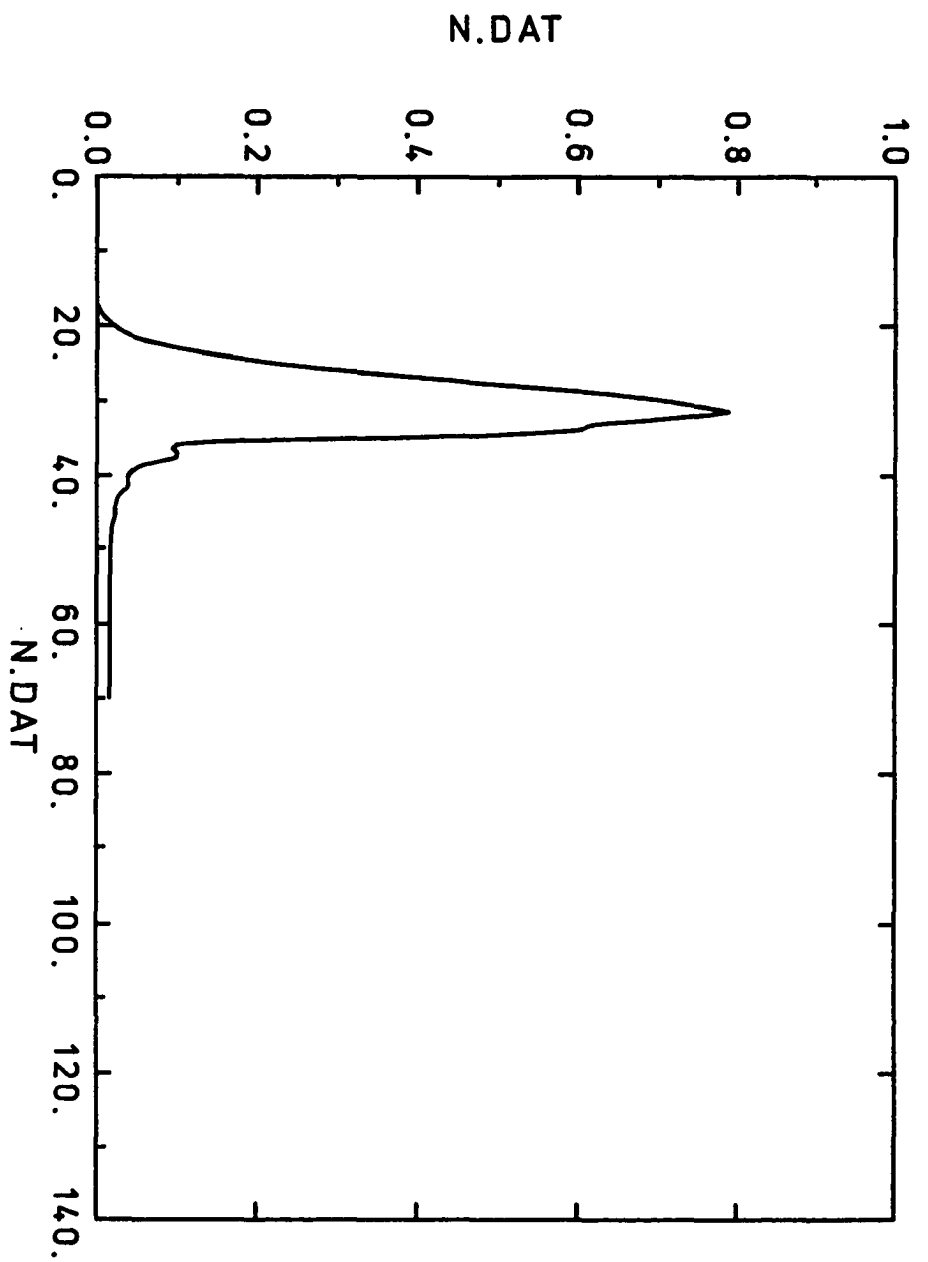

Figure 4.14 Computed population inversion using a finite difference algorithm. Here, M=10 and E_p=200 mJ. Results are shown at the second interior grid point.

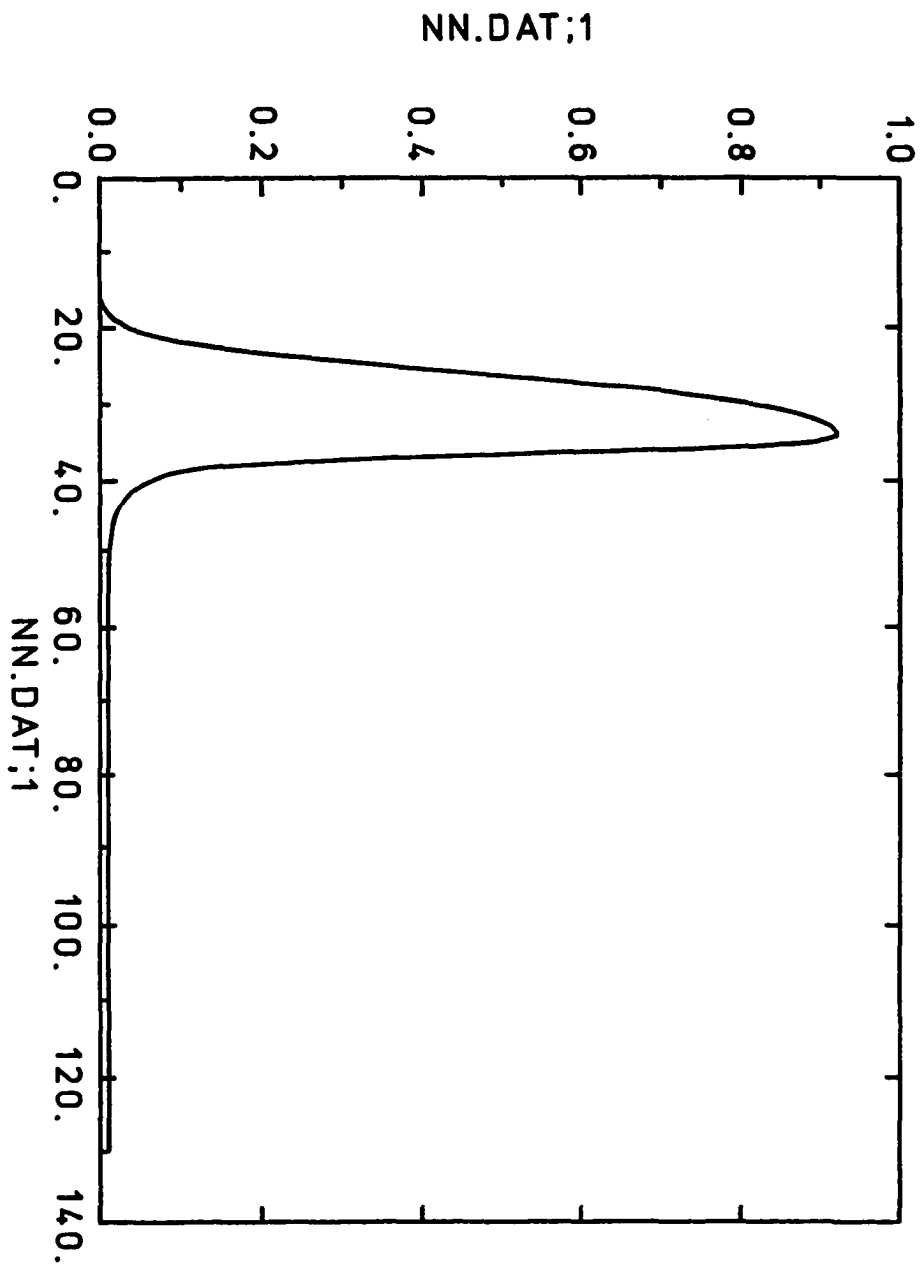

Figure 4.15 Computed population inversion using a finite difference algorithm. In this case, M=50 and E_p=200 mJ. Results are shown at the tenth interior grid point.

Euler Method with $M = 5$ required one-fourth the CPU time necessary to run the first order finite difference method with $M = 10$. The Modified Euler prodecure, with $M = 5$ was almost forty times faster in terms of CPU time than the finite difference approximation for $M = 50$ and only then are the solutions comparable. It is evident that integration along the characteristics using a Modified Euler Algorithm with a spatial and temporal discretization described here represents a significant improvement in the accuracy of the computed solutions while providing a significant savings in computational effort over that required for comparable solutions using the finite difference algorithm.

One observation that can be made from the plots of the populaiton inversion is that this quantity appears to decay very slowly, unlike the corresponding situation in the spatially averaged version of the model. It was proved in 4.2 that the population inversion is integrable as a function of t for fixed position $\bar{x}$. To see that this result is not violated by the numerical approximation of the solution, note that it is evident that for some time T, the quantities $N_1(\bar{x},t), \phi_{\pm}(\bar{x},t), and W(\bar{x},t)$ are negligible for $t \geq T$ so that the differential equation for N is approximated by

$$\frac{dN}{dt} \approx c_{11}N$$

and so

$$N(\bar{x},t) \sim N(\bar{x},T)e^{c_{11}(t-T)} \text{ for } t > T$$

where c_{11} is small in magnitude and negative.

To study the effects on the solutions of changes in the pump pulse, the Modified Euler Method was used to compute the numerical solutions. Figs. 4.16 and 4.17 show the temporal development of the population inversion and photon concentrations at each interior grid points for a system in which no injection is present and the pump pulse is constant with $E_p = 10mJ$. The laser crystal is assumed to be end pumped so the pump pulse is absorbed as it moves through the crystal. Consequently, it is expected that at a position in the crystal closer to the pump, the inverted population density will be greater than at a position further from the pump source. It is also expected that the photon density will increase due to stimulated emission as photons propagate through the crystal and that density of the clockwise traveling photons will dominate the counterclockwise traveling photons so that the total photon concentration will increase as one moves through the crystal. These qualitative properties are observed in the numerical results as is evident from Fig. 4.16 and 4.17. The oscillatory behavior is consistent with the results from the spatially averaged version of the model assuming similar conditions. If the pump energy is increased to $E_p = 20mJ$, (Fig. 4.18 and 4.19) the oscillations appear to be damped out more quickly, which is also consistent with the results of spatially averaged version.

Figs. 4.20 and 4.21 display the effect of introducing an injected signal of the type described earlier. In these examples, the pump pulse at the boundary of the crystal is a Gaussian pulse with $E_p = 10mJ$ and $E_p = 20mJ$. Again, the

results are consistent with the dynamics of the spatially averaged model.

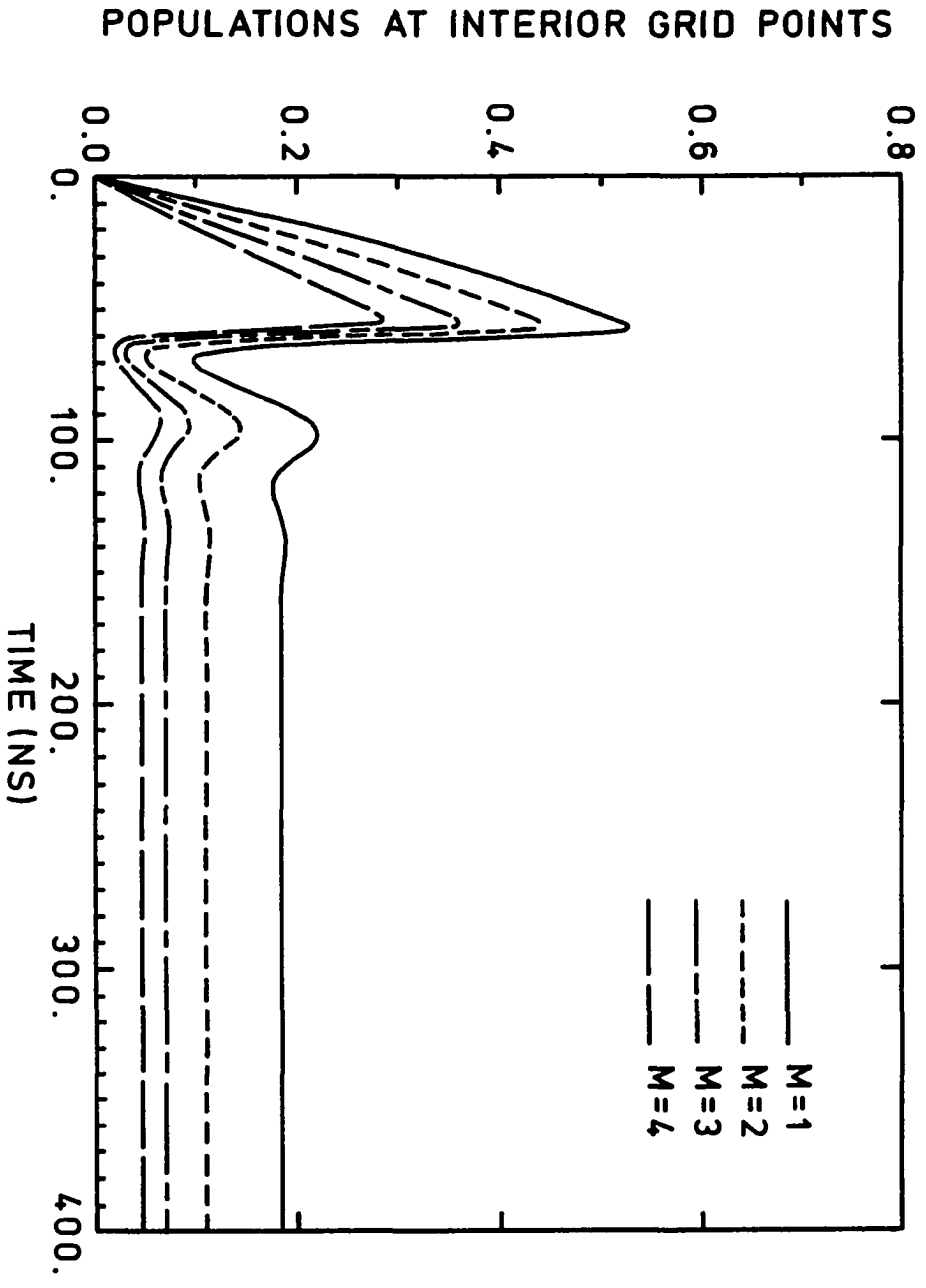

Figure 4.16 Population inversion computed at each of the interior grid points in a system with constant pump, E_p=10 mJ.

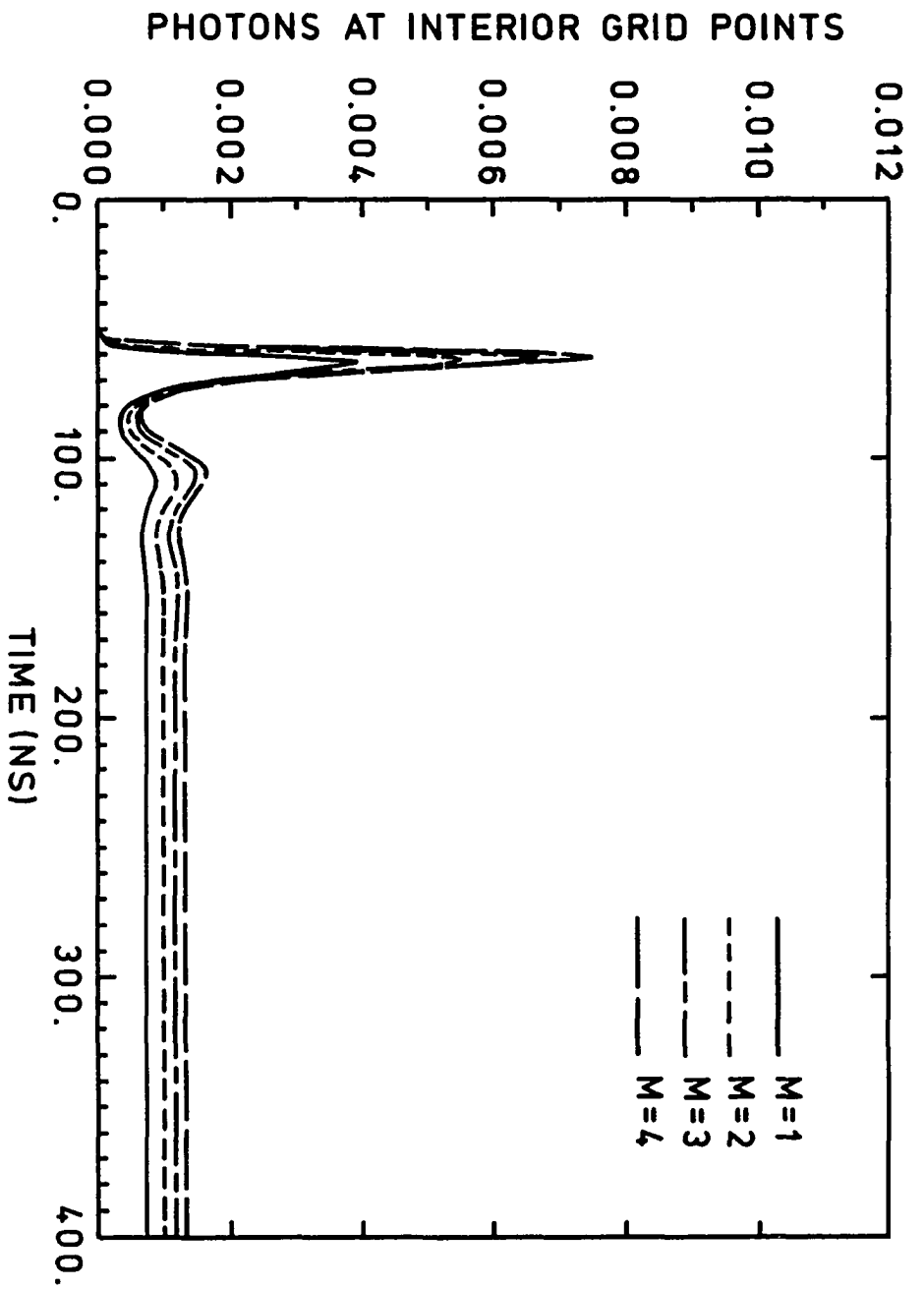

Figure 4.17 Total photon concentration at each interiore grid point in a system with constant pump, E_p=10 mJ.

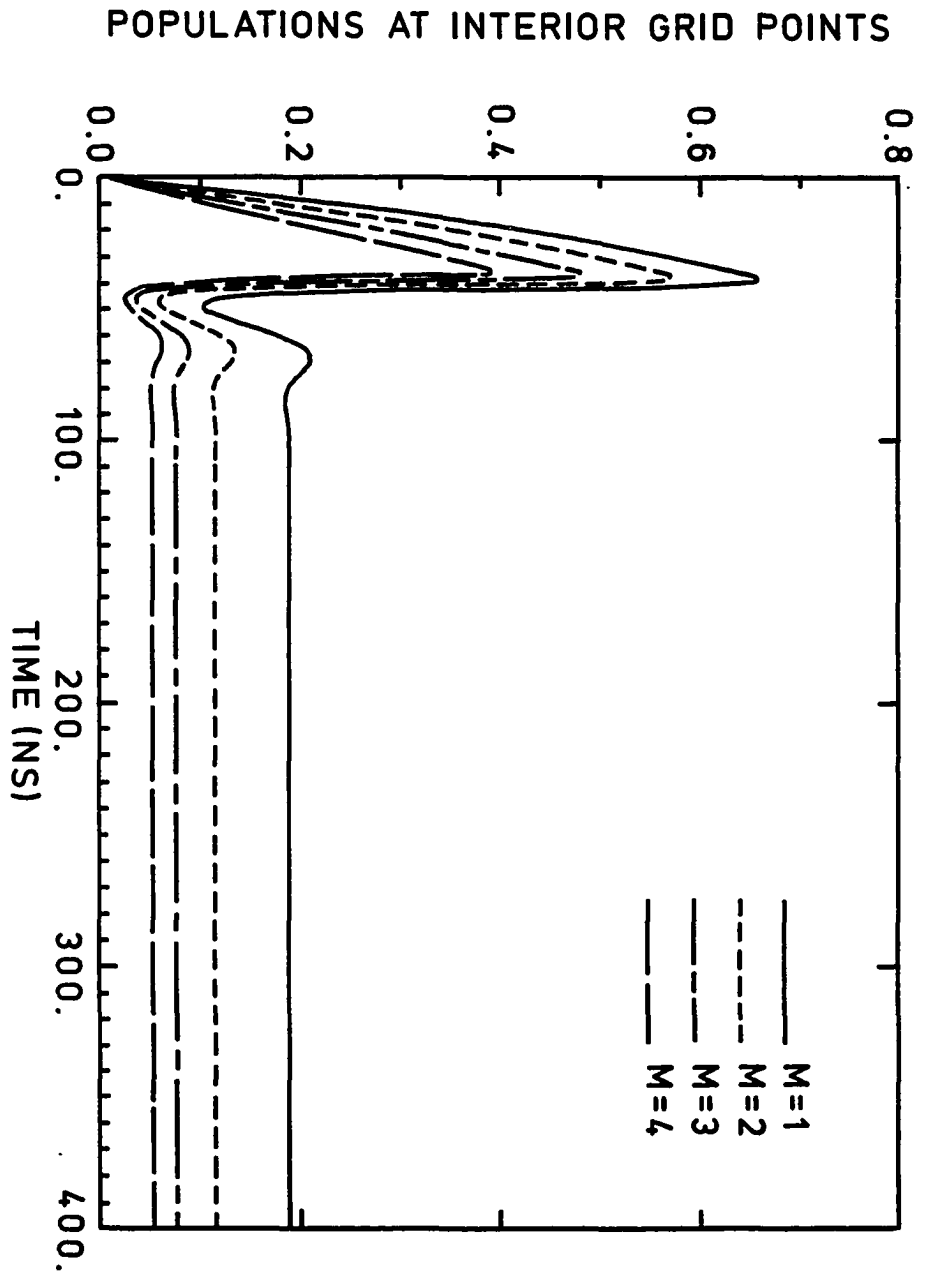

Figure 4.18 Population inversion at each interior grid point in a system with constant pump, E_p=20 mJ.

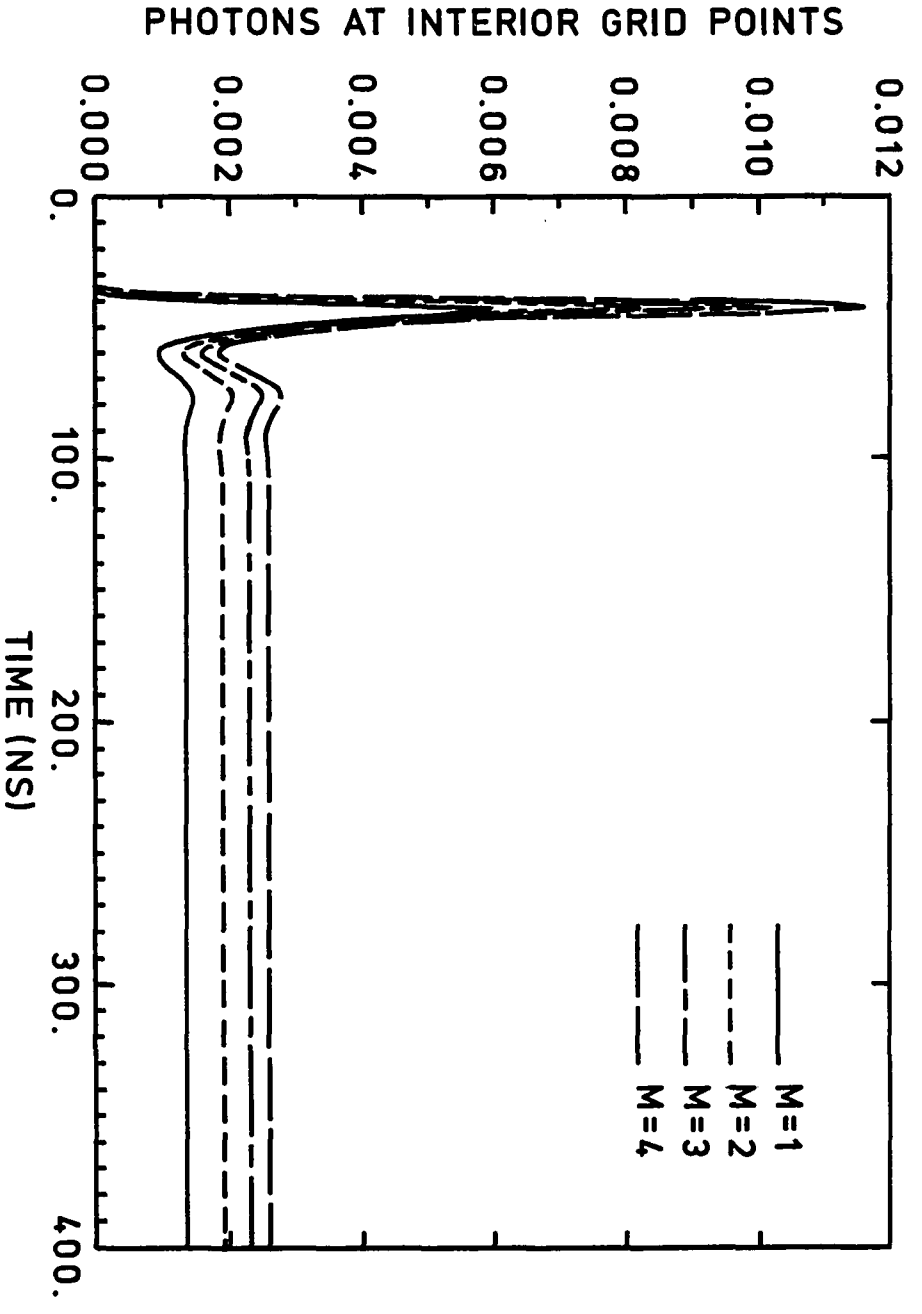

Figure 4.19 Total photon concentration at each interior grid point in a system with constant pump, E_p=20 mJ.

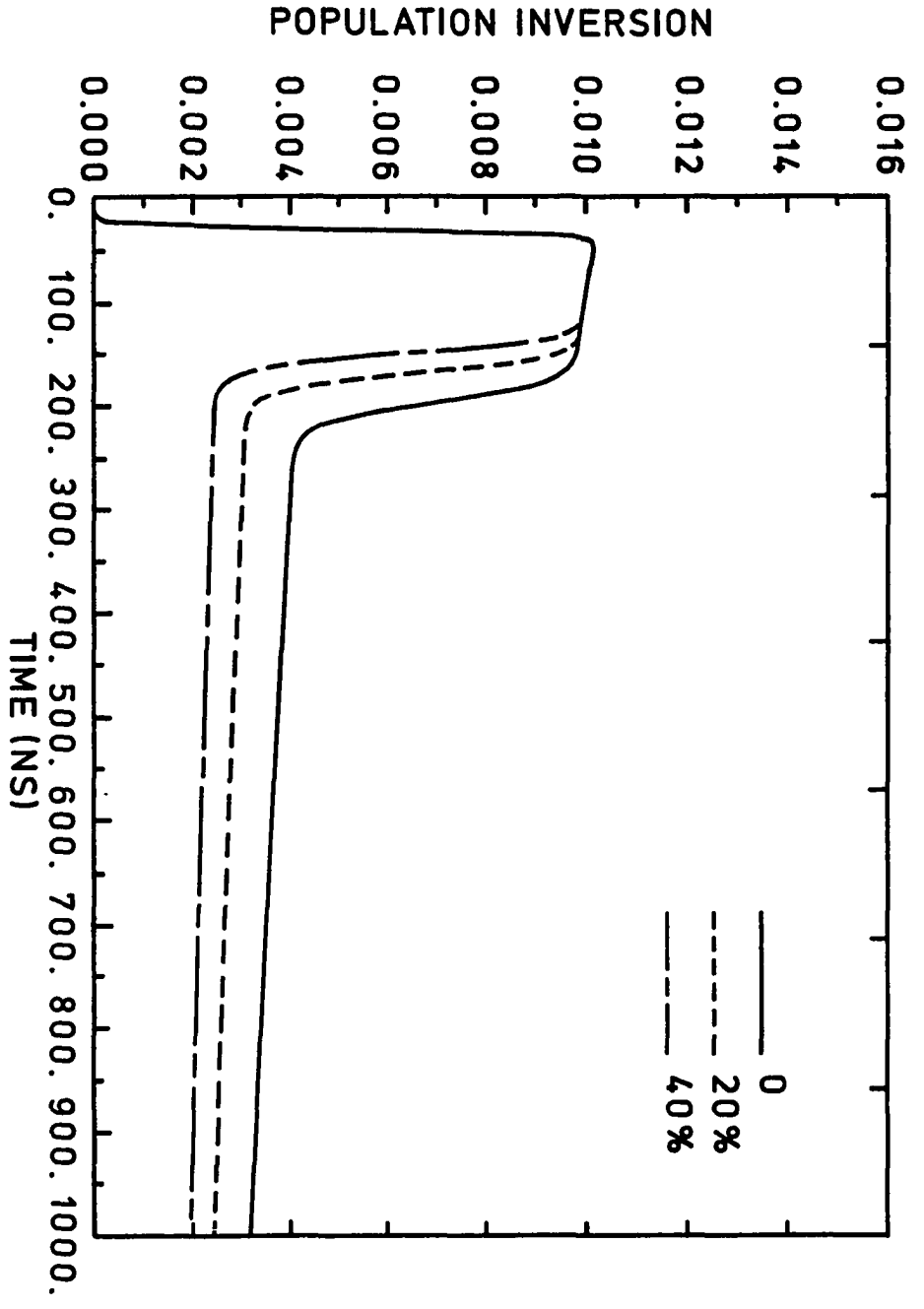

Figure 4.20 Curves showing the effect on the population inversion of the presence of an injection signal. Results are shown for varying amounts of output pulse reintroduced intthe system. Her, E_p=20mJ and Gaussian boundary distribution of the pump pulse.

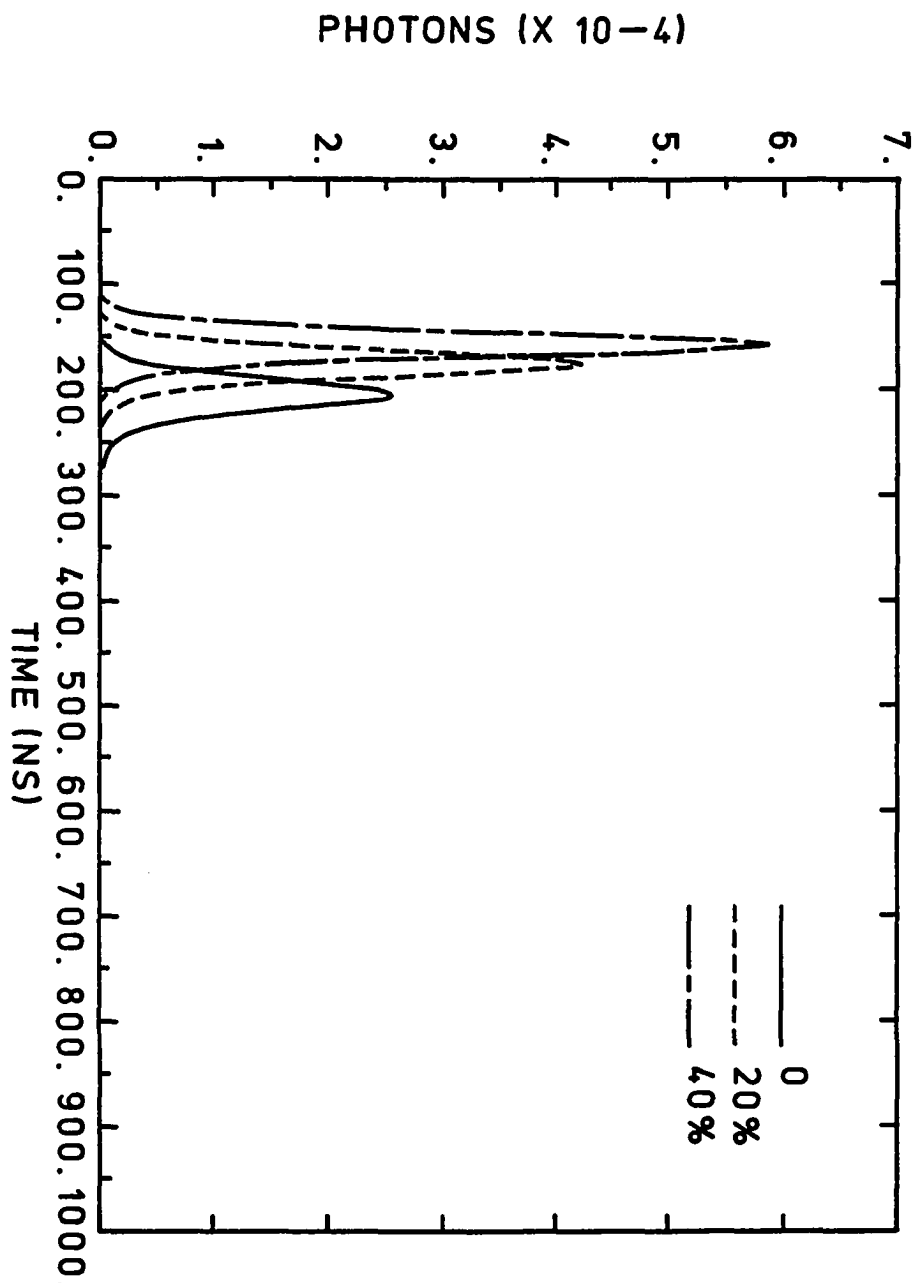

Figure 4.21 Curves showing the effect on the total photon concentration of the presence of an injection signal. Results are shown for varying amounts of output pulse reintroduced into the system. Here, E_p=20 mJ and Gaussian boundary distribution of the pump pulse.

Chapter 5

Concluding Remarks

The analytical study of both the spatial and temporal model and the spatially averaged version of the model verify that the solutions satisfy physically realistic qualitative properties under realsitic assumptions about the laser material and the operating environment of the laser.

While the spatially averaged version of the model does not offer specific information on spatial variations in the laser dynamics, it does provide insight into the effects on the solutions of changes in the physical parameters, and pump pulse. It allows the introduction of an injection signal so that injection seeding as a line narrowing technique may be studied. The stability analysis provides estimates on laser threshold conditions that must be exceeded in order for stimulated emission to occur.

The spatial and temporal model is complete in the sense that it provides the capability of analyzing the dynamics at any point in the laser cavity. It also

includes the dependence of the photons on discrete wavelengths in the emission spectrum. While the study was based on a simple ring cavity configuration, the numerical procedure developed here gives approximate solutions which agree favorably with the results from a stable finite difference algorithm that required many more grid points and hence much more computer effort to obtain comparable accuracy. The solutions generated by the Modified Euler Method in conjunction with the method of characteristics also agreed favorably with anticipated qualitative properties.

The spatial and temporal model, together with the qualitative and numerical analysis here, provide a powerful analytical tool for the study of an optically pumped four-level solid state laser system.

References

1. Birkhoff, G. and Gian-Carlo Rota, Ordinary Differential Equations, Ginn and Company, 1972.

2. Brauer, F. and J. Nohel, Qualitative Theory of Ordinary Differential Equations, W.A. Benjamin, New York, 1969.

3. Brockman, P., C.H. Bair, J.C. Barnes, R.V. Hess, and E.V. Browel, Optics Letters, Vol. 11, No.11, 1986, pp. 712-714.

4. Byvik, C.E. and A.M. Buoncristiani, IEEE J. Quantum Electron, QE-21, 1985, p. 1619.

5. Buoncristiani, A.M., J.J. Swetits, L.F. Roberts, "Model of an End- pumped, Injection Seeded Solid-State Laser", Math. Comput. Modelling, To Appear.

6. Buoncristiani, A.M. Private communication.

7. Burden, R.L.and D.T. Faires, Numerical Analysis, Prindle, Weber and Schmidt, Boston, 1978.

8. Courant, R. and Lax, Ph.D., "On Nonlinear Partial Differential Equations with Two Independent Variables", Pure Appl. Math., Vol. 2, 1949, ppp. 253-273.

9. Ganiel, U., A. Hardy, and G. Neumann, "Amplified Spontaneous Emission and Signal Amplification in Dye-laster Systems", IEEE J. Quantum Electron, QE-11, 1975, pp. 881-892.

10. Ganiel, U., A. hardy, and D. Treves, "Analysis of Injection Locking in Pulsed Dye Laser Systems", IEEE J. Quantum Electron, QER-12, 1976, pp. 704-715.

11. Garabedian, P., Partial Differential Equations, Chelsea, New York, 1964.

12. Koechner, W., Solid-State Laser Engineering, Chelsea, New York, 1964.

13. Langley Research Center Implementation of LSODE, and ODE software package based on the GEAR and GEARB packages (A.C. Hindmarsh, Lawrence Livermore Lab.)

14. Lapidus, L. and G.F. Pinder, Numerical Solutions of Partial Differential Equations in Science and Engineering, Wiley interscience, New York, 1982.

15. Meis, T. and U. Marcowitz, Numerical Solution of Partial Differential Equations in Science and Engineering, Wiley Interscience, New York, 1982.

16. Meis, T. and U. Marcowitz, Numerical Solution of Partial Differential Equations, Springer-Verlag, New York, 1981.

17. Moulton, P., "An Investigation of the Co:MgF_2 Laser System", IEEE J. Quantum Electron, QE-21, 1985, pp. 1582-1595.

18. Moulton, P., "Spectroscopic and Laser Characteristics of Ti:Al_2O_3", Jour. Opt. Soc. Am. B, Vol. 3, NO. 1, 1986, pp. 125- 133.

19. Moulton, P., "Titanium Doped Sapphire Laser Research and Design Study", NASA Contractor Report 4093, 1987.

20. Nair, L.G., and K. Dasgupta, "Amplified Spontaneous Emission in Narrow-Band Pulsed Dye Laser Systems", IEEE J. Quantum Electron, QE-21, 1985.

21. Sanchez, D.A., Ordinary Differential Equations and Stability Theory: Theory: An Introduction, Dover, New York, 1979.

22. Sneddon, I., Elements of Partial Differential Equations, McGraw-Hill, New York, 1957.

23. Struble, R.A., Nonlinear Differential Equations, McGraw-Hill, New York, 1962.

24. Tarasov, L.V. Laser Physics, MIR, Moscow, 1983.

Appendix I

Computer Program: Equilibrium

```
CCCCCCCCCCCCCCCCCCCCCCCCCCCCCCCCCCCCCCCCCCCCCCCCCCCCCCCCCCCCCC
C    THIS PROGRAM CALCULATES THE EQUILIBRIUM POINTS
C    OF THE FOUR-LEVEL THREE EQUATION MODEL.  IT
C    DETERMINES THE STABILITY PROPERTIES OF THE
C    EQUILIBRIUM POINTS.  IN ADDITION, IT ALSO FINDS
C    THE EIGENVALUES OF THE LINEARIZED SYSTEM BY
C    NEWTON'S METHOD TO FIND THE FIRST EIGENVALUE
C   THEN FACTORS THE REMAINING
C   QUADRATIC TO DETERMINE
C   THE  OTHER TWO EIGENVALUES.
CCCCCCCCCCCCCCCCCCCCCCCCCCCCCCCCCCCCCCCCCCCCCCCCCCCCCCCCCCCCCC
      PROGRAM EQUILIBRIUM
      IMPLICIT DOUBLE PRECISION(A-H,O-Z)
CCCCCCCCCCCCCCCCCCCCCCCCCCCCCCCCCCCCCCCCCCCCCCCCCCCCCCCCCCCCCC
C     OPEN DATA FILES:
C         EQUILPT4.DAT EQUILIBRIUM POINTS
C         DISPT1.DAT   STABILITY PROPERTIES AND
C                      NATURE  OF THE LINEARIZED
C                      EIGENVALUES
C         DISPT2.DAT   STABILITY PROPERTIES AND
C                      NATURE OF THE LINEARIZED
C                      EIGENVALUES
      OPEN(UNIT=1,FILE='EQUILPT4.DAT',STATUS='NEW')
      OPEN(UNIT=2,FILE='DISPT2.DAT',STATUS='NEW')
      OPEN(UNIT=3,FILE='DISPT1.DAT',STATUS='NEW')
C*****TI:SAPPHIRE PHYSICAL PARAMETERS*****
      G21=2.0D0/3.0D0
      SIGMA=3.0D-19
      C=3.0D10
      DEX=1.76D0
      V=C/DEX
      TOTAL=1.0D18
      TAUFL=3800.0D0
      TAU1=1.0D0
      TAUC=16.5D0
      TAUN=1.0D-09
      TAU2=3000.0D0
C*****PUMP PARAMETER*********
      WP=.001
C*****SPONTANEOUS EMISSION PARAMETER**********
      SPO=1.0D-04
      GAMMA=G21+1.0D0
C*****DIFFERENTIAL EQUATION COEFFICIENTS******
      ALPHA=SIGMA*V*TOTAL*TAUN
      C11=-(1.0D0/TAU2+G21/TAUFL)
      C12=-G21*(-C11-1.0D0/TAU1)
      C21=1.0D0/TAUFL
      C22=G21/TAUFL-1.0D0/TAU1
      C31=SPO/TAUFL
      C32=G21*C31
      C33=-1.0D0/TAUC
C*******CALCULATION OF EQUILIBRIUM POINTS*******
      D21=C31-C21
```

```
          D22=C32-C22
          B11=C11-WP
          B12=C12-GAMMA*WP
          D11=B11+GAMMA*C21
          D12=B12+GAMMA*C22
          DET=D11*D22-D12*D21
          A=ALPHA*D12*C33
          B=C33*(C21*B12-C22*B11)-ALPHA*WP*D22
          C=WP*(C22*C31-C21*C32)
          DISCR=B*B-4.0D0*A*C
          IF(DISCR.LT.0.0D0)THEN
             TYPE 201
 201      FORMAT(' IMAGINARY ROOTS')
          GO TO 30
          ELSE
            D=2.0D0*A
CCCCCCCCCCCCCCCCCCCCCCCCCCCCCCCCCCCCCCCCCCCCCCCCCCCCCCCCCCC
C     EQUILIBRIUM POINTS
C          FIRST EQUILIBRIUM POINT
C            (X1,Y1,Z1)
C             WHERE X1=POPULATION INVERSION
C                   Y1=LOWER LASER LEVEL POPULATION
C                   Z1=PHOTON CONCENTRATION
C          SECOND EQUILIBRIUM POINT
C             (X2,Y2,Z2)
C              WHERE X2=POPULATION INVERSION
C                    Y2=LOWER LASER LEVEL POPULATION
C                    Z2=PHOTON CONCENTRATION
CCCCCCCCCCCCCCCCCCCCCCCCCCCCCCCCCCCCCCCCCCCCCCCCCCCCCCCCCCC
            Z1=(-B-DSQRT(DISCR))/D
            Z2=(-B+DSQRT(DISCR))/D
            X1=(-WP*D22+D12*C33*Z1)/DET
            X2=(-WP*D22+D12*C33*Z2)/DET
            Y1=(WP*D21-D11*C33*Z1)/DET
            Y2=(WP*D21-D11*C33*Z2)/DET
            WRITE(1,100)WP,X1,Y1,Z1
CCCCCCCCCCCCCCCCCCCCCCCCCCCCCCCCCCCCCCCCCCCCCCCCCCCCCCCCCCC
C     INFORMATION FLAGS:
C        ITFLAG IF=0 THEN NEWTON'S METHOD SUCCEEDS,
C                IF=1, NEWTON'S METHOD FAILS--TOO
C                      MANY ITERATIONS.
C        ISTAB IF=0 EQUIL. PT. IS STABLE
C              IF=1 EQUIL. PT. IS UNSTABLE
C        IEIGEN IF=0 EIGENVALUE IS REAL
C               IF=1 EIGENVALUE IS COMPLEX
C        MFLAG  IF=0 NO MULTIPLICITY OF EIGENVALUES
C               IF=1 MULTIPLICITY OF EIGENVALUES
C        IROOT  IF=0 NEWTON'S METHOD CONVERGED TO
C                    ROOT WITHIN SPECIFIED
C                    TOLERANCE
C               IF=1 NEWTON'S METHOD DID NOT
C                    CONVERGE TO ROOT
C                    WITHIN TOLERANCE
```

```
            ITFLAG=0
            IROOT=0
            IEIGEN=0
            MFLAG=0
            ISTAB=0
CCCCCCCCCCCCCCCCCCCCCCCCCCCCCCCCCCCCCCCCCCCCCCCCCCCCCCCC
C     CALCULATION OF CUBIC DISCRIMINANT FOR FIRST
C      EQUIL.PT
CCCCCCCCCCCCCCCCCCCCCCCCCCCCCCCCCCCCCCCCCCCCCCCCCCCCCCCC
            A111=C11-ALPHA*GAMMA*Z1-WP
            A121=C12-WP*GAMMA
            A131=-ALPHA*GAMMA*X1
            A211=C21+ALPHA*Z1
            A221=C22
            A231=ALPHA*X1
            A311=C31+ALPHA*Z1
            A321=C32
            A331=C33+ALPHA*X1
            BETA1=-(A111+A221+A331)
            GAMMA1=-(A231*A321+A211*A121+
     1            A311*A131-A111*A221-A331*A111-
     2            A331*A221)
            SIGMA1=-(A111*A221*A331-
     1            A111*A231*A321-A211*A121*A331
     2            +A211*A321*A131+A311*
     3            A121*A231-A311*A131*A221)
            P=-(1.0D0/3.0D0)*BETA1*BETA1+GAMMA1
            Q=-GAMMA1*BETA1/3.0D0+SIGMA1+2.0D0*BETA1
     1          *BETA1*BETA1/27.0D0
            DIS=-27.0D0*Q*Q-4.0D0*P*P*P
            TEST=BETA1*GAMMA1-SIGMA1
C  STABILITY CHECK FOR FIRST EQUILIBRIUM POINT
               IF(BETA1.GT.0.0D0.AND.SIGMA1.GT.0.0D0
     1            .AND.TEST.GT.0.0D0)THEN
              ISTAB=1
              WRITE(1,101)ISTAB
              WRITE(2,200)WP,DIS,ISTAB
            ELSE
              ISTAB=0
              WRITE(1,101)ISTAB
              WRITE(2,200)WP,DIS,ISTAB
            END IF
C   CHECK FOR NATURE OF EIGENVALUES
            IF(DIS.LT.0.0D0) THEN
              IEIGEN=1
              WRITE(1,102)IEIGEN
            ELSE
              IF(DIS.GT.0.0D0) THEN
               IEIGEN=0
               WRITE(1,102)IEIGEN
              ELSE
               IEIGEN=0
               MFLAG=1
```

```
              WRITE(1,103)IEIGEN,MFLAG
             END IF
            END IF
CCCCCCCCCCCCCCCCCCCCCCCCCCCCCCCCCCCCCCCCCCCCCCCCCCCCCCCCCCCCCC
C  CALCULATION OF EIGENVALUES--FIRST DETERMINED BY
C  NEWTON'S METHOD.  REMAINING TWO DETERMINED FROM
C  REDUCED QUADRATIC.
            CALL ANEWTON(BETA1,GAMMA1,SIGMA1,E1,
     1                   ITFLAG)
             IF(ITFLAG.EQ.1)GO TO 10
             CALL ROOTS(E1,BETA1,GAMMA1,SIGMA1
     1                 ,E2R,E2I,E3R,E3I,IROOT)
             IF(IROOT.EQ.1)GO TO 10
             WRITE(1,105)E1,E2R,E2I,E3R,E3I
  10        CONTINUE
            WRITE(1,104)ITFLAG,IROOT
            WRITE(1,150)WP,X2,Y2,Z2
C  CHECK FOR STABILITY OF SECOND EQUILIBRIUM POINT
C   CHECK FOR NATURE OF EIGENVALUES
            ITFLAG=0
            IROOT=0
            IEIGEN=0
            MFLAG=0
            ISTAB=0
            A112=C11-ALPHA*GAMMA*Z2-WP
            A122=C12-WP*GAMMA
            A132=-ALPHA*GAMMA*X2
            A212=C21+ALPHA*Z2
            A222=C22
            A232=ALPHA*X2
            A312=C31+ALPHA*Z2
            A322=C32
            A332=C33+ALPHA*X2
            BETA2=-(A112+A222+A332)
            GAMMA2=-(A232*A322+
     1              A212*A122+A312*A132-A112*A222
     2              -A332*A112-A332*A222)
          SIGMA2=-(A112*A222*A332-
     1             A112*A232*A322-A212*A122*A332
     2             +A212*A322*A132+
     3             A312*A122*A232-A312*A132*A222)
             P=-(1.0D0/3.0D0)*BETA2*BETA2+GAMMA2
             Q=-GAMMA2*BETA2/3.0D0+SIGMA2+
     1          2.0D0*BETA2*BETA2*BETA2/27.0D0
             DIS=-27.0D0*Q*Q-4.0D0*P*P*P
             TEST=BETA2*GAMMA2-SIGMA2
             IF(BETA2.GT.0.0D0.AND.SIGMA2.GT.0.0D0.
     1         AND.TEST.GT.0.0D0)THEN
               ISTAB=1
               WRITE(1.101)ISTAB
               WRITE(3,200)WP,DIS,ISTAB
             ELSE
               ISTAB=0
```

```
              WRITE(1,101)ISTAB
              WRITE(3,200)WP,DIS,ISTAB
            END IF
            IF(DIS.LT.0.0D0) THEN
              IEIGEN=1
              WRITE(1,102)IEIGEN
            ELSE
              IF(DIS.GT.0.0D0)THEN
                IEIGEN=0
                WRITE(1,102)IEIGEN
              ELSE
                IEIGEN=0
                MFLAG=1
                WRITE(1,103)IEIGEN,MFLAG
              END IF
            END IF
            CALL ANEWTON(BETA2,GAMMA2,SIGMA2,
     1                   E1,ITFLAG)
            IF(ITFLAG.EQ.1)GO TO 20
            CALL ROOTS(E1,BETA2,GAMMA2,SIGMA2,
     1                 E2R,E2I,E3R,E3I,IROOT)
            IF(IROOT.EQ.1)GO TO 20
            WRITE(1,105)E1,E2R,E2I,E3R,E3I
          END IF
 20       CONTINUE
          WRITE(1,104)ITFLAG,IROOT
 30       CONTINUE
 45       CONTINUE
 100      FORMAT(' WP=',G22.9,/,' 2ND EQUILIBRIUM
          1        POINT',3G15.8)
 101      FORMAT(' STABILITY FLAG',I10)
 102      FORMAT(' COMPLEX EIGENVALUE FLAG',I10)
 103      FORMAT(' COMPLEX EIGENVALUE FLAG',I10,/,
         1       ' MULTIPLICITY FLAG',I10)
 104      FORMAT(' ITERATION FLAG',I10,' ROOT CHECK
          1      FLAG',I10)
 105      FORMAT(' EIGENVALUES',/,G22.8,/,2(2G22.8,/))
 150      FORMAT(' WP=',G22.8,/,' 1ST EQUILIBRIUM
         1       POINT',3G15.8)
 200      FORMAT(2G22.8,I10)
          STOP
          END
CCCCCCCCCCCCCCCCCCCCCCCCCCCCCCCCCCCCCCCCCCCCCCCCCCCCCCCCCCCCCCCCCCC
          SUBROUTINE ANEWTON(B,C,D,X,ITFLAG)
C          INPUT:
C                B,C,D=COEFFICIENTS OF CUBIC
C          OUTPUT:
C                X=COMPUTED ROOT
C                ITFLAG=ITERATION FLAG
          IMPLICIT DOUBLE PRECISION(A-H,O-Z)
          ITFLAG=0
          TOL=1.0D-12
          MAXIT=200
```

```
      X1=B*.5D0
      DO 10 I=1,MAXIT
        DENOM=DERIV(B,C,X1)
        DNUMER=FUNCT(B,C,D,X1)
        DNUX=X1-DNUMER/DENOM
        TEST=FUNCT(B,C,D,DNUX)
        TE=DABS(DNUX-X1)
        IF(DABS(TE).LT.TOL.AND.TEST.LT.TOL)GO TO 20
        X1=DNUX
 10   CONTINUE
      ITFLAG=1
      GO TO 30
 20   CONTINUE
      X=DNUX
 30   CONTINUE
      RETURN
      END
CCCCCCCCCCCCCCCCCCCCCCCCCCCCCCCCCCCCCCCCCCCCCCCCCCCCCCCCCCCCCCCCCC
      FUNCTION DERIV(B,C,X)
C     FUNCTION CALLED BY NEWTON'S METHOD TO COMPUTE
C        DERIVATIVE
      IMPLICIT DOUBLE PRECISION(A-H,O-Z)
      BETAM=3.0D0*X+2.0D0*B
      DERIV=X*BETAM+C
      RETURN
      END
CCCCCCCCCCCCCCCCCCCCCCCCCCCCCCCCCCCCCCCCCCCCCCCCCCCCCCCCCCCCCCCCCC
      FUNCTION FUNCT(B,C,D,X)
C     FUNCTION CALLED BY NEWTON TO EVALUATE CUBIC
      IMPLICIT DOUBLE PRECISION (A-H,O-Z)
      BETAF=X+B
      GAMMAF=X*BETAF+C
      FUNCT=X*GAMMAF+D
      RETURN
      END
CCCCCCCCCCCCCCCCCCCCCCCCCCCCCCCCCCCCCCCCCCCCCCCCCCCCCCCCCCCCCCCCCC
      FUNCTION ROOTS(X,B,C,D,R1R,R1I,R2R,R2I,IROOT)
C     FUNCTION COMPUTES ROOTS OF REDUCED QUADRATIC
      IMPLICIT DOUBLE PRECISION (A-H,O-Z)
      IROOT=0
      BETAR=X+B
      GAMMAR=X*BETAR+C
      TEST=X*GAMMAR+D
      IF(TEST.LT.1.0D-12) THEN
        DISC=BETAR*BETAR-4.0D0*GAMMAR
        IF(DISC.LT.0.0D0)THEN
          R1R=-BETAR/2.0D0
          R2R=R1R
          R1I=DSQRT(-DISC)/2.0D0
          R2I=-R1I
        ELSE
          R1I=0.0D0
          R2I=R1I
```

```
      R1R=-BETAR/2.0D0+DSQRT(DISC)/2.0D0
      R2R=-BETAR/2.0D0-DSQRT(DISC)/2.0D0
    END IF
  ELSE
    IROOT=1
  END IF
  RETURN
  END
```

Appendix II

Computer Program: Ring

```
CCCCCCCCCCCCCCCCCCCCCCCCCCCCCCCCCCCCCCCCCCCCCCCCCCCCCCCCCCCCCCCCCCCC
CCCCCCCCCCCCCCCCCCCCCCCCCCCCCCCCCCCCCCCCCCCCCCCCCCCCCCCCCCCCCCCCCCCC
      PROGRAM RING
C   RING COMPUTES APPROXIMATE SOLUTIONS TO THE PDE MODEL
C   OF A RING LASER USING THE MODIFIED EULER METHOD
C   THE RING LASER CAVITY IS ASSUMED TO BE EQUILATERAL
C   IF THIS IS NOT THE CASE SOME MODIFICATION TO THE
C   GRID WILL BE NECESSARY.
C
C   SUBROUTINES:
C         SWITCH
C         PHICAV
C         DQ1
C         DQ2
C         PUMP
C
CCCCCCCCCCCCCCCCCCCCCCCCCCCCCCCCCCCCCCCCCCCCCCCCCCCCCCCCCCCCCCCCCCCC
CCCCCCCCCCCCCCCCCCCCCCCCCCCCCCCCCCCCCCCCCCCCCCCCCCCCCCCCCCCCCCCCCCCC
C  DISCRETIZATION PARAMETERS
C
C     NXCR=#SPATIAL INCREMENTS IN CRYSTAL
C     NXTOTAL=MAXIMUM NUMBER OF SPATIAL INCREMENTS IN
C             CAVITY
C     NL=NUMBER OF WAVELENGTHS IN EMISSION SPECTRUM OF
C        CONCERN
CCCCCCCCCCCCCCCCCCCCCCCCCCCCCCCCCCCCCCCCCCCCCCCCCCCCCCCCCCCCCCCCCCCC
C  DISCRETIZATION PARAMETERS
C
C     NX    CR=#SPATIAL INCREMENTS IN CRYSTAL
C     NXTOTAL=MAXIMUM NUMBER OF SPATIAL INCREMENTS IN
C             CAVITY
C     NL=NUMBER OF WAVELENGTHS IN EMISSION SPECTRUM OF
C        CONCERN
CCCCCCCCCCCCCCCCCCCCCCCCCCCCCCCCCCCCCCCCCCCCCCCCCCCCCCCCCCCCCCCCCCCC
C   DEPENDENT VARIABLES: (CURRENT VALUES)
C     X--ARRAY OF LENGTH NXCR+1.  POPULATION INVERSION
C     X1-ARRAY OF LENGTH NXCR+1.  LOWER LEVEL POPULATION
C     W--ARRAY OF LENGTH NXCR+1.  PUMP
C     PHI-ARRAY OF DIMENSIONS 2xNXTOTL+1xNL.  RIGHT AND
C         LEFT TRAVELING PHOTON CONCENTRATIONS IN THE
C         ACTIVE REGION AND IN THE CAVITY
CCCCCCCCCCCCCCCCCCCCCCCCCCCCCCCCCCCCCCCCCCCCCCCCCCCCCCCCCCCCCCCCCCCC
C     TEMPORARY VALUES OF THE DEPENDENT VARIABLES ARE
C     STORED IN THE ARRAYS
C       XTMP,X1TMP,WTMP,PHITMP.
C     PREVIOUS VALUES OF THE DEPENDENT VARIABLES ARE
C     STORED IN THE ARRAYS
C       XOLD,X1OLD,WOLD,PHIOLD.
C     NEWLY COMPUTED VALUES OF THE DEPENDENT VARIABLES
C     ARE STORED IN THE ARRAYS
C       XNEW,X1NEW,WNEW,PHINEW.
CCCCCCCCCCCCCCCCCCCCCCCCCCCCCCCCCCCCCCCCCCCCCCCCCCCCCCCCCCCCCCCCCCCC
C     VALUES OF THE DIRECTIONAL DERIVATIVES
```

```
C     ARE STORED IN THE ARRAYS
C       DWOLD(NXCR+1),DXOLD(2,NXCR+1),DPHOLD(2,NXCR+1,NL)
C       DW(NXCR+1),DX(2,NXCR+1),DPHI(2,NXCR+1,NL)
C       DWTMP(NXCR+1),DXTMP(2,NXCR+1),DPTMP(2,NXCR+1,NL)
CCCCCCCCCCCCCCCCCCCCCCCCCCCCCCCCCCCCCCCCCCCCCCCCCCCCCCCCCCCCCCCCCC
      PARAMETER(NXCR=5,NXTOTL=1000,NL=24)
CCCCCCCCCCCCCCCCCCCCCCCCCCCCCCCCCCCCCCCCCCCCCCCCCCCCCCCCCCCCCCCCCC
C  DECLARATIONS
C  CALCULATIONS DONE IN REAL DOUBLE PRECISION
      IMPLICIT DOUBLE PRECISION(A-H,L,O-Z)
CCCCCCCCCCCCCCCCCCCCCCCCCCCCCCCCCCCCCCCCCCCCCCCCCCCCCCCCCCCCCCCCCC
      DIMENSION X(0:NXCR),X1(0:NXCR),XTMP(0:NXCR),
     1          X1TMP(0:NXCR),XNEW(0:NXCR),X1NEW(0:NXCR),
     2          W(0:NXCR),WNEW(0:NXCR),WTMP(0:NXCR),
     3          PHI(2,0:NXTOTL,NL),PHINEW(2,0:NXTOTL,NL),
     4          DWOLD(0:NXCR),DXOLD(2,0:NXCR),DW(0:NXCR),
     5          DX(2,0:NXCR),LAM(NL),OUTPUT(2,NL),
     6          DPHI(2,0:NXCR,NL),PHITMP(2,0:NXTOTL,NL),
     7          XONEW(0:NXCR),DPHOLD(2,0:NXCR,NL),
     8          DWTMP(0:NXCR),DXTMP(2,0:NXCR),
     9          DPTMP(2,0:NXCR,NL),SIG(NL),
     A          WOLD(0:NXCR),PHIOLD(2,0:NXTOTL,NL),
     B          XOLD(0:NXCR),X1OLD(0:NXCR)
CCCCCCCCCCCCCCCCCCCCCCCCCCCCCCCCCCCCCCCCCCCCCCCCCCCCCCCCCCCCCCCCCC
C   WAVELENGTHS IN MICRONS
      DATA LAMBDA/.650D0,.675D0,.6875D0,.700D0,.712D0,
     1            .725D0,.7375D0,.750D0,.7625D0,.775D0,
     2            .7875D0,.800D0,.812D0,
     3            .825D0,.8375D0,.850D0,
     4            .8625D0,.875D0,.8875D0,.900D0,.9125D0,
     5            .925D0,.9375D0,.950D0/
CCCCCCCCCCCCCCCCCCCCCCCCCCCCCCCCCCCCCCCCCCCCCCCCCCCCCCCCCCCCCCCCCC
C   CROSS SECTIONS IN CM^2
      DATA SIGMA/3.48D-20,8.0D-20,1.2D-19,1.6D-19,2.0D-19,
     1           2.4D-19,2.8D-19,3.22D-19,
     2           3.52D-19,3.79D-19,3.88D-19,
     3           3.944D-19,3.88D-19,3.8D-19,3.48D-19,
     4           3.272D-19,3.12D-19,2.9D-19,2.62D-19,
     5           2.432D-19,2.28D-19,2.00D-19,1.86D-19,
     6           1.60D-19/
CCCCCCCCCCCCCCCCCCCCCCCCCCCCCCCCCCCCCCCCCCCCCCCCCCCCCCCCCCCCCCCCCC
C   ABSORPTION COEFFICIENTS IN 1/CM
      DATA ALPHA/.07D0,.07D0,.07D0,.07D0,.07D0,.07D0,
     1           .07D0,.07D0,.07D0,.07D0,.07D0,.07D0,
     2           .07D0,.07D0,.07D0,.07D0,.07D0,.07D0,
     3           .07D0,.07D0,.07D0,.07D0,.07D0,.07D0/
CCCCCCCCCCCCCCCCCCCCCCCCCCCCCCCCCCCCCCCCCCCCCCCCCCCCCCCCCCCCCCCCCC
C     COMMON BLOCKS
      COMMON/COEFF/C11,C12,C21,C22,GAMMA,V,TOTALN
     1      XNORM,TNORM,BETA,BETAG,PFACTR,XNORML
      COMMON/SP/L,R,DEX,DELTAX,DLAMBDA(NL)
      COMMON/REFL/TS,R1,R2,R3,T1,FRACTN,AREA
      COMMON/DISCRT/N1,N2,MIDX
```

```
      COMMON/WPUMP/SIGMAA,BWAIST,ETAP,PLMBDA,ETOTL,TAUP,T0
      COMMON/WAVL/SIGMA(NL),ALPHA(NL),NLMBDA,LAMBDA(NL)
CCCCCCCCCCCCCCCCCCCCCCCCCCCCCCCCCCCCCCCCCCCCCCCCCCCCCCCCCCC
C    TI:SAPPHIRE PARAMETERS:
C               G2G1=RATIO OF DEGENERACIES
C               DEX=INDEX OF REFRACTION
C               TAUFL=FLUORESCENCE LIFETIME(NS)
C               TAU2
C               TAU1
C               TS=FRESNEL TRANSMISSION COEFFICIENT
      G2G1=2.0D0/3.0D0
      DEX=1.76D0
      TAUFL=3870.0D0
      TAU2=3150.0D0
      TAU1=1.0D0
      TS=4.0D0*DEX/((DEX+1.0D0)*(DEX+1.0D0))
CCCCCCCCCCCCCCCCCCCCCCCCCCCCCCCCCCCCCCCCCCCCCCCCCCCCCCCCCCC
C     CRYSTAL PARAMETERS
C              TOTALN=CONCENTRAION OF DOPANT IONS(/CM^3)
C              L=LENGTH(CM)
C              R=RADIUS(CM)
       TOTALN=1.26D19
      L=2.5D0
      R=.05D0
CCCCCCCCCCCCCCCCCCCCCCCCCCCCCCCCCCCCCCCCCCCCCCCCCCCCCCCCCCC
C     PUMP PARAMETERS
C
C              ETOTL=ENERGY OF PUMP (mJ)
C              TAUP,T0=GAUSSIAN BEAM PARAMETERS(NS)
C              BWAIST=BEAM WAIST(CM)
C              ETAP=BRANCHING RATIO
C              PLMBDA=PUMP WAVELENGTH(MICRON)
C              SIGMAA=ABSORPTION CROSS SECTION(CM^2)
      ETOTL=200.0D0
      TAUP=10.0D0
      T0=30.0D0
      BWAIST=.05D0
      ETAP=1.0D0
      PLMBDA=.532D0
      PLMBDA=PLMBDA*1.0D-04
      SIGMAA=5.12D-20
CCCCCCCCCCCCCCCCCCCCCCCCCCCCCCCCCCCCCCCCCCCCCCCCCCCCCCCCCCC
C     CAVITY PARAMETERS
C         LP=LENGTH OF CAVITY
C         R1=REFLECTION OF 1ST MIRROR
C         T1=TRANSMISSION OF 1ST MIRROR
C         R2=REFLECTION OF 2ND MIRROR
C         R3=REFLECTION OF 3RD MIRROR
      LP=120.0D0
      R1=.4D0
      T1=.5D0
      R2=0.9D0
      R3=0.9D0
```

```
CCCCCCCCCCCCCCCCCCCCCCCCCCCCCCCCCCCCCCCCCCCCCCCCCCCCCCCCCCCCCCCCCC
C     BEGIN-END TIMES(NS)
C
      TBEGIN=0.0D0
      TEND=130.0D0
CCCCCCCCCCCCCCCCCCCCCCCCCCCCCCCCCCCCCCCCCCCCCCCCCCCCCCCCCCCCCCCCCC
C     REFLECTIVITY OF REVERSE WAVE SUPRESSOR MIRROR
C
      FRACTN=0.0D0
CCCCCCCCCCCCCCCCCCCCCCCCCCCCCCCCCCCCCCCCCCCCCCCCCCCCCCCCCCCCCCCCCC
C     OPEN DATA OUTPUT FILES (USER DEPENDENT)
C     FOR EXAMPLE:  THE FOLLOWING MAY BE OPENED TO
C     PRINT THE VALUES OF THE POPULATION INVERSION,
C     PHOTON CONCENTRATION AND PUMP AT A PARTICULAR GRID
C     POINT:
      OPEN(4,FILE='N.DAT',STATUS='NEW')
      OPEN(5,FILE='PHI.DAT',STATUS='NEW')
      OPEN(6,FILE='PUMP.DAT',STATUS='NEW')
CCCCCCCCCCCCCCCCCCCCCCCCCCCCCCCCCCCCCCCCCCCCCCCCCCCCCCCCCCCCCCCCCC
C NUMBER OF WAVELENGTHS IN THIS EXAMPLE
C  NLMBDA MUST BE LESS THAN OR EQUAL TO NL-1
      NLMBDA=NL-1
C COMPUTE DLAMBDAS AND XSECTION AND WAVELENGTH AVERAGES
      DO 5 I=1,NLMBDA
           DLAMBDA(I)=LAMBDA(I+1)-LAMBDA(I)
           SIG(I)=.5D0*(SIGMA(I+1)+SIGMA(I))
           LAM(I)=.5D0*(LAMBDA(I+1)+LAMBDA(I))
 5    CONTINUE
C   RENAME SIG AND LAM--CONVERT LAMBDAS AND DLAMBDAS TO CM
      DO 8 I=1,NLMBDA
           SIGMA(I)=SIG(I)
           LAMBDA(I)=LAM(I)*1.0D-04
           DLAMBDA(I)=DLAMBDA(I)*1.0D-04
 8    CONTINUE
CCCCCCCCCCCCCCCCCCCCCCCCCCCCCCCCCCCCCCCCCCCCCCCCCCCCCCCCCCCCCCCCCC
C  NORMALIZING CONSTANTS
      XNORM=TOTALN
      TNORM=1.0D-09
CCCCCCCCCCCCCCCCCCCCCCCCCCCCCCCCCCCCCCCCCCCCCCCCCCCCCCCCCCCCCCCCCC
C  OUTPUT PARAMETER--WILL PRINT EVERY IOth VALUE TO DATA
C    FILE
      IO=1
CCCCCCCCCCCCCCCCCCCCCCCCCCCCCCCCCCCCCCCCCCCCCCCCCCCCCCCCCCCCCCCCCC
C    PHYSICAL CONSTANTS
C    C=SPEED OF LIGHT IN VACUUM(CM/SEC)
C    H=PLANCK'S CONSTANT(mJ-SEC)
      C=3.0D10
      H=6.6262D-31
C    COMPUTED CONSTANTS
      PI=4.0D0*DATAN(1.0D0)
      AREA=PI*BWAIST*BWAIST
CCCCCCCCCCCCCCCCCCCCCCCCCCCCCCCCCCCCCCCCCCCCCCCCCCCCCCCCCCCCCCCCCC
C  COEFFICIENTS IN RATE EQUATIONS
```

```
C
      GAMMA=1.0D0+G2G1
      V=C/DEX
      C11=-1.0D0/TAU2-G2G1/TAUFL
      C12=-G2G1*(-C11-1.0D0/TAU1)
      C21=1.0D0/TAUFL
      C22=G2G1/TAUFL-1.0D0/TAU1
      PFACTR=-SIGMAA*XNORM
      BETA=V*XNORM*TNORM
      BETAG=BETA*GAMMA
      XNORML=TOTALN/XNORM
CCCCCCCCCCCCCCCCCCCCCCCCCCCCCCCCCCCCCCCCCCCCCCCCCCCCCCCCCCCCCCCCC
      T=TBEGIN
      TMAX=TEND
CCCCCCCCCCCCCCCCCCCCCCCCCCCCCCCCCCCCCCCCCCCCCCCCCCCCCCCCCCCCCCCCC
C     GRID MESH SELECTION                                          C
C     MUST BE MODIFIED IF CAVITY IS NOT EQUILATERAL                C
C     NXCR=# SPATIAL INCREMENTS IN CRYSTAL                         C
C     N1=# SPATIAL INCREMENTS FROM EDGE OF CRYSTAL TO              C
C          1ST MIRROR                                              C
C     N2=# SPATIAL INCREMENTS FROM 1ST MIRROR TO EDGE OF           C
C          CRYSTAL                                                 C
      CAV=LP/3.0D0
      L1=.5D0*(CAV+L)
      L2=2.0D0*CAV+L1
      DENOM=DBLE(NXCR)
      DELTAT=L/(V*DENOM*TNORM)
      DTBY2=DELTAT/2.0D0
      DELTAX=L/DENOM
      DXBY2=DELTAX/2.0D0
      DENOM1=C*DELTAT*TNORM
      N1=IDNINT((L1-L)/DENOM1)
      N2=IDNINT((L2-L)/DENOM1)
CCCCCCCCCCCCCCCCCCCCCCCCCCCCCCCCCCCCCCCCCCCCCCCCCCCCCCCCCCCCCCCCC
C   INITIAL CONDITIONS                                             C
C   POPULATIONS
      DO 20 I=0,NXCR
            X0(I)=XNORML
            X(I)=0.0D0
            X1(I)=0.0D0
 20   CONTINUE
C   PUMP
      W(0)=PUMP(T)
      DO 25 I=1,NXCR
          W(I)=0.0D0
 25   CONTINUE
C    PHOTONS + AND -
      DO 30 I=0,NXCR+N1+N2
            DO 29 J=1,NLMBDA
                  PHI(1,I,J)=0.0D0
                  PHI(2,I,J)=0.0D0
 29         CONTINUE
 30   CONTINUE
```

```
C  CALCULATE DERIVATIVES AT THE INITIAL POINTS
      CALL DQ1(T,X,X1,W,PHI,DW,DX)
      CALL DQ2(T,X,X1,PHI,DPHI)
C  FIRST VALUES COMPUTED BY EULER'S METHOD AND BOUNDARY
C  CONDITIONS
      M=1
      IOUT=MOD(M,IO)
      T=T+DELTAT
      DO 40 I=0,NXCR
         IF(I.EQ.0)THEN
           WNEW(0)=PUMP(T)
         ELSE
           WNEW(I)=W(I-1)+DELTAX*DW(I-1)
         END IF
         XNEW(I)=X(I)+DELTAT*DX(1,I)
         X1NEW(I)=X1(I)+DELTAT*DX(2,I)
         DO 50 J=1,NLMBDA
            IF(I.EQ.0)THEN
              PHINEW(1,I,J)=TS*R2*R3*
     1                       PHI(1,NXCR+N1+N2-1,J)
            ELSE
              PHINEW(1,I,J)=PHI(1,I-1,J)+
     1                       DELTAX*DPHI(1,I-1,J)
            END IF
 50      CONTINUE
 40   CONTINUE
      CALL PHICAV(PHI,PHINEW,OUTPUT)
C     PHIMINUS IN CRYSTAL
      DO 55 I=NXCR,1,-1
          DO 60 J=1,NLMBDA
             PHINEW(2,I-1,J)=PHI(2,I,J)+
     1                        DELTAX*DPHI(2,I,J)
 60       CONTINUE
 55   CONTINUE
C   CALCULATES PHIMINUS GOING OUT OF CRYSTAL
      DO 70 J=1,NLMBDA
          PHINEW(2,NXCR+N1+N2,J)=TS*PHINEW(2,0,J)
 70   CONTINUE
C     SWITCH VALUES
      CALL SWITCH(W,WNEW,X,XNEW,X1,X1NEW,PHI,
     1            PHINEW,DW,DX,DPHI,WOLD,XOLD,X1OLD,
     2            PHIOLD,DWOLD,DXOLD,DPHOLD,T)
      IF(IOUT.EQ.0)GO TO 400
 150  CONTINUE
      M=M+1
      IOUT=MOD(M,IO)
C  CALCULATE DERIVATIVES AT CURRENT TIME
      CALL DQ1(T,X,X1,W,PHI,DW,DX)
      CALL DQ2(T,X,X1,PHI,DPHI)
CCCCCCCCCCCCCCCCCCCCCCCCCCCCCCCCCCCCCCCCCCCCCCCCCCCCCCCC
C EULER'S METHOD IS USED FOR THE FIRST GUESS AT NEW TIME
CCCCCCCCCCCCCCCCCCCCCCCCCCCCCCCCCCCCCCCCCCCCCCCCCCCCCCCC
      T=T+DELTAT
```

```
      IF(T.GT.TMAX)GO TO 500
C LOOP 80 COMPUTES FIRST GUESS FOR THE PUMP AND
C POPULATIONS
C INTEGRATION FOR PUMP ALONG CHARACTERISTIC PARALLEL TO
C X=VT
C INTEGRATION FOR POPULATIONS ALONG CHARACTERISTICS
C X=CONSTANT
      DO 80 I=0,NXCR
C   BOUNDARY CONDITIONS FOR THE PUMP
         IF(I.EQ.0)THEN
            WTMP(0)=PUMP(T)
         ELSE
            WTMP(I)=W(I-1)+DELTAX*DW(I-1)
         END IF
         XTMP(I)=X(I)+DELTAT*DX(1,I-1)
         X1TMP(I)=X1(I)+DELTAT*DX(2,I-1)
 80   CONTINUE
C    BOUNDARY CONDITIONS FOR PHOTONS CLOCKWISE AND
C    CCLOCKWISE
      DO 85 J=1,NLMBDA
         PHITMP(1,0,J)=TS*R2*R3*PHI(1,NXCR+N1+N2-1,J)
         PHITMP(2,NXCR,J)=TS*PHI(2,NXCR+1,J)
C     LOOP 90 COMPUTES FIRST GUESS FOR THE CLOCKWISE
C     PHOTONS
C     INTEGRATION ALONG CHARACTERISTIC PARALLEL TO X=VT
        DO 90 I=1,NXCR
         PHITMP(1,I,J)=PHI(1,I-1,J)+DELTAX*(DPHI(1,I-1,J))
 90     CONTINUE
C     LOOP 95 COMPUTES FIRST GUESS FOR CCLOCKWISE PHOTONS
C     INTEGRATION ALONG CHARACTERISTIC PARALLEL TO X=-VT
        DO 95 I=NXCR-1,0,-1
            PHITMP(2,I,J)=PHI(2,I+1,J)+
     1                    DELTAX*(DPHI(2,I+1,J))
 95     CONTINUE
 85   CONTINUE
CCCCCCCCCCCCCCCCCCCCCCCCCCCCCCCCCCCCCCCCCCCCCCCCCCCCCC
C           IMPROVEMENTS ON FIRST GUESS
C            BY MODIFIED EULER'S METHOD
CCCCCCCCCCCCCCCCCCCCCCCCCCCCCCCCCCCCCCCCCCCCCCCCCCCCCC
      K=0
 300  CONTINUE
      K=K+1
C    EVALUATE DERIVATIVES AT THE PREDICTED VALUES
      CALL DQ1(T,XTMP,X1TMP,WTMP,PHITMP,DWTMP,DXTMP)
      CALL DQ2(T,XTMP,X1TMP,PHITMP,DPTMP)
C    MAKE IMPROVEMENT
C    LOOP 310 CORRECTS PUMP AND POPULATIONS
      DO 310 I=0,NXCR
         IF(I.EQ.0)THEN
           WNEW(I)=WTMP(I)
         ELSE
           WNEW(I)=W(I-1)+DXBY2*(DWTMP(I)+DW(I-1))
         END IF
```

```
            XNEW(I)=X(I)+DTBY2*(DXTMP(1,I)+DX(1,I))
            X1NEW(I)=X1(I)+DTBY2*(DXTMP(2,I)+DX(2,I))
 310  CONTINUE
      DO 320 J=1,NLMBDA
C     LOOP 325 CORRECTS CLOCKWISE PHOTONS
        DO 325 I=0,NXCR
          IF(I.EQ.0)THEN
            PHINEW(1,I,J)=PHITMP(1,I,J)
          ELSE
            PHINEW(1,I,J)=PHI(1,I-1,J)+DXBY2*(DPTMP(1,I,J)+
     1                    DPHI(1,I-1,J))

          END IF
 325    CONTINUE
C     LOOP 330 CORRECTS CCLOCKWISE PHOTONS
        DO 330 I=NXCR,1,-1
          IF(I.EQ.NXCR)THEN
           PHINEW(2,I,J)=PHITMP(2,I,J)
          ELSE
           PHINEW(2,I-1,J)=PHI(2,I,J)+DXBY2*(DPTMP(2,I-1,J)+
     1                     DPHI(2,I,J))
          END IF
 330    CONTINUE
 320  CONTINUE
C    SECOND ITERATION IN MODIFIED EULER'S METHOD
C    REPLACE TEMPORARY VALUES WITH NEW VALUES CALCULATED
C    ABOVE
C    GO THROUGH IMPROVEMENTS AGAIN.
       IF(K.EQ.1)THEN
          XTMP(I)=XNEW(I)
          X1TMP(I)=X1NEW(I)
          WTMP(I)=WNEW(I)
          DO 345 J=1,NLMBDA
             PHITMP(1,I,J)=PHINEW(1,I,J)
             PHITMP(2,NXCR-I,J)=PHINEW(2,NXCR-I,J)
 345      CONTINUE
 340    CONTINUE
        GO TO 300
        END IF
 420    CONTINUE
C CALCULATE PHOTONS IN THE REST OF THE CAVITY
       CALL PHICAV(PHI,PHINEW,OUTPUT)
C    SWITCH VALUES
       CALL SWITCH(W,WNEW,X,XNEW,X1,X1NEW,PHI,PHINEW,DW,
      1            DX,DPHI,WOLD,XOLD,X1OLD,PHIOLD,DWOLD,
      2            DXOLD,DPHOLD,T)
C  IF M IS A MULTIPLE OF IO THEN WRITE TO DATA FILES
 400  CONTINUE
       IF(IOUT.EQ.0)THEN
         WRITE(4,700)T,X(1)
         WRITE(6,700)T,W(1)
         SUM1=0.0D0
         DO 410 J=1,NLMBDA
```

```
        SUM1=SUM1+PHI(1,1,J)+PHI(2,1,J)
 410    CONTINUE
        WRITE(5,700)T,SUM1
      GO TO 150
 500  STOP
 700  FORMAT(2E18.6)
      END
CCCCCCCCCCCCCCCCCCCCCCCCCCCCCCCCCCCCCCCCCCCCCCCC
C          SUBROUTINE TO SWITCH VALUES
CCCCCCCCCCCCCCCCCCCCCCCCCCCCCCCCCCCCCCCCCCCCCCCC
C  ARGUMENTS:  W=PUMP (ON INPUT CURRENT VALUES FOR
C                      FOR PUMP. ON OUTPUT NEW VALUES
C                      FOR PUMP)
C              WNEW=NEWLY CALCULATED VALUES FOR PUMP
C              WOLD=ON INPUT OLD VALUES FOR PUMP.  ON
C                   OUTPUT CURRENT VALUES FOR PUMP
C              X=POPULATION INVERSION (ON INPUT CURRENT
C                FOR POP. INVERSION.  ON OUTPUT NEW
C                VALUES FOR PUMP)
C              XNEW=NEWLY CALCULATED VALUES FOR POP.INV.
C              XOLD=ON INPUT OLD VALUES FOR POP.INV. ON
C                   OUTPUT CURRENT VALUES FOR POP. INV.
C              X1=LOWER LASER LEVEL POPULATION.  ON INPUT
C                 CURRENT VALUES FOR L.L.POP. ON OUTPUT
C                 NEW VALUES FOR L.L.POP.
C              X1NEW=NEWLY CALCULATED VALUES FOR L.L.POP
C              X1OLD=ON INPUT OLD VALUES FOR L.L.POP.ON
C                    OUTPUT CURRENT VALUES FOR L.L.POP
C              PHI=PHOTON CONCENTRATIONS. ON INPUT
C                  CURRENT VALUES FOR PHOTON CONC.
C                  ON OUTPUT NEW VALUES FOR PHOTON CONC.
C              PHINEW=NEWLY CALCULATED VALUES FOR PHOTON
C                     CONC.
C              PHIOLD=ON INPUT OLD VALUES FOR PHOTON CONC.
C                     ON OUTPUT CURRENT VALUES FOR PHOTON
C                     CONC.
C              DX=CURRENT DERIVATIVE VALUES OF POPULATIONS
C              DXOLD=ON INPUT OLD DERIVATIVE VALUES. ON
C                 OUTPUT CURRENT DERIVATIVES OF POP.
C              DW=CURRENT DERIVATIVES OF PUMP
C              DWOLD=ON INPUT OLD DERIVATIVES OF
C                 PUMP.ON OUTPUT CURRENT DERIV. OF PUMP
C              DPHI=CURRENT DERIVATIVES OF PHOTON.
C              DPHIO=ON INPUT OLD DERIV. OF PHOTON. ON
C                 OUTPUT CURR. DERIV. OF PHOTON.
      SUBROUTINE SWITCH(W,WNEW,X,XNEW,X1,X1NEW,PHI,PHINEW,
     1           DW,DX,DPHI,WOLD,XOLD,X1OLD,PHIOLD,DWOLD,
     2           DXOLD,DPHIO,T)
      PARAMETER(NXCR=5,NL=24,NXTOTL=1000)
      IMPLICIT DOUBLE PRECISION(A-H,L,O-Z)
      DIMENSION W(0:NXCR),WNEW(0:NXCR),X(0:NXCR),
     1    XNEW(0:NXCR),X1NEW(0:NXCR),PHI(2,0:NXTOTL,NL),
     2    X1(0:NXCR),PHINEW(2,0:NXTOTL,NL),
```

```
     3     DW(0:NXCR),DX(2,0:NXCR),
     4     DPHI(2,0:NXCR,NL),WOLD(0:NXCR),XOLD(0:NXCR),
     5     X1OLD(0:NXCR),PHIOLD(2,0:NXTOTL,NL),
     6     DWOLD(0:NXCR)DXOLD(2,0:NXCR),DPHIO(2,0:NXCR,NL)
      COMMON/DISCRT/N1,N2,MIDX
      COMMON/WAVL/SIGMA(NL),ALPHA(NL),NLMBDA,LAMBDA(NL)
      DO 15 I=0,NXCR
            XOLD(I)=X(I)
            X1OLD(I)=X(I)
            WOLD(I)=W(I)
            X(I)=XNEW(I)
            X1(I)=X1NEW(I)
            W(I)=WNEW(I)
            DXOLD(1,I)=DX(1,I)
            DXOLD(2,I)=DX(2,I)
            DWOLD(I)=DW(I)
15    CONTINUE
      DO 30 K=1,2
         DO 20 J=1,NLMBDA
            DO 25 I=0,NXCR+N1+N2
                PHIOLD(K,I,J)=PHI(K,I,J)
                PHI(K,I,J)=PHINEW(K,I,J)
25          CONTINUE
            DO 35 I=0,NXCR
                DPHIO(K,I,J)=DPHI(K,I,J)
35          CONTINUE
20       CONTINUE
30    CONTINUE
      RETURN
      END
CCCCCCCCCCCCCCCCCCCCCCCCCCCCCCCCCCCCCCCCCCCCCCCCCCCCCCCCCCCCCCCC
CCCCCCCCCCCCCCCCCCCCCCCCCCCCCCCCCCCCCCCCCCCCCCCCCCCCCCCCCCCCCCCC
C     SUBROUTINE TO SOLVE HOMOGENEOUS PDES IN CAVITY
CCCCCCCCCCCCCCCCCCCCCCCCCCCCCCCCCCCCCCCCCCCCCCCCCCCCCCCCCCCCCCCC
      SUBROUTINE PHICAV(PHI,PHINEW,OUTPUT)
      PARAMETER(NXCR=5,NXTOTL=1000,NL=24)
      IMPLICIT DOUBLE PRECISION (A-H,L,O-Z)
      DIMENSION PHI(2,0:NXTOTL,NL),PHINEW(2,0:NXTOTL,NL),
     1      OUTPUT(2,NL),Z(2,NL)
      COMMON/REFL/TS,R1,R2,R3,T1,FRACTN,AREA
      COMMON/DISCRT/N1,N2,MIDX
      COMMON/WAVL/SIGMA(NL),ALPHA(NL),NLMBDA,LAMBDA(NL)
C    CALCULATES PHIPLUS AT THE BOUNDARY X=L
      DO 60 J=1,NLMBDA
            PHINEW(1,NXCR,J)=TS*PHINEW(1,NXCR,J)
C     CALCULATES PHIPLUS BETWEEN CRYSTAL AND OUTPUT COUPLER
            DO 65 I=NXCR,NXCR+N1-1
               PHINEW(1,I+1,J)=PHI(1,I,J)
 65         CONTINUE
C     CALCULATES PHIMINUS GOING OUT OF CRYSTAL
            PHINEW(2,NXCR+N1+N2,J)=TS*PHINEW(2,0,J)
C     CALCULATES PHIMINUS FROM EDGE OF CRYSTAL TO OUTPUT
C     COUPLER
```

```
            DO 75 I=NXCR+N1+N2,NXCR+N1+1,-1
               PHINEW(2,I-1,J)=PHI(2,I,J)
 75         CONTINUE
C     CALCULATES OUTPUT(BOTH PHI+ AND PHI-)
            DO 80 I=1,2
               OUTPUT(I,J)=T1*PHINEW(I,NXCR+N1,J)*AREA
 80         CONTINUE
C     CALCULATES INJECTION TERM
            Z(1,J)=T1*FRACTN*OUTPUT(1,J)/AREA
            Z(2,J)=0.0D0
C     CALCULATES PHIPLUS AND PHIMINUS AT FIRST MIRROR
          PHINEW(1,NXCR+N1,J)=R1*PHINEW(1,NXCR+N1,J)+Z(1,J)
          PHINEW(2,NXCR+N1,J)=R1*R2*R3*
     1                       PHINEW(2,NXCR+N1,J)+Z(2,J)
C    CALCULATES PHIPLUS FROM OUTPUT COUPLER TO EDGE OF
C    CRYSTAL
            DO 85 I=NXCR+N1,NXCR+N1+N2-1
              PHINEW(1,I+1,J)=PHI(1,I,J)
 85         CONTINUE
C    CALCULATES PHIPLUS GOING INTO THE CRYSTAL
            PHINEW(1,0,J)=TS*R2*R3*PHINEW(1,NXCR+N1+N2,J)
C    CALCULATES PHIMINUS FROM OUTPUT COUPLER TO EDGE OF
C    CRYSTAL
            DO 90 I=NXCR+N1,NXCR+1,-1
               PHINEW(2,I-1,J)=PHI(2,I,J)
 90         CONTINUE
C     CALCULATES PHIMINUS AT EDGE OF CRYSTAL
            PHINEW(2,NXCR,J)=TS*PHINEW(2,NXCR,J)
 60    CONTINUE
       RETURN
       END
CCCCCCCCCCCCCCCCCCCCCCCCCCCCCCCCCCCCCCCCCCCCCCCCCCCCCCCCCCCCCCCCCC
C
CCCCCCCCCCCCCCCCCCCCCCCCCCCCCCCCCCCCCCCCCCCCCCCCCCCCCCCCCCCCCCCCCC
C          SUBROUTINES TO COMPUTE DERIVATIVES
CCCCCCCCCCCCCCCCCCCCCCCCCCCCCCCCCCCCCCCCCCCCCCCCCCCCCCCCCCCCCCCCCC
CCCCCCCCCCCCCCCCCCCCCCCCCCCCCCCCCCCCCCCCCCCCCCCCCCCCCCCCCCCCCCCCCC
C            PUMP AND POPULATION DERIVATIVES
CCCCCCCCCCCCCCCCCCCCCCCCCCCCCCCCCCCCCCCCCCCCCCCCCCCCCCCCCCCCCCCCCC
C     X=(INPUT)POPULATION INVERSION
C     Y=(INPUT)LOWER LASER LEVEL POPULATION
C     W=(INPUT)PUMP
C     PH=(INPUT)PHOTON CONCENTRATIONS
C     DX=(OUTPUT)DERIVATIVES OF POPULATIONS
C     DW=(OUTPUT)DERIVATIVES OF PUMP
      SUBROUTINE DQ1(T,X,Y,W,PH,DW,DX)
      PARAMETER(NXCR=5,NL=24,NXTOTL=1000)
      IMPLICIT DOUBLE PRECISION(A-H,L,O-Z)
      DIMENSION W(0:NXCR),X(0:NXCR),
     1          Y(0:NXCR),PH(2,0:NXTOTL,NL),
     2          DW(0:NXCR),DX(2,0:NXCR)
       COMMON/COEFF/C11,C12,C21,C22,GAMMA,V,TOTALN,XNORM,
     1             TNORM,BETA,BETAG,PFACTR,XNORML
```

```
      COMMON/WAVL/SIGMA(NL),ALPHA(NL),NLMBDA,LAMBDA(NL)
      DO 10 I=0,NXCR
          A=XNORML-X(I)-GAMMA*Y(I)
          IF(A.GT.0.0D0)THEN
             X0=A
          ELSE
             X0=0.0D0
          END IF
          WP=X0*W(I)
          DW(I)=PFACTR*WP
          SUM=0.0D0
          DO 15 J=1,NLMBDA
              SUM=SUM+(PH(1,I,J)+PH(2,I,J))*SIGMA(J)
 15       CONTINUE
          DX(1,I)=C11*X(I)+C12*Y(I)-BETAG*X(I)*SUM+WP
          DX(2,I)=C21*X(I)+C22*Y(I)+BETA*X(I)*SUM
 10   CONTINUE
      RETURN
      END
CCCCCCCCCCCCCCCCCCCCCCCCCCCCCCCCCCCCCCCCCCCCCCCCCCCCCCCCCCCCCCCCC
C                  PHOTON DERIVATIVES IN CRYSTAL
CCCCCCCCCCCCCCCCCCCCCCCCCCCCCCCCCCCCCCCCCCCCCCCCCCCCCCCCCCCCCCCCC
C     X=(INPUT)POPULATION INVERSION
C     Y=(INPUT)LOWER LASER LEVEL POPULATION
C     PH=(INPUT)PHOTON CONCENTRATIONS
C     DP=(OUTPUT)DERIVATIVES OF PHOTON CONCENTRATTONS
      SUBROUTINE DQ2(T,X,Y,PH,DP)
      PARAMETER(NXCR=5,NL=24,NXTOTL=1000)
      IMPLICIT DOUBLE PRECISION(A-H,L,O-Z)
      DIMENSION X(0:NXCR),Y(0:NXCR),
     1          PH(2,0:NXTOTL,NL),DP(2,0:NXCR,NL),
     2          S(2,0:NXCR,NL)
     COMMON/COEFF/C11,C12,C21,C22,GAMMA,
     1          V,TOTALN,XNORM,TNORM,
     2          BETA,BETAG,PFACTR,XNORML
      COMMON/WAVL/SIGMA(NL),ALPHA(NL),NLMBDA,LAMBDA(NL)
      COMMON/SP/L,R,DEX,DELTAX,DLAMBDA(NL)
      COMMON/WPUMP/SIGMAA,BWAIST,ETAP,PLMBDA,ETOTL,TAUP,T0
CCCCCCCCCCCCCCCCCCCCCCCCCCCCCCCCCCCCCCCCCCCCCCCCCCCCCCCCCCCCCCCCC
C    CALCULATION OF SPONTANEOUS EMISSION CONTRIBUTION
      PI=4.0D0*DATAN(1.0D0)
      T4=2.0D0*DEX*DEX*DEX/(PI*BWAIST*BWAIST)
      DO 20 J=1,NLMBDA
            LMBDA2=LAMBDA(J)*LAMBDA(J)
            T2=T4*SIGMA(J)*DLAMBDA(J)/LMBDA2
          DO 10 I=0,NXCR
               T1=X(I)+(GAMMA-1.0D0)*Y(I)
               T3=T1*T2
               S(1,I,J)=T3
               S(2,I,J)=T3
 10       CONTINUE
 20   CONTINUE
CCCCCCCCCCCCCCCCCCCCCCCCCCCCCCCCCCCCCCCCCCCCCCCCCCCCCCCCCCCCCCCCC
```

```
C        CALCULATION OF PHOTON DERIVATIVES
       DO 60 J=1,NLMBDA
          SIG=SIGMA(J)*XNORM
          DO 50 I=0,NXCR
            DP(1,I,J)=(SIG*X(I)-ALPHA(J))*
     1                    PH(1,I,J)+S(1,I,J)
 50       CONTINUE
          DO 55 I=NXCR,0,-1
            DP(2,I,J)=(SIG*X(I)-ALPHA(J))
     1                     *PH(2,I,J)+S(2,I,J)
 55       CONTINUE
 60       CONTINUE
       RETURN
       END
CCCCCCCCCCCCCCCCCCCCCCCCCCCCCCCCCCCCCCCCCCCCCCCCCCCCCCCCCCCCCCCC
C     PUMP FUNCTION
CCCCCCCCCCCCCCCCCCCCCCCCCCCCCCCCCCCCCCCCCCCCCCCCCCCCCCCCCCCCCCCC
       FUNCTION PUMP(T)
       IMPLICIT DOUBLE PRECISION(A-H,L,O-Z)
       COMMON/WPUMP/SIGMAA,BWAIST,ETAP,PLMBDA,ETOTL,TAUP,T0
CCCCCCCCCCCCCCCCCCCCCCCCCCCCCCCCCCCCCCCC
C      C IS IN CM/SEC
C      H IS IN mJ-SEC
C      BWAIST IS IN CM
C      ETOTL IS IN MILLIJOULES
C      PLMBDA IS IN CM
C      SIGMAA IS IN CM^2
C      TAUP,T0 ARE IN NS
CCCCCCCCCCCCCCCCCCCCCCCCCCCCCCCCCCCCCCCC
       C=3.0D10
       PI=4.0D0*DATAN(1.0D0)
       FACTOR=SIGMAA/(PI*BWAIST*BWAIST)
       H=6.6262D-31
       PUMP=ETAP*(ETOTL/TAUP)*(PLMBDA/(H*C))*FACTOR
       BDLOG=DLOG(2.0D0)
       PUMP=PUMP*2.0D0*DSQRT(BDLOG/PI)*
      1     EXP(-BDLOG*((T-T0)/(.5D0*TAUP))**2)
       RETURN
       END
```

Biographical Statement

Lila Freeman Roberts was born in Asheville, North Carolina on December 21, 1954. As an undergraduate student, she attended Western Carolina University in Cullowhee, N.C. in 1973 and North Carolina State University in Raleigh, N.C. from 1974 to 1977.

After receiving a Bachelor of Science Degree in Mathematics Education from North Carolina State University in May, 1977, Ms. Roberts taught secondary school Mathematics with the Virginia Beach City Public Schools in Virginia Beach Virginia from 1977 to 1981 and with the Norfolk City Public Schools in Norfolk, Virginia in 1982.

Ms Roberts attended Old Dominion University in Norfolk, Virginia from 1983 to 1988 and received her Master of Science Degree in Computational and Applied Mathematics in August, 1986. She was a teaching assistant from 1983 to 1986. In 1986, she was elected to the honor society of Phi Kappa Phi. During the years 1985 to 1988, she conducted research at NASA Langley Research Center in Hampton, Virginia under a NASA Graduate Student Fellowship.

Currently, Ms Roberts is Assistant Professor of Mathematics at Randolph-Macon Woman's College in Lynchburg, Virginia. She resides in Madison Heights, Virginia with her husband. She will receive her Doctor of Philosophy Degree in Computational and Applied Mathematics from Old Dominion University in December 1988.